ABSTRACT

Title of Dissertation: ENGINEERING CELL-PENETRATING PEPTIDES FOR TRANSLOCATION AND INTRACELLULAR CARGO DELIVERY IN CANDIDA SPECIES

Zifan Gong, Doctor of Philosophy, 2017

Dissertation directed by: Professor Amy J. Karlsson, Department of Chemical and Biomolecular Engineering

Fungal infections caused by *Candida* species, particularly *C. albicans* and *C. glabrata*, have become a serious threat to public health. The rising drug resistance has prevented effective treatment and increased the mortal rate. Novel approaches to improve the therapeutic effects of antifungal agents and allow delivery of agents that are not normally cell-permeable are in demand.

In order to improve the intracellular delivery of antifungal agents, we have investigated using cell-penetrating peptides as drug carriers for treating fungal infections. CPPs have been widely studied as tools for delivering a variety of molecular cargo into cells, including DNA, RNA, proteins, and nanoparticles. Previous work with CPPs has mainly focused on their uptake in mammalian cells, but CPPs also have potential as drug delivery and research tools in other organisms, including *Candida* pathogens.

We have explored various well-studied CPPs to identify peptides that retain their translocation capability with *Candida* cells, including pVEC, penetratin, MAP, MPG,

SynB, TP-10 and cecropin B. The CPPs pVEC, penetratin, MAP and cecropin B show a higher level in the cytosol adopt direct translocation mechanisms and exhibit toxicity towards *C. albicans*. Our peptide localization and mechanistic studies allow better understanding of the mode of translocation for different CPPs, which is related to the potential toxicity towards *Candida* pathogens.

To further understand the molecular mechanisms of translocation of CPP, we investigated the biophysical properties of the peptides. CPPs that previously were shown to use direct translocation mechanisms (pVEC, MAP, and cecropin B) exhibit helical conformations upon interaction with cells due to the hydrophobic interaction with the core of bilayers. Membrane associations of peptides that entered cells via endocytosis were controlled by electrostatic forces. Our novel structure characterization methods using circular dichroism with live fungal cells, along with Monte Carlo simulations, allow us to understand how CPPs interact with cell membranes and how the membrane association affects the translocation mechanisms.

After beginning to understand the structure-function relationships of CPPs, we engineered two CPPs, pVEC and SynB, to enable better translocation efficacy and manipulation of translocation mechanisms. We tuned the properties of the peptides, including the net charge and the hydrophobicity, to alter intracellular fates and the level of antifungal activity. These results are promising and motivate better peptide engineering for specific purposes.

Our work with CPPs and fungal pathogens contributes to the understanding of structure-function relationship of CPPs in *Candida* species. We have provided the foundation for further peptide engineering and explorations into applications of CPPs in treating fungal infections.

ENGINEERING CELL-PENETRATING PEPTIDES FOR TRANSLOCATION AND INTRACELLULAR CARGO DELIVERY IN CANDIDA SPECIES

by

Zifan Gong

Dissertation submitted to the Faculty of the Graduate School of the
University of Maryland, College Park, in partial fulfillment
of the requirements for the degree of
Doctor of Philosophy
2017

Advisory Committee:
Professor Amy J. Karlsson, Chair
Professor Jeffery Klauda
Professor Ganesh Sriram
Professor Zhongchi Liu
Professor Taylor Woehl

Acknowledgements

My 5-year Ph.D. life has been an incredible experience. The one that deserves the most credit is my advisor Dr. Amy Karlsson. Amy and I have witnessed the lab from many unpacked boxes to a fully functional, advanced biological lab for protein engineering. Her hands-on training and mentoring at the early days really helped me build the foundation of my research projects, while her trust and giving me space for innovation enabled me to become an independent researcher. She is always very supportive and encouraging, which helps me survive from the tough days. I never realized the importance of a great advisor, but now I believe choosing Amy as my advisor is one of the biggest right decision I have made in my life.

I am extremely fortunate and grateful to work in such a lab with nice people and warm culture. Svetlana Ikonomova and I started to work in the lab at the same time. I quickly learned how to fit into the American culture from her and she certainly helped me to practice my English speaking. As we became more and more independent and familiar with the projects, she provided me so many great ideas and suggestions that helped my projects moving forward. I also would like to thank Parisa Moghaddam-Taaheri for her help in the lab. She is the “cool girl” of our group and she not only brings a lot of expertise but also a lot of laughter into the lab. Her extra talent in organization definitely helps to maintain a clean and well-organized lab. Sayanee Adhikari was recently joined the lab and I closely worked with her on some projects. She has patiently listened to all of my experience in the projects and

instruments, and now she has turned to another expert in cell-penetrating peptides in the lab.

In addition to the graduate students in my group, I need to thank all the undergraduate students and high school students that extensively worked on my projects. I thank Kirsten Smulovitz, Thomas Wescott, Alisha Karley for their preliminary work on the CPP projects. I also thank Mackenzie Walls for his great work on my first published work. Turki Alahmadi and Rosemary Iwuala made a lot of progress recently and I would like to thank them for their nice work.

Many people from other research labs have contributed time, expertise and materials to make my projects possible. The members from Dr. Chris Jewell's lab, Dr. Lisa H. Tostanoski, Dr. Peipei Zhang and Dr. Xiangbin Zeng have helped me a lot in flow cytometry training and data interpretation. Mary Doolin and I worked together on testing CPPs on mammalian cell lines, and I am truly grateful to work with such a talented student. I would like to thank Jason Hustedt for his help in CD training and trouble shooting. I also want to thank Vincent Kuo and Ting Guo from Dr. John Fisher's lab to help me with the fluorescence assays.

One of the most valuable asset I have at UMD is the friends I made in these years. They may not directly contribute to my research projects, but they offer me huge help in my life outside the lab. Guanghui Zhu, Fudong Han, Tao Gao and I started at the same time, and I am really grateful to have them as my close friends. They helped me survived from the first year of being alone in the United States. Their intelligence and innovation also helped me to keep me myself motivated and moving forward. Jing Yan has been my closest friend and now she is my life partner. Her

positive life attitude and her enthusiasm encourage through most of graduate school. I really appreciate her support and her help especially toward the end of my Ph.D. My friendship with Yiqing Wu, Yujia Liang, Jiaojie Tan, Xiyang Dai is also my greatest fortune.

Debbie Goldberg is another life mentor for me. I worked with her while I was her intern at MedImmune, and now she has begun a new career in my department at UMD. Without Debbie, I could never become who I am today. She is always there when I need future career advice. I am really grateful that I went to MedI and got to know her.

Finally, I want to thank my parents for supporting me to pursue my Ph.D. in the United States. Thank you for teaching me how to be a good son, a good student and a good man.

Table of Contents

List of Tables

List of Figures

Chapter 7. Future work

List of Abbreviations

CD	Circular dichroism
CDC	Centers for Disease Control and Prevention
CFPS	Cell-free protein synthesis
CFU	Colony-forming unit
CPP	Cell-penetrating peptide
DIC	Differential interference contrast microscopy
$DiSC_3(5)$	3,3′-Dipropylthiadicarbocyanine iodide
FAM	Carboxyfluorescein
FPLC	Fast protein purification liquid chromatography
GFP	Green fluorescent protein
IEX	Ion exchange chromatography
IMAC	Immobilized metal affinity chromatography
LB	Lysogeny broth
LPS	Lipopolysaccharides
MC	Monte Carlo simulation
MIC_{50}	Minimum inhibitory concentration required to inhibit 50% of the growth
NAA	Non-natural amino acids
NLS	Nuclear localization sequence
OD	Optical density
PBS	Phosphate-buffered saline
PG	Phosphatidylglycerol
PI	Propidium iodide
PS	Phosphatidylserine
SEC	Size exclusion chromatography
TFE	Trifluoroethanol
YPD	Yeast extract peptone dextrose medium

Chapter 1. Introduction

Yeast infections can be caused by *Candida* species and other fungal species, and the most common clinically isolated strains are *C. albican*s and *C. glabrata* [1]. These fungi can develop drug resistance to traditional antifungal agents rapidly [2, 3]. The Centers for Disease Control and Prevention (CDC) has listed fluconazole-resistant *Candida* species as a "serious threat" to public health and estimated an increased healthcare cost of $6000-$9000 per infection case [4]. Although these fungal infections can currently still be treated, the drug resistance can be problematic as it can delay the initial diagnosis of infection and the administration of an effective drug [5].

Opportunistic *Candida* species can be isolated from the human digestive tract and other mucosal surfaces, such as the oral cavity. They typically do not initiate infections or symptoms. However, for patients with suppressed immune systems, such as people with AIDS or those undergoing chemotherapy, fungi can cause serious systemic infections, which are hard to treat and have a high mortality rate. Treating fungal infections is a growing concern due to the limited drug targets and the rapidly rising drug resistance to the traditional antifungal agents, which motivates research into novel therapeutic methods or drug delivery vehicles to improve the efficacy of antifungal agents.

1.1. *Candida* species and traditional antifungal agents

Currently, the first-line treatment for fungal infections includes antifungal drugs such as polyenes and azoles [6]. The most commonly used polyenes drugs are

A

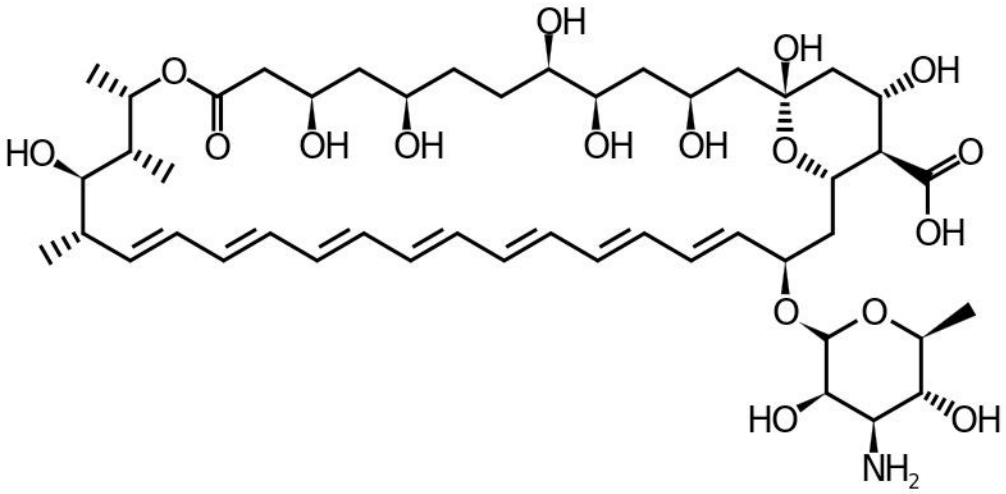

Amphotericin B

B

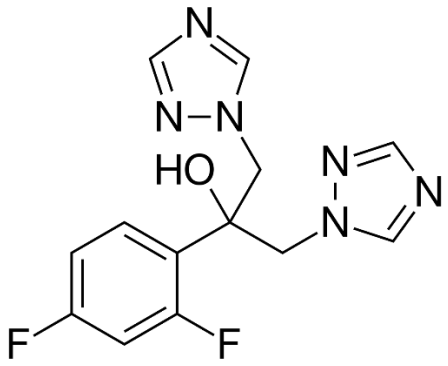

Fluconazole

Figure 1.1 Example of antifungal drugs that commonly used for treating fungal infections caused by *C. albicans*. (A) Amphotericin B, polyene drug. (B) Fluconazole, azole drug.

amphotericin B (Figure 1.1A) formulations. Amphotericin B is an effective antifungal agent for treating infections caused by *C. albicans*, yet it has reduced activity towards *C. glabrata*. Amphotericin B binds to the ergosterol in the cell membrane of fungi, causing pore formation and cell leakage, leading to cell death [7]. Although drug resistance of amphotericin B is rarely reported, the drug has severe side effects such as high fever, shaking chills, and even organ damage including kidney damage [8]. Azole drugs, including fluconazole (Figure 1.1A) and itraconazole, are also commonly used to treat infections caused by *C. albicans*. Their antifungal mechanism

involves inhibition of ergosterol synthesis [9]. They inhibit the activity of a cytochrome P450 enzyme, 14-α-demethylase, the intracellular enzyme that converts lanosterol to ergosterol and affect membrane integrity. Azole drugs are mostly effective towards *C. albicans*, but not towards *C. glabrata* due to the differences in membrane enzyme compositions [10]. Even for *C. albicans*, cells can develop resistance to azoles through multiple mechanisms, including Erg3p inactivation and activation of major facilitator superfamily transporters (MFS) [9]. Although the toxicity of azoles to patients is not as significant as for amphotericin B, the rapid development of drug resistance still makes azole treatment less effective.

Although amphotericin B, azoles, and other drugs are effective antifungal agents, the severe side effects and rising drug resistance demand novel therapeutic methods. As treatment with these traditional drugs continue, *C. albicans* and other fungal pathogens will evolve more mechanisms to reduce the therapeutic effects, leading to an increased number of drug-resistant infections, delaying the treatment and causing a higher mortality rate. Thus the discovery of novel drugs or drug delivery approaches is becoming more essential to prevent rising drug resistance.

1.2. Application of cell-penetrating peptides (CPPs)

One potential new therapeutic method is to use cell-penetrating peptides (CPPs) as a novel drug delivery vehicle. CPPs are small peptides, approximately 30 amino acids [11, 12] or fewer, with the capability to cross cellular membranes. These short peptides are often positively charged with several lysine or arginine residues in the sequence. The polar/charged residues and the non-polar/hydrophobic residues are

commonly arranged in an alternating pattern that leads to an amphipathic secondary structure [12].

The first CPP, the Tat peptide, was discovered from the HIV virus in 1988 [11]. Tat is the trans-activating transcriptional activator of the virus, which assists in uptake of the virus by mammalian cells in culture. Over three decades of research, more than 100 CPPs have been discovered or synthesized [12]. Studying natural peptides allows exploration of the highly varied structures of CPPs. *De novo* synthesized peptides such as MAP and $(KFF)_3K$, can be designed to have a highly organized amphipathic structure and show significant translocation efficacy [13, 14], which enables a better understanding of CPPs.

CPPs can carry molecular cargos as they cross into the cytosol. They have been exploited to deliver various biomolecular cargos into cells, including DNA [15-19], siRNA [20, 21], and nanoparticles [22]. More importantly, CPPs are widely used for delivering proteins into mammalian cells including insulin [23], green fluorescent protein (GFP) [24], β-galactosidase [25], and antibody fragments [26].

1.3. Limited use of CPPs with fungal pathogens

Although CPPs show promise for applications in cargo delivery and cell recognition, limitations exist in their development for therapeutic applications, especially for applications that target fungal pathogens. Most CPPs were discovered or screened in mammalian cells. The translocation process is better understood in mammalian cells, with limited information about the translocation toward other types of cells, such as bacterial and fungal cells [27-32]. In order to utilize CPPs for enhanced drug delivery to combat fungal infection, a more detailed study of CPP

translocation in fungal cells is needed to identify the peptides that can be used in fungi.

In addition, although CPPs have been widely used with mammalian cells, a clear explanation of their translocation mechanisms is often still lacking. Several mechanisms have been proposed to explain the translocation in mammalian cells, but no comprehensive mechanistic study of cellular uptake has been done in fungal cells. In order to use CPPs in fungal cells, or further engineer CPPs for fungi-specific cargo delivery, a more detailed mechanistic study is needed.

1.4. Overview of dissertation

This dissertation describes my work to understand CPPs and cargo delivery in fungal cells, as well as to engineer CPPs for enhanced translocation and cell-specific cargo delivery. In Chapter 2, I review relevant literature of CPPs and their mechanisms of action. I also explore the limitation of applying CPPs for drug delivery and the opportunities of studying CPPs in *Candida* species. In Chapter 3, I present a screening study of CPPs in fungal cells. Subcellular localization of several well-studied CPPs was carefully analyzed to reveal the trafficking of the peptides Chapter 4 expands on the work in Chapter 3. It provides biophysical information about CPP structure and how it affects the interaction between CPPs and fungal cells. In Chapter 5, I present my study on cargo delivery into *C. albicans* using CPPs. Using direct genetic fusion of CPPs to cargo and recombinant expression, I was able to produce CPP-green fluorescent protein (GFP) fusion proteins with the capability for intracellular translocation. In Chapter 6, I present my preliminary data on CPP engineering. I modified biophysical properties of CPPs to understand the structure-

function relationship of CPPs. Finally, Chapter 7 describes several possible future projects that build on my work in Chapters 3-6.

1.5. References

1. Silva, S., M. Negri, M. Henriques, R. Oliveira, D.W. Williams, and J. Azeredo, *Candida glabrata, Candida parapsilosis and Candida tropicalis: biology, epidemiology, pathogenicity and antifungal resistance.* Fems Microbiology Reviews, 2012. **36**(2): p. 288-305.
2. Mayer, F.L., D. Wilson and B. Hube, *Candida albicans pathogenicity mechanisms.* Virulence, 2013. **4**(2): p. 119-28.
3. Helmerhorst, E.J., C. Venuleo, A. Beri and F.G. Oppenheim, *Candida glabrata is unusual with respect to its resistance to cationic antifungal proteins.* Yeast, 2005. **22**(9): p. 705-714.
4. *Centers for Disease Control and Prevention. Antibiotic Resistance Threats in the United States, 2013.*: p. http://www.cdc.gov/drugresistance/threat - report - 2013/ Accessed July 2014.
5. Cannon, R.D., E. Lamping, A.R. Holmes, K. Niimi, K. Tanabe, M. Niimi, and B.C. Monk, *Candida albicans drug resistance - another way to cope with stress.* Microbiology-Sgm, 2007. **153**: p. 3211-3217.
6. Pappas, P.G., J.H. Rex, J.D. Sobel, S.G. Filler, W.E. Dismukes, T.J. Walsh, and J.E. Edwards, *Guidelines for treatment of candidiasis.* Clinical Infectious Diseases, 2004. **38**(2): p. 161-189.
7. O'Keeffe, J., S. Doyle and K. Kavanagh, *Exposure of the yeast Candida albicans to the anti-neoplastic agent adriamycin increases the tolerance to amphotericin B.* Journal of Pharmacy and Pharmacology, 2003. **55**(12): p. 1629-1633.
8. Spellberg, B.J., S.G. Filler and J.E. Edwards, *Current treatment strategies for disseminated candidiasis.* Clinical Infectious Diseases, 2006. **42**(2): p. 244-251.
9. Ghannoum, M.A. and L.B. Rice, *Antifungal agents: Mode of action, mechanisms of resistance, and correlation of these mechanisms with bacterial resistance.* Clinical Microbiology Reviews, 1999. **12**(4): p. 501-+.
10. Xiao, M., X. Fan, S.C.A. Chen, H. Wang, Z.Y. Sun, K. Liao, S.L. Chen, Y. Yan, M. Kang, Z.D. Hu, Y.Z. Chu, T.S. Hu, Y.X. Ni, G.L. Zou, F.R. Kong, and Y.C. Xu, *Antifungal susceptibilities of Candida glabrata species complex, Candida krusei, Candida parapsilosis species complex and Candida tropicalis causing invasive candidiasis in China: 3 year national surveillance.* Journal of Antimicrobial Chemotherapy, 2015. **70**(3): p. 802-810.
11. Feng, S. and E.C. Holland, *Hiv-1 Tat Trans-Activation Requires the Loop Sequence within Tar.* Nature, 1988. **334**(6178): p. 165-167.
12. Alhakamy, N.A., A.S. Nigatu, C.J. Berkland and J.D. Ramsey, *Noncovalently associated cell-penetrating peptides for gene delivery applications.* Ther Deliv, 2013. **4**(6): p. 741-57.
13. Hallbrink, M., A. Floren, A. Elmquist, M. Pooga, T. Bartfai, and U. Langel, *Cargo delivery kinetics of cell-penetrating peptides.* Biochim Biophys Acta, 2001. **1515**(2): p. 101-9.

14. Vaara, M. and M. Porro, *Group of peptides that act synergistically with hydrophobic antibiotics against gram-negative enteric bacteria.* Antimicrobial Agents and Chemotherapy, 1996. **40**(8): p. 1801-1805.
15. Stetsenko, D.A. and M.J. Gait, *Efficient conjugation of peptides to oligonucleotides by "native ligation".* J Org Chem, 2000. **65**(16): p. 4900-4908.
16. Fisher, L., U. Soomets, V. Cortes Toro, L. Chilton, Y. Jiang, U. Langel, and K. Iverfeldt, *Cellular delivery of a double-stranded oligonucleotide NFkappaB decoy by hybridization to complementary PNA linked to a cell-penetrating peptide.* Gene Ther, 2004. **11**(16): p. 1264-72.
17. El-Andaloussi, S., H. Johansson, A. Magnusdottir, P. Jarver, P. Lundberg, and U. Langel, *TP10, a delivery vector for decoy oligonucleotides targeting the Myc protein.* J Control Release, 2005. **110**(1): p. 189-201.
18. Zielinski, J., K. Kilk, T. Peritz, T. Kannanayakal, K.Y. Miyashiro, E. Eiriksdottir, J. Jochems, U. Langel, and J. Eberwine, *In vivo identification of ribonucleoprotein-RNA interactions.* P Natl Acad Sci USA, 2006. **103**(5): p. 1557-62.
19. Liu, Y., J. Yan and M.R. Prausnitz, *Can ultrasound enable efficient intracellular uptake of molecules? A retrospective literature review and analysis.* Ultrasound Med Biol, 2012. **38**(5): p. 876-888.
20. Muratovska, A. and M.R. Eccles, *Conjugate for efficient delivery of short interfering RNA (siRNA) into mammalian cells.* Febs Lett, 2004. **558**(1-3): p. 63-68.
21. Chiu, Y.L., A. Ali, C.Y. Chu, H. Cao, and T.M. Rana, *Visualizing a correlation between siRNA localization, cellular uptake, and RNAi in living cells.* Chem Biol, 2004. **11**(8): p. 1165-1175.
22. Olson, E.S., T. Jiang, T.A. Aguilera, Q.T. Nguyen, L.G. Ellies, M. Scadeng, and R.Y. Tsien, *Activatable cell penetrating peptides linked to nanoparticles as dual probes for in vivo fluorescence and MR imaging of proteases.* P Natl Acad Sci USA, 2010. **107**(9): p. 4311-4316.
23. Khafagy, E.S., M. Morishita, K. Isowa, J. Imai, and K. Takayama, *Effect of cell-penetrating peptides on the nasal absorption of insulin.* Journal of Controlled Release, 2009. **133**(2): p. 103-108.
24. Gong Z., W., MT., Karley AN., Karlsson AJ., *Effect of a flexible linker on recombinant expression of cell-penetrating peptide fusion proteins and their translocation into fungal cells.* Mol Biotechnol, 2016.
25. Myrberg, H., M. Lindgren and U. Langel, *Protein delivery by the cell-penetrating peptide YTA2.* Bioconjugate Chemistry, 2007. **18**(1): p. 170-174.
26. Weisbart, R.H., J.F. Gera, G. Chan, J.E. Hansen, E. Li, C. Cloninger, A.J. Levine, and R.N. Nishimura, *A Cell-Penetrating Bispecific Antibody for Therapeutic Regulation of Intracellular Targets.* Molecular Cancer Therapeutics, 2012. **11**(10): p. 2169-2173.
27. Rajarao, G.K., N. Nekhotiaeva and L. Good, *Peptide-mediated delivery of green fluorescent protein into yeasts and bacteria.* Fems Microbiol Lett, 2002. **215**(2): p. 267-272.

28. Holm, T., S. Netzereab, M. Hansen, U. Langel, and M. Hallbrink, *Uptake of cell-penetrating peptides in yeasts.* FEBS Lett, 2005. **579**(23): p. 5217-22.
29. Parenteau, J., R. Klinck, L. Good, U. Langel, R.J. Wellinger, and S.A. Elela, *Free uptake of cell-penetrating peptides by fission yeast.* Febs Lett, 2005. **579**(21): p. 4873-4878.
30. Palm, C., S. Netzerea and M. Hallbrink, *Quantitatively determined uptake of cell-penetrating peptides in non-mammalian cells with an evaluation of degradation and antimicrobial effects.* Peptides, 2006. **27**(7): p. 1710-1716.
31. Munoz, A., E. Harries, A. Contreras-Valenzuela, L. Carmona, N.D. Read, and J.F. Marcos, *Two functional motifs define the interaction, internalization and toxicity of the cell-penetrating antifungal peptide paf26 on fungal cells.* Plos One, 2013. **8**(1).
32. Rajarao, G.K., N. Nekhotiaeva and L. Good, *The signal peptide NPFSD fused to ricin A chain enhances cell uptake and cytotoxicity in Candida albicans.* Biochem Bioph Res Co, 2003. **301**(2): p. 529-534.

Chapter 2. Cell-penetrating peptides

CPPs, also known known as protein translocation domain (PTD) or Trojan horse peptides, can transport biomolecules with various sizes and properties. Compared with other drug delivery vehicles such as virus vectors, CPPs are less toxic to host cells and can be easily engineered or designed for specific purposes [1-3]. I review the structures, properties, translocation mechanisms, and potential applications of CPPs in this chapter.

2.1. Classes of CPPs

Currently no unified method exists to classify CPPs. They can be categorized by either their origins or their properties. Based on their origin, there are three major types of CPPs: (1) protein-derived peptides, such as penetratin, Tat, and pVEC, which came from natural proteins; (2) model peptides, which are *de novo* designed, like MAP and $(Arg)_8$; and (3) chimeric peptides, such as MPG, Pep-1, and transportan that include multiple regions from different origins, which help the peptides to enter cells and achieve specific subcellular localization [1].

Another way to categorize CPPs is based on their structural and functional characteristics: (1) cationic peptides, (2) hydrophobic peptides, (3) amphipathic peptides, and (4) antimicrobial peptides [3]. Some peptides may belong to more than one category. Example of CPPs in all chapters are listed in **Table 2.1** and defined by their origin or structural or functional characteristics. The structural classes of CPPs are discussed in more detail below.

Table 2.1 Class of CPPs

Peptides	Sequence	Class		Ref
		Property	Origin	
MTS	AAVALLPAVLLALLAP	Hydrophobic	κ-fibroblast growth factor (protein-derived)	[4]
Integrin β3 signal peptide	VTVLALGALAGVGV	Hydrophobic	Integrin β3 (natural peptide)	[5]
Penetratin	RQIKIWFQNRRMKWKK	Cationic	Antennapedia protein (protein-derived)	[6]
CyLoP	CRWRWKCCKK	Cationic	Crotamine (protein-derived)	[7]
Tat	RKKRRQRRR	Cationic	HIV virus (protein-derived)	[8]
Transportan	GWTLNSAGYLLGKINLKALAA LAKKIL	Cationic	Mastoparan (protein-derived)	[9]
TP-10	AGYLLGKINLKALAALAKKIL	Cationic	Transportan (protein-derived)	[10]
SynB	RGGRLSYSRRRFSTSTGR	Cationic	Protegrin (protein-derived)	[11]
R_9F_2	RRRRRRRRRFF	Cationic	Model	[12]
R_n (n=6-9)	R_n (n=6-9)	Cationic	Model	[13]
MPG	GALFLGFLGAAGSTMGAWSQ PKKKRKV	Amphipathic	Chimeric	[14]
Pep-1	KETWWETWWTEWSQPKKKR KV	Amphipathic	Chimeric	[15]
S413-PV	ALWKTLLKKVLKAPKKKRKV C	Amphipathic	Chimeric	[16]
YTA 2	YTAIAWVKAFIRKLRK	Amphipathic	Model	[17]
YTA 4	IAWVKAFIRKLRKGPLG	Amphipathic	Model	[17]
$(KFF)_3K$	KFFKFFKFFK	Amphipathic	Model	[18]
KALA	WEAKLAKALAKALAKHLAKA LAKALKACEA	Amphipathic	Model	[19]
MAP	KLALKLALKALKAALKLA	Amphipathic	Model	[19]
pVEC	LLIILRRRIRKQAHAHSK	Amphipathic	Vascular endothelial cadherin (protein-derived)	[20]
Ctyptdin-4	GLLCYCRKGHCKRGERVRGT CGIRFLYCCPRR	Amp	Alpha-defensin (protein-derived)	[21]
Tachyplesin I	KWCFRVCRGICYRRCR	Amp	Hemocytes (protein-derived)	[22]
Cecropin A	KWKLFKKIEKVGQNIRDGIIKA GPAVAVVGQATQIAK	Amp	Hemolymph (protein-derived)	[23]
Cecropin B	KWKVFKKIEKMGRNIRNGIVK AGPAIAVLGEAKAL	Amp	Hemolymph (protein-derived)	[23]
PAF 26	RKKWFW	Amp	Model	[24]
Dermaseptin S	ALWKTMLKKLGTMALHAGK AALGAAADTISQGTQ	Amp	*Phyllomedusa sauvagii* skin (natural peptide)	[25]
Histatin-5	DSHAKRHHGYKRKFHEKHHS HRGY	Amp	Saliva (natural peptide)	[26]
Buforin-2	TRSSRAGLQFPVGRVHRLLRK	Amp	Toad stomach tissue (natural peptide)	[27]
hCT	LGTYTQDFNKTFPQTAIGVGA P		Human calcitonin (protein-derived)	[28]

2.1.1. Cationic peptides

Positively charged CPPs are widely seen and studied. Most of these peptides have several arginine or lysine residues in the primary sequences. Dedicated research about arginine residues in the peptides indicates that poly-arginine peptides (R_7, R_8, and R_9) have better transmembrane capabilities than the original arginine-rich Tat (RKKRRQRRR) peptides [29, 30]. Meanwhile, other lysine-rich peptides including penetratin (RQIKIWFQNRRMKWKK) and TP-10 (AGYLLGKINLKAL-AALAKKIL) have also shown great translocation efficacy. The high surface charge of cationic CPPs enables stronger membrane association, which increases the translocation efficacy. However, for some peptides, such as Tat and TP-10, these net charges and closer membrane association lead to membrane damage towards mammalian cells [31].

2.1.2. Hydrophobic peptides

Hydrophobic CPPs normally consist of several regions: a positively charged domain, a hydrophobic domain (h-region), as well as a negatively charged domain [32]. The hydrophobic domain controls the translocation of this class of peptides. The h-region of Kaposi fibroblast growth factor (AAVALLPAVLLALLAP, K-FGF) was incorporated into the SKP peptides, which showed intracellular translocation and nuclear localization [32]. The integrin β3 signaling peptide has an h-region with a 15-amino acid fragment (VTVLALGALAGVGV) [5] that was used as a CPP for a translocation study in mammalian cells.

2.1.3. Amphipathic CPPs

The amphipathic class of CPPs is the most commonly seen class. Upon forming their secondary structure, these peptides have a polar side with charged residues and a non-polar hydrophobic side with hydrophobic amino acids in the primary sequence. The helical structure, many of these amphipathic CPPs form, has been proposed to be directly related to their translocation process [33]. While amphipathic CPPs have a random coil conformation in aqueous solution, some studies indicate α-helical or β-sheet structures form when these peptides closely interact with the membrane [19, 34, 35]. The anionic cell membrane helps attract peptides onto the membrane surface through electrostatic forces, and the conformational transition due to the hydrophobic interaction from the non-polar residues promotes the insertion of the peptides into the lipid bilayer. Protein-derived CPPs like penetratin [6], pVEC [36], and CyLoP [37], as well as synthesized CPPs including MAP [38], KALA [19], and $(KFF)_3K$ [39], with such amphipathic properties have shown great translocation efficacy and structure transition behavior.

2.1.4. Antimicrobial peptides

Some peptides not only interact with the cell membrane, but also directly affect the viability of the cells. These peptides, commonly referred as AMP, include histatin-5 and cecropin A and B [40, 41]. Many members of this class of peptides have an amphipathic, α-helical conformation that promotes membrane interaction and leads to cytosolic toxicity to host cells [42]. Some AMPs, such as histatin-5 and S413-PV, target intracellular targets (mitochondria for histatin-5 [43]) and nucleus for

S413-PV [16]), whereas other AMPs, including tachyplesin I, cryptdin-4, and buforin-2, cause toxicity via pore formation [44].

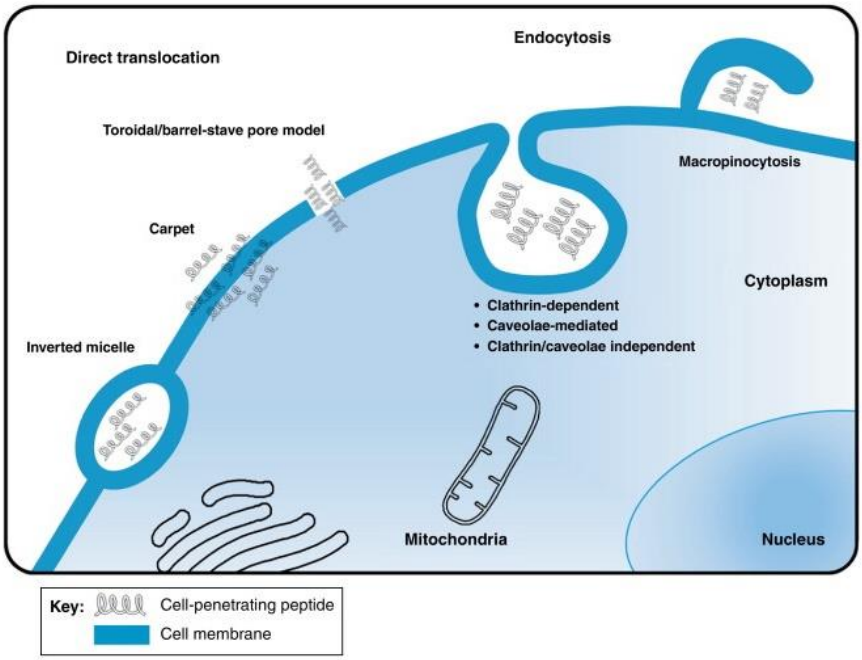

Figure 2.1 Potential pathways of cell entry for CPPs. Figure from [21]

2.2. CPP translocation mechanisms

Although CPPs have been widely studied for decades, a clear explanation of the translocation process is still lacking. Initially, people believed that CPPs entered the cells via an energy-independent direct transmembrane process like pore formation [45]. However, more research has suggested multiple potential mechanisms (Figure 2.1), including direct translocation (inverse micelles, "carpet", and pore formation) or endocytosis (for example, clathrin dependent endocytosis and macropinocytosis) [2].

2.2.1. Direct translocation mechanisms

Inverted Micelles. Penetratin, also known as pAntp, was the first peptide known to use the inverted micelles mode for internalization [6]. Based on results from

confocal microscopy, electron microscopy, [6] and NMR studies [46], Derossi *et al.* suggest that peptides initially associate with the lipid layers. Due to the hydrophobic interaction, peptides subsequently interact with the cell membrane and induce membrane reorganization and inversion. Hydrophobic residues like tryptophan, previously known as an inducer of inverted micelles [47], promote the formation of inverted micelles that carry the peptides. Although this mechanism explains how cationic CPPs that also have hydrophobic residues (like penetratin) can enter cells, it cannot explain the internalization of peptides that lack hydrophobic residues, such as the arginine-rich peptides $(Arg)_9$ and SynB, since they cannot interact with the hydrophobic domain in the bilayer in the same way.

Carpet Mode. The carpet mode of translocation was first proposed to describe the mechanism of the AMP dermaseptin S [25] and was later used to explain the mode of action for other peptides including AMPs and CPPs [22, 48-52]. The peptides first interact with the negatively charged membrane lipids such as phosphatidylinositol (PI), phosphatidylserine (PS), and phosphatidylglycerol (PG) via electrostatic interaction, triggering a conformational change of the peptides. The positively charged amino acid side chains turn towards the lipid hydrophilic surface, which allows the hydrophobic side chains to interact with the core of the bilayer. As the critical concentration of the peptides is reached, CPPs disrupt the membrane and cause internalization of the peptides [53]. The rearrangement of the peptides on the surface could also reduce the surface tension of the membrane, which would also promote the internalization of CPPs [53].

Pore formation. Pore formation has been observed mostly for amphipathic CPPs with a potential α-helical conformation upon membrane association. When many peptide units closely associate with the lipid membrane, they assemble into a "barrel", displaying all hydrophobic side chains outwards to allow deeper membrane association with the hydrophobic core. The bundled peptide clusters act like pores to permeabilize the membrane and allow more internalization of the peptides [53-55].

2.2.2. Endocytosis-dependent mechanisms

Instead of directly translocating into the cytosol of cells, CPPs internalized via endocytosis, commonly pinocytosis, are initially included in intracellular vesicles. These vesicles will be either guided to other cellular organelles [43, 56-58] or will escape from endosomes [59-62]. These pinocytosis processes can be classified into 1) clathrin-mediated, 2) caveolae-mediated, or 3) macropinocytosis. Clathrin-mediated pinocytosis and caveolae-mediated pinocytosis are both receptor-mediated endocytosis processes that require specific membrane receptors to allow vesicles formation [63], whereas macropinocytosis is independent of a receptor [64]. Some peptides may adopt multiple mechanisms dependent on the concentration and the cargo properties. TAT was suggested to use caveolae-mediated endocytosis with protein cargo, but to utilize a clathrin-mediated process when attached to small molecules [53]. Macropinocytosis, a non-specific endocytosis process, was recently suggested to be a widely used mode of internalization [64, 65]. It can occur in different types of cells without a specific receptor requirement and is easily distinguished from other types of pinocytosis by the pattern of membrane

perturbation, where macropinocytosis involves actin cytoskeleton rearrangement at the plasma membrane leading to the formation of membrane ruffles [64].

2.2.3. Factors determining the translocation mechanism

CPPs with different types of properties may have different modes of intracellular translocation and sometimes one CPP may even have multiple mechanisms. Several properties are useful in evaluating the mode of action for intracellular translocation, such as cargo type and size, concentration of the peptides, target cell type, amphipathicity of the peptide and net charge of the peptide. For direct translocation processes, physiochemical properties can greatly affect the efficacy of translocation [66, 67].

In some cases, the biophysical (structural) properties of the peptides also affect the membrane association and translocation processes. The amphipathic property of CPPs and net surface charges of the peptides can greatly affect the interaction between peptides and cell membranes [68]. The primary sequence of the peptides and the hydrophobicity of the environment has a huge impact on the secondary structure of the peptides, which is closely related to the translocation mechanism [69]. CPPs like pVEC and penetration remain in random coil conformation in aqueous solutions but form helical structures in hydrophobic solutions or when interacting with model membranes [70]. Eiríksdóttir *et al.* suggested that conformational change can be directly associated with the membrane interaction and affect the translocation mechanisms and efficacy of peptides, such as MAP and TP10 [70].

2.3. Current applications of CPPs

Since Tat was first discovered at 1988 [71], researchers have widely studied CPPs due to their great cargo delivery potential. Compared with other delivery methods, CPPs have some promising advantages, such as high delivery efficiency, specificity, and flexibility in cargo properties [57]. CPPs can translocate various types of biomolecules including DNA [10, 72-75], siRNA [76, 77], proteins [78-82], and nanoparticles [83]. These cargos can be either covalently conjugated to the peptides by chemical reaction or recombinant gene expression or non-covalently conjugated. The variety of properties and the high compatibility of different cargo molecules have allowed CPPs to become promising drug delivery vehicles.

2.3.1. Protein cargo delivery

Therapeutic proteins and peptides are great options for treating many diseases. People have been working with CPPs to deliver protein cargos with sizes ranging from 25 kDa (e.g. scFv [84]) to 150 kDa (e.g. IgG [85]). The 120-kDa protein β-galactosidase can be delivered into mouse tissues, even in the brain, while maintaining its biological activity [86]. CPPs like Tat, penetratin, or Pep-1 have been shown to yield significant tissue localization *in vivo* with protein cargos consisting of antibody fragments ([87]). Not only useful in mammalian cells, CPPs can also deliver proteins into other types of cells including bacterial cells [88] and fungal pathogens [89, 90], suggesting CPPs can play a great role in drug delivery for different purposes.

CPP-assisted protein delivery has shown therapeutic effects towards diseases such as cancer and strokes. Tat and penetratin successfully delivered elastin-like

polypeptides fused to a cyclin-dependent kinase inhibitor p21 that could inhibit proliferation of cancer cells [91]. Tat was also used to deliver a cellular antigen of $CD8^+$ T cells, (Tp2), to stimulate $CD8^+$ T cells. Other proteins delivered by CPPs include postsynaptic density protein PSD-95 [92] and Bcl-x_L [93] and could also prevent tissue damage caused by cancer cells *in vivo*. Bigger molecules such as antibodies that are difficult to deliver intracellularly can also be translocated by CPPs. CPPs have successfully been used to deliver anti-mouse immunoglobulin (IgG) [94] and anti-p21 antibody for sensitizing cancer cells [95].

2.3.2. Nucleic acid cargo delivery

CPPs have been used to deliver nucleic acids for gene regulation related to diseases including cancer. Peptide-nucleic acid complexes, or polyplexes, allow easy conjugation and rational design to improve delivery efficacy and cellular targeting. Non-covalent conjugation of siRNA to MPG, a chimeric CPP with a nuclear-localization sequence (NLS), allowed intracellular delivery into mammalian cells and *in vivo* gene regulation [96]. Palm-Apergi *et al.* showed that MAP, a model amphipathic CPP, can transport DNA or plasmid inside bacterial ghosts, empty cell envelopes of Gram-negative bacteria, into cancer cells without further lysis or ghost reloading [97]. When siRNA is encapsulated in liposomes, the poly-arginine CPP R_8 enhances the intracellular delivery of the nucleic acid and maintains the biological functions [98]. Tat was also studied to deliver the gene for GFP into HeLa cells with a high transfection efficiency and biological activity [99]. The easy conjugation and high translocation efficacy allows CPPs to be a promising tool for gene editing and gene therapy [100].

2.3.3. Small molecule delivery

CPPs have also been studied for delivering small molecules into cells via chemical conjugation of the CPPs to the small molecules. The arginine-rich CPP R_9F_2 successfully delivered phosphorodiamidate morpholino oligomers with a high internalization efficacy and *in vivo* gene regulation function in cultures of primary murine leukocytes [101]. Cancer cells resistance to methotrexate (MTX) could be inhibited by conjugating MTX to YTA2 and YTA4 CPPs [102]. Longhu *et al.* used Tat to deliver 2′,5′-oligoadenylate tetramer (2-5A) to enable *in vivo* activation of RNase L, which provided a new method to destroy HIV RNA [103]. As more small molecule drugs are approved for treating cancer, CPPs could improve the therapeutic effects by increasing the specificity and efficacy.

2.4. Limitations of CPPs in drug delivery

Although CPPs are promising tools for drug delivery, they do have limitations that must be considered. For CPPs that enter the cells via endocytosis, endosomal escape is necessary for intracellular delivery. However, the exact mechanisms of endosomes escape are still unknown[59, 104]. After the release of the CPPs into the cytosol, the target loctation of the peptides is often non-specific and how the cellular targeting can be controlled is still not fully understood. Although the nuclear localization of CPPs like Pep-1 and MPG can be explained by the incorporation of an NLS sequence, a general explanation for other CPPs is still under debate.

The cytotoxicity of CPPs could be a potential safety issue for applying CPPs to *in vivo* cargo delivery. The potential toxicity of cationic peptides from disrupting the cell membranes and affecting other cellular organelles would directly affect the

viability of host cells. Even though CPPs can be used to kill cancer or bacterial cells, the specificity of the peptides needs to be addressed to reduce nonspecific cargo delivery into normal cells.

The stability of CPPs is another major issue that needs to be considered while studying CPPs for cargo delivery. As the surface charges are very important for the initial membrane association, the pH and ionic strength of the buffer hugely impacts translocation efficacy. Secreted proteases from the host cells can degrade the peptides before internalization happens, significantly reducing the efficacy of the peptides [105]. After internalization, the pH/salt concentration shift and intracellular proteases will also significantly affect the integrity of the peptides [106-108]. In addition, the immunogenicity of CPPs has not been fully studied [1, 109], so there is not clear understanding whether the immune system will rapidly eliminate peptides before internalization happens.

2.5. Opportunities for studying CPPs in fungal pathogens

Despite the limitations in applying CPPs in mammalian cells, the advantages of these short peptides can still be widely applied to fungal cells. Due to the limited work done previously in fungal cells, I explored the application of CPPs in treating fungal infections or delivering antifungal agents into pathogens to enhance the therapeutics. Studying translocation mechanisms from both biological and molecular perspectives will benefit the understanding of structure-function relationship of CPPs. My engineering work of rational CPPs design applies the knowledge of structure-function relationships and enables better rational design of CPPs for improved

translocation efficacy, as well as specific cell targeting. This work has been done in my thesis and will be fully discussed in the following chapters.

2.6. Reference

1. Langel, Ü., *Cell-Penetrating Peptides*, in *Methods and Protocols*, Ü. Langel, Editor. 2011, Humana Press. p. 1-586.
2. Koren, E. and V.P. Torchilin, *Cell-penetrating peptides: breaking through to the other side.* Trends in Molecular Medicine, 2012. **18**(7): p. 385-393.
3. Copolovici, D.M., et al., *Cell-penetrating peptides: design, synthesis, and applications.* ACS Nano, 2014. **8**.
4. Moutal, A., et al., *Differential neuroprotective potential of CRMP2 peptide aptamers conjugated to cationic, hydrophobic, and amphipathic cell penetrating peptides.* Frontiers in Cellular Neuroscience, 2014. **8**: p. 471.
5. Liu, X.Y., et al., *Identification of a functionally important sequence in the cytoplasmic tail of integrin beta(3) by using cell-permeable peptide analogs.* Proceedings of the National Academy of Sciences of the United States of America, 1996. **93**(21): p. 11819-11824.
6. Derossi, D., et al., *Cell internalization of the third helix of the antennapedia homeodomain is receptor-independent.* Journal of Biological Chemistry, 1996. **271**(30): p. 18188-18193.
7. Jha, D., et al., *CyLoP-1: a novel cysteine-rich cell-penetrating peptide for cytosolic delivery of cargoes.* Bioconjug Chem, 2011. **22**(3): p. 319-28.
8. Feng, S. and E.C. Holland, *Hiv-1 Tat Trans-Activation Requires the Loop Sequence within Tar.* Nature, 1988. **334**(6178): p. 165-167.
9. Pooga, M., et al., *Cell penetration by transportan.* Faseb Journal, 1998. **12**(1): p. 67-77.
10. El-Andaloussi, S., et al., *TP10, a delivery vector for decoy oligonucleotides targeting the Myc protein.* J Control Release, 2005. **110**(1): p. 189-201.
11. Rousselle, C., et al., *New advances in the transport of doxorubicin through the blood-brain barrier by a peptide vector-mediated strategy.* Molecular Pharmacology, 2000. **57**(4): p. 679-686.
12. Nelson, M.H., et al., *Arginine-rich peptide conjugation to morpholino oligomers: effects on antisense activity and specificity.* Bioconjug Chem, 2005. **16**(4): p. 959-66.
13. Herce, H.D., et al., *Arginine-Rich Peptides Destabilize the Plasma Membrane, Consistent with a Pore Formation Translocation Mechanism of Cell-Penetrating Peptides.* Biophysical Journal, 2009. **97**(7): p. 1917-1925.
14. Morris, M.C., et al., *A new peptide vector for efficient delivery of oligonucleotides into mammalian cells.* Nucleic Acids Research, 1997. **25**(14): p. 2730-2736.
15. Deshayes, S., et al., *Insight into the mechanism of internalization of the cell-penetrating carrier peptide Pep-1 through conformational analysis.* Biochemistry, 2004. **43**(6): p. 1449-1457.
16. Mano, M., et al., *Cellular uptake of S413-PV peptide occurs upon conformational changes induced by peptide-membrane interactions.* Biochim Biophys Acta, 2006. **1758**(3): p. 336-46.

17. Lindgren, M., et al., *Overcoming methotrexate resistance in breast cancer tumour cells by the use of a new cell-penetrating peptide.* Biochem Pharmacol, 2006. **71**(4): p. 416-25.
18. Holm, T., et al., *Uptake of cell-penetrating peptides in yeasts.* Febs Letters, 2005. **579**(23): p. 5217-5222.
19. Wyman, T.B., et al., *Design, synthesis, and characterization of a cationic peptide that binds to nucleic acids and permeabilizes bilayers.* Biochemistry, 1997. **36**(10): p. 3008-3017.
20. Elmquist, A., et al., *VE-cadherin-derived cell-penetrating peptide, pVEC, with carrier functions.* Experimental Cell Research, 2001. **269**(2): p. 237-244.
21. Cummings, J.E. and T.K. Vanderlick, *Kinetics of Cryptdin-4 Translocation Coupled with Peptide-Induced Vesicle Leakage.* Biochemistry, 2007. **46**(42): p. 11882-11891.
22. Matsuzaki, K., *Why and how are peptide-lipid interactions utilized for self-defense? Magainins and tachyplesins as archetypes.* Biochim Biophys Acta, 1999. **1462**(1-2): p. 1-10.
23. Moore, A.J., et al., *Antimicrobial activity of cecropins.* J Antimicrob Chemother, 1996. **37**(6): p. 1077-89.
24. Lopez-Garcia, B., E. Perez-Paya, and J.F. Marcos, *Identification of novel hexapeptides bioactive against phytopathogenic fungi through screening of a synthetic peptide combinatorial library.* Applied and Environmental Microbiology, 2002. **68**(5): p. 2453-2460.
25. Pouny, Y., et al., *Interaction of antimicrobial dermaseptin and its fluorescently labeled analogues with phospholipid membranes.* Biochemistry, 1992. **31**(49): p. 12416-23.
26. Oppenheim, F.G., et al., *Histatins, a novel family of histidine-rich proteins in human parotid secretion. Isolation, characterization, primary structure, and fungistatic effects on Candida albicans.* J Biol Chem, 1988. **263**(16): p. 7472-7.
27. Cho, J.H., B.H. Sung, and S.C. Kim, *Buforins: Histone H2A-derived antimicrobial peptides from toad stomach.* Biochimica et Biophysica Acta (BBA) - Biomembranes, 2009. **1788**(8): p. 1564-1569.
28. Schmidt, M.C., et al., *Translocation of human calcitonin in respiratory nasal epithelium is associated with self-assembly in lipid membrane.* Biochemistry, 1998. **37**(47): p. 16582-16590.
29. Wender, P.A., et al., *The design, synthesis, and evaluation of molecules that enable or enhance cellular uptake: Peptoid molecular transporters.* Proceedings of the National Academy of Sciences of the United States of America, 2000. **97**(24): p. 13003-13008.
30. Chang, M., J.-C. Chou, and H.-J. Lee, *Cellular Internalization of Fluorescent Proteins via Arginine-rich Intracellular Delivery Peptide in Plant Cells.* Plant and Cell Physiology, 2005. **46**(3): p. 482-488.
31. Saar, K., et al., *Cell-penetrating peptides: A comparative membrane toxicity study.* Analytical Biochemistry, 2005. **345**(1): p. 55-65.
32. Lin, Y.Z., et al., *Inhibition of nuclear translocation of transcription factor NF-kappa B by a synthetic peptide containing a cell membrane-permeable*

motif and nuclear localization sequence. J Biol Chem, 1995. **270**(24): p. 14255-8.
33. Scheller, A., et al., *Evidence for an amphipathicity independent cellular uptake of amphipathic cell-penetrating peptides.* European Journal of Biochemistry, 2000. **267**(19): p. 6043-6049.
34. Jiao, C.Y., et al., *Translocation and endocytosis for cell-penetrating peptide internalization.* J Biol Chem, 2009. **284**(49): p. 33957-65.
35. Wada, S.-i., et al., *Cellular uptake of Aib-containing amphipathic helix peptide.* Bioorganic & Medicinal Chemistry Letters, 2011. **21**(19): p. 5688-5691.
36. Elmquist, A., M. Hansen, and U. Langel, *Structure-activity relationship study of the cell-penetrating peptide pVEC.* Biochim Biophys Acta, 2006. **1758**(6): p. 721-9.
37. Jha, D., et al., *CyLoP-1: A Novel Cysteine-Rich Cell-Penetrating Peptide for Cytosolic Delivery of Cargoes.* Bioconjugate Chemistry, 2011. **22**(3): p. 319-328.
38. Scheller, A., et al., *Structural requirements for cellular uptake of alpha-helical amphipathic peptides.* Journal of Peptide Science, 1999. **5**(4): p. 185-194.
39. Vaara, M. and M. Porro, *Group of peptides that act synergistically with hydrophobic antibiotics against gram-negative enteric bacteria.* Antimicrobial Agents and Chemotherapy, 1996. **40**(8): p. 1801-1805.
40. Tati, S., et al., *Histatin 5 Resistance of Candida glabrata Can Be Reversed by Insertion of Candida albicans Polyamine Transporter-Encoding Genes DUR3 and DUR31.* Plos One, 2013. **8**(4).
41. Andra, J., O. Berninghausen, and M. Leippe, *Cecropins, antibacterial peptides from insects and mammals, are potently fungicidal against Candida albicans.* Med Microbiol Immunol, 2001. **189**(3): p. 169-173.
42. Zelezetsky, I. and A. Tossi, *Alpha-helical antimicrobial peptides--using a sequence template to guide structure-activity relationship studies.* Biochim Biophys Acta, 2006. **1758**(9): p. 1436-49.
43. Helmerhorst, E.J., et al., *The cellular target of histatin 5 on Candida albicans is the energized mitochondrion.* Journal of Biological Chemistry, 1999. **274**(11): p. 7286-7291.
44. Nicolas, P., *Multifunctional host defense peptides: intracellular-targeting antimicrobial peptides.* Febs j, 2009. **276**(22): p. 6483-96.
45. Tréhin, R. and H.P. Merkle, *Chances and pitfalls of cell penetrating peptides for cellular drug delivery.* European Journal of Pharmaceutics and Biopharmaceutics, 2004. **58**(2): p. 209-223.
46. Derossi, D., et al., *The third helix of the Antennapedia homeodomain translocates through biological membranes.* J Biol Chem, 1994. **269**(14): p. 10444-50.
47. De Kruijff, B., et al., *Progress in Protein-Lipid Interactions*. 1985: Elsevier. Science Publishers, BV, Amsterdam. 89-142.
48. Gazit, E., et al., *Interaction of the Mammalian Antibacterial Peptide Cecropin P1 with Phospholipid Vesicles.* Biochemistry, 1995. **34**(36): p. 11479-11488.

49. Gazit, E., et al., *Mode of Action of the Antibacterial Cecropin B2: A Spectrofluorometric Study.* Biochemistry, 1994. **33**(35): p. 10681-10692.
50. Ghosh, J.K., et al., *Selective cytotoxicity of dermaseptin S3 toward intraerythrocytic Plasmodium falciparium and the underlying molecular basis.* Journal of Biological Chemistry, 1997. **272**(50): p. 31609-31616.
51. Gazit, E., et al., *Structure and Orientation of the Mammalian Antibacterial Peptide Cecropin P1 within Phospholipid Membranes.* Journal of Molecular Biology, 1996. **258**(5): p. 860-870.
52. Ding, B., et al., *Physiologically-Relevant Modes of Membrane Interactions by the Human Antimicrobial Peptide, LL-37, Revealed by SFG Experiments.* Scientific Reports, 2013. **3**: p. 1854.
53. Shin, M.C., et al., *Cell-penetrating peptides: achievements and challenges in application for cancer treatment.* Journal of biomedical materials research. Part A, 2014. **102**(2): p. 575-587.
54. Ciobanasu, C., J.P. Siebrasse, and U. Kubitscheck, *Cell-Penetrating HIV1 TAT Peptides Can Generate Pores in Model Membranes.* Biophysical Journal, 2010. **99**(1): p. 153-162.
55. Sun, D., et al., *Effect of arginine-rich cell penetrating peptides on membrane pore formation and life-times: a molecular simulation study.* Phys Chem Chem Phys, 2014. **16**(38): p. 20785-95.
56. Allen, T.D., et al., *The nuclear pore complex: mediator of translocation between nucleus and cytoplasm.* J Cell Sci, 2000. **113 (Pt 10)**: p. 1651-9.
57. Stewart, K.M., K.L. Horton, and S.O. Kelley, *Cell-penetrating peptides as delivery vehicles for biology and medicine.* Org Biomol Chem, 2008. **6**(13): p. 2242-55.
58. Kogure, K., et al., *Multifunctional envelope-type nano device (MEND) as a non-viral gene delivery system.* Adv Drug Deliv Rev, 2008. **60**(4-5): p. 559-71.
59. Erazo-Oliveras, A., et al., *Improving the Endosomal Escape of Cell-Penetrating Peptides and Their Cargos: Strategies and Challenges.* Pharmaceuticals (Basel, Switzerland), 2012. **5**(11): p. 10.3390/ph5111177.
60. Feng, J. and L. Tang, *The cell-type specificity and endosomal escape of cell-penetrating peptides.* Curr Pharm Des, 2015. **21**(10): p. 1351-6.
61. Madani, F., et al., *Modeling the endosomal escape of cell-penetrating peptides using a transmembrane pH gradient.* Biochimica et Biophysica Acta (BBA) - Biomembranes, 2013. **1828**(4): p. 1198-1204.
62. Yang, S.-T., et al., *Cell-Penetrating Peptide Induces Leaky Fusion of Liposomes Containing Late Endosome-Specific Anionic Lipid.* Biophysical Journal, 2010. **99**(8): p. 2525-2533.
63. Sorkin, A. and M.A. Puthenveedu, *Clathrin-Mediated Endocytosis,* in *Vesicle Trafficking in Cancer,* Y. Yarden and G. Tarcic, Editors. 2013, Springer New York: New York, NY. p. 1-31.
64. Lim, J.P. and P.A. Gleeson, *Macropinocytosis: an endocytic pathway for internalising large gulps.* Immunol Cell Biol, 2011. **89**(8): p. 836-43.

65. Jones, A.T., *Macropinocytosis: searching for an endocytic identity and role in the uptake of cell penetrating peptides.* J Cell Mol Med, 2007. **11**(4): p. 670-84.
66. Nakase, I., et al., *Methodological and cellular aspects that govern the internalization mechanisms of arginine-rich cell-penetrating peptides.* Adv Drug Deliv Rev, 2008. **60**(4-5): p. 598-607.
67. Patel, L.N., J.L. Zaro, and W.C. Shen, *Cell penetrating peptides: Intracellular pathways and pharmaceutical perspectives.* Pharmaceutical Research, 2007. **24**(11): p. 1977-1992.
68. Lins, L., et al., *Relationships between the orientation and the structural properties of peptides and their membrane interactions.* Biochimica et Biophysica Acta (BBA) - Biomembranes, 2008. **1778**(7–8): p. 1537-1544.
69. Su, Y., et al., *Reversible Sheet–Turn Conformational Change of a Cell-Penetrating Peptide in Lipid Bilayers Studied by Solid-State NMR.* Journal of molecular biology, 2008. **381**(5): p. 1133-1144.
70. Eiríksdóttir, E., et al., *Secondary structure of cell-penetrating peptides controls membrane interaction and insertion.* Biochimica et Biophysica Acta (BBA) - Biomembranes, 2010. **1798**(6): p. 1119-1128.
71. Ruben, S., et al., *Structural and functional characterization of human immunodeficiency virus tat protein.* Journal of Virology, 1989. **63**(1): p. 1-8.
72. Stetsenko, D.A. and M.J. Gait, *Efficient conjugation of peptides to oligonucleotides by "native ligation".* Journal of Organic Chemistry, 2000. **65**(16): p. 4900-4908.
73. Fisher, L., et al., *Cellular delivery of a double-stranded oligonucleotide NFkappaB decoy by hybridization to complementary PNA linked to a cell-penetrating peptide.* Gene Ther, 2004. **11**(16): p. 1264-72.
74. Zielinski, J., et al., *In vivo identification of ribonucleoprotein-RNA interactions.* Proc Natl Acad Sci U S A, 2006. **103**(5): p. 1557-62.
75. Liu, Y., J. Yan, and M.R. Prausnitz, *Can ultrasound enable efficient intracellular uptake of molecules? A retrospective literature review and analysis.* Ultrasound Med Biol, 2012. **38**(5): p. 876-888.
76. Muratovska, A. and M.R. Eccles, *Conjugate for efficient delivery of short interfering RNA (siRNA) into mammalian cells.* Febs Letters, 2004. **558**(1-3): p. 63-68.
77. Chiu, Y.L., et al., *Visualizing a correlation between siRNA localization, cellular uptake, and RNAi in living cells.* Chemistry & Biology, 2004. **11**(8): p. 1165-1175.
78. Wadia, J.S., R.V. Stan, and S.F. Dowdy, *Transducible TAT-HA fusogenic peptide enhances escape of TAT-fusion proteins after lipid raft macropinocytosis.* Nature Medicine, 2004. **10**(3): p. 310-315.
79. Jain, M., et al., *Penetratin improves tumor retention of single-chain antibodies: A novel step toward optimization of radioimmunotherapy of solid tumors.* Cancer Research, 2005. **65**(17): p. 7840-7846.
80. Cao, L.M., et al., *Intracellular localization and sustained prodrug cell killing activity of TAT-HSVTK fusion protein in hepatocelullar carcinoma cells.* Molecules and Cells, 2006. **21**(1): p. 104-111.

81. Theisen, D.M., et al., *Targeting of HIV-1 Tat traffic and function by transduction-competent single chain antibodies.* Vaccine, 2006. **24**(16): p. 3127-3136.
82. Shokolenko, I.N., et al., *TAT-mediated protein transduction and targeted delivery of fusion proteins into mitochondria of breast cancer cells.* DNA Repair, 2005. **4**(4): p. 511-518.
83. Olson, E.S., et al., *Activatable cell penetrating peptides linked to nanoparticles as dual probes for in vivo fluorescence and MR imaging of proteases.* Proceedings of the National Academy of Sciences of the United States of America, 2010. **107**(9): p. 4311-4316.
84. Lim, K.J., et al., *A Cancer Specific Cell-Penetrating Peptide, BR2, for the Efficient Delivery of an scFv into Cancer Cells.* PLOS ONE, 2013. **8**(6): p. e66084.
85. Masuda, R., K. Yamamoto, and T. Koide, *Cellular Uptake of IgG Using Collagen-Like Cell-Penetrating Peptides.* Biol Pharm Bull, 2016. **39**(1): p. 130-4.
86. Schwarze, S.R., et al., *In vivo protein transduction: delivery of a biologically active protein into the mouse.* Science, 1999. **285**(5433): p. 1569-72.
87. Kameyama, S., et al., *Effects of cell-permeating peptide binding on the distribution of 125I-labeled Fab fragment in rats.* Bioconjug Chem, 2006. **17**(3): p. 597-602.
88. Rajarao, G.K., N. Nekhotiaeva, and L. Good, *Peptide-mediated delivery of green fluorescent protein into yeasts and bacteria.* Fems Microbiology Letters, 2002. **215**(2): p. 267-272.
89. Gong Z., W., MT., Karley AN., Karlsson AJ., *Effect of a flexible linker on recombinant expression of cell-penetrating peptide fusion proteins and their translocation into fungal cells.* Mol Biotechnol, 2016.
90. Parenteau, J., et al., *Free uptake of cell-penetrating peptides by fission yeast.* Febs Letters, 2005. **579**(21): p. 4873-4878.
91. Massodi, I., G.L. Bidwell Iii, and D. Raucher, *Evaluation of cell penetrating peptides fused to elastin-like polypeptide for drug delivery.* Journal of Controlled Release, 2005. **108**(2–3): p. 396-408.
92. Aarts, M., et al., *Treatment of ischemic brain damage by perturbing NMDA receptor- PSD-95 protein interactions.* Science, 2002. **298**(5594): p. 846-50.
93. Nakachi, N., et al., *Transduction of Anti–Cell Death Protein FNK Suppresses Graft Degeneration After Autologous Cylindrical Osteochondral Transplantation.* Journal of Histochemistry and Cytochemistry, 2009. **57**(3): p. 197-206.
94. Cornelissen, B., et al., *Cellular penetration and nuclear importation properties of 111In-labeled and 123I-labeled HIV-1 tat peptide immunoconjugates in BT-474 human breast cancer cells.* Nucl Med Biol, 2007. **34**(1): p. 37-46.
95. Kersemans, V. and B. Cornelissen, *Targeting the Tumour: Cell Penetrating Peptides for Molecular Imaging and Radiotherapy.* Pharmaceuticals, 2010. **3**(3): p. 600-620.

96. Simeoni, F., et al., *Insight into the mechanism of the peptide-based gene delivery system MPG: implications for delivery of siRNA into mammalian cells.* Nucleic Acids Research, 2003. **31**(11): p. 2717-2724.
97. Palm-Apergi, C. and M. Hallbrink, *A new rapid cell-penetrating peptide based strategy to produce bacterial ghosts for plasmid delivery.* J Control Release, 2008. **132**(1): p. 49-54.
98. Wang, W., et al., *Cell penetrating peptides enhance intracellular translocation and function of siRNA encapsulated in Pegylated liposomes.* Yao Xue Xue Bao, 2006. **41**(2): p. 142-8.
99. Jeong, C., et al., *A branched TAT cell-penetrating peptide as a novel delivery carrier for the efficient gene transfection.* Biomaterials Research, 2016. **20**(1): p. 28.
100. Reilly, M.J., J.D. Larsen, and M.O. Sullivan, *Histone H3 tail peptides and poly(ethylenimine) have synergistic effects for gene delivery.* Mol Pharm, 2012. **9**(5): p. 1031-40.
101. Marshall, N.B., et al., *Arginine-rich cell-penetrating peptides facilitate delivery of antisense oligomers into murine leukocytes and alter pre-mRNA splicing.* Journal of Immunological Methods, 2007. **325**(1–2): p. 114-126.
102. Lindgren, M., et al., *Overcoming methotrexate resistance in breast cancer tumour cells by the use of a new cell-penetrating peptide.* Biochemical Pharmacology, 2006. **71**(4): p. 416-425.
103. Zhou, L., et al., *Delivery of 2-5A cargo into living cells using the Tat cell penetrating peptide: 2-5A-tat.* Bioorganic & Medicinal Chemistry, 2006. **14**(23): p. 7862-7874.
104. Lönn, P., et al., *Enhancing Endosomal Escape for Intracellular Delivery of Macromolecular Biologic Therapeutics.* Scientific Reports, 2016. **6**: p. 32301.
105. Bochenska, O., et al., *The action of ten secreted aspartic proteases of pathogenic yeast Candida albicans on major human salivary antimicrobial peptide, histatin 5.* Acta Biochim Pol, 2016. **63**(3): p. 403-10.
106. Palm, C., et al., *Peptide degradation is a critical determinant for cell-penetrating peptide uptake.* Biochimica et Biophysica Acta (BBA) - Biomembranes, 2007. **1768**(7): p. 1769-1776.
107. Holm, T., *Cell-penetrating peptides: Uptake, stability and biological activity*. 2011, Department of Neurochemistry, Stockholm University.
108. Ruttekolk, I.R., et al., *Measurements of the intracellular stability of CPPs.* Cell-Penetrating Peptides: Methods and Protocols, 2011: p. 69-80.
109. Lim, S., et al., *Identification of a Novel Cell-Penetrating Peptide from Human Phosphatidate Phosphatase LPIN3.* Molecules and Cells, 2012. **34**(6): p. 577-582.

Chapter 3. Translocation of CPPs into *Candida* fungal pathogens[1]

3.1. Introduction

CPPs have shown great potential in drug delivery in mammalian cells and have been extensively studied to understand the translocation mechanisms. However, the structural and functional diversity of CPPs complicates studies of their interactions with cells. Previous mechanistic research on CPP translocation suggests some peptides penetrate cells via an energy-dependent endocytosis process. These CPPs include MAP (synthetic, highly amphiphilic model peptide [1]), TP-10 (fragment of transportan [2]), hCT (derivative of calcitonin [3]), SynB (derivative of the antimicrobial peptide protegrin 1 [4]), and PAF26 (hexapeptide with antimicrobial activity [5]). In contrast, other CPPs may enter cells via macropinocytosis [6], including pVEC (derivative of murine vascular endothelium cadherin [7]) and penetratin (fragment of antennaedia homeodomain [8]). The mechanism of translocation may also include transient pore formation [9], which is suspected for MPG (derivative of two viruses [10]) and Pep-1 (synthetic peptide [11]). MPG and Pep-1 also contain nuclear localization sequences, which promote the translocation efficacy and solubility of the peptides [9]. For other CPPs, such as $(KFF)_3K$

[1] This chapter has been accepted in the Protein Science Journal and appears in this thesis with the journal's permission:
Gong Z, Karlsson AJ
Translocation of cell-penetrating peptides into *Candida* fungal pathogens
DOI: 10.1002/pro.3203

(synthetic peptide [12]), additional work is required to elucidate the mechanism of translocation. These examples highlight the diversity of CPPs as delivery vehicles and the challenges in understanding their interaction with cells.

Most studies on the translocation mechanisms of CPPs have focused on translocation in mammalian cells, and studies of the interactions of CPPs with fungal cells, including *Candida* cells, are very limited [13-18]. To expand the application of CPPs to delivering molecules to *Candida* species, an improved understanding of the interaction of CPPs with *Candida* cells is required. One key structural difference between mammalian cells and fungal cells is the presence of a cell wall in fungal cells. The cell wall is composed of chitin, glucans, mannans, and glycoproteins and provides an additional barrier for CPP transport into fungal cells compared to mammalian cells [19]. Another key difference is that fungal cells have vacuoles, which are involved in a number of biological processes in fungal cells, including endocytosis, pH and salt balance maintenance, and phosphate degradation [20]. The effect of these structures on CPP translocation and trafficking has not been described previously, and an understanding of their role will facilitate the use and design of CPPs for delivering molecular cargo to fungal cells.

To improve the understanding of how CPPs translocate into fungal cells, we studied the translocation of known CPPs into two *Candida* pathogens, *C. albicans* and *C. glabrata*. We evaluated the translocation and toxicity of the CPPs and

Table 3.1 CPPs tested in this chapter

Peptide	Sequence	MW (Da)	Net Charge[a]
pVEC	LLIILRRRIRKQAHAHSK	2209.7	+8
$(KFF)_3K$	KFFKFFKFFK	1413.8	+4
Penetratin	RQIKIWFQNRRMKWKK	2246.8	+7
MAP	KLALKLALKALKAALKLA	1876.0	+5
Pep-1	KETWWETWWTEWSQPKKKRKV	2848.3	+2
hCT	LGTYTQDFNKTFPQTAIGVGAP	2326.6	0
SynB	RGGRLSYSRRRFSTSTGR	2100.3	+6
MPG	GALFLGFLGAAGSTMGAWSQPKKKRKV	2807.4	+5
PAF26	RKKWFW	950.2	+3
TP-10	AGYLLGKINLKALAALAKKIL	2182.8	+4
Cecropin B	KWKVFKKIEKMGRNIRNGIVKAGPAIAVLGEAKAL	3835.7	+9

[a] **Includes only charges due to amino acid side chains (pH 7) and not N-terminal FAM (-3)**

explored their mechanisms of translocation. Some peptides previously shown to enter mammalian cells were also translocated into *Candida* species, while others exhibited little to no translocation. Our analysis of subcellular localization of CPPs provides insight into intracellular trafficking of the peptides, as well as translocation mechanisms. Further experiments to explore the translocation mechanism indicate the translocation of some CPPs in fungal cells may differ from the mechanisms proposed for mammalian cells. Our data suggest translocation of CPPs into fungal cells often correlates with toxicity toward the cells, but some peptides are taken up by *Candida* cells with little effect on viability.

3.2. Materials and Methods

3.2.1. Peptides

The peptides listed in **Table 3.1** were commercially synthesized at >95% purity with an N-terminal 5-carboxyfluorescein (FAM) (Genscript, Piscataway, NJ). The lyophilized peptides were reconstituted in sterile, ultrapure H_2O and diluted to a final concentration of 10 mM Na_2HPO_4 buffer.

3.2.2. Strains and culture conditions

C. albicans strain SC5314 and *C. glabrata* strain ATCC2001 were purchased from American Type Culture Collection (ATCC, Manassas, VA). *Candida* cells were inoculated from yeast-peptone-dextrose (YPD) agar plates (1% w/v yeast extract), 2% w/v peptone, 2% w/v glucose, and 2% w/v agar) into 5 mL of liquid YPD medium (1% w/v yeast extract, 2% w/v peptone, and 2% w/v glucose) and grown overnight at 30 °C while shaking at 230 rpm. The cells in the overnight culture were subcultured into 5 mL of fresh YPD medium at OD_{600}=0.1 (equivalent to ~2×10^6 CFU/mL). The culture was then grown at 30 °C to OD_{600}=0.5 (equivalent to ~1×10^7 CFU/mL) while shaking. Cells were harvested by centrifugation at 4,000 × g for 10 min and washed twice with 10 mM Na_2HPO_4 buffer before use in downstream assays.

3.2.3. Fluorescence imaging

For each peptide, 100 µL of peptide solution (2–100 µM), depending on the experiment) was prepared in 10 mM Na_2HPO_4 buffer, mixed with 100 µL of cell suspension containing 5×10^5 cells in 10 mM Na_2HPO_4 and incubated at 30 °C for 60 min. Cells were collected by centrifugation at 5,000 ×g for 10 min at 4 °C and washed once with 10 mM Na_2HPO_4. The cell pellet was then incubated with 200 µL

of 0.025% trypsin (Invitrogen, Waltham, MA) at 37 °C for 10 min to remove surface-bound peptide [21]. Cells were collected and washed again with 10 mM Na_2HPO_4. For vacuole staining, 1 µM of CellTracker Blue CMAC (Invitrogen Molecular Probes, Waltham, MA) was added into the washed cell suspension and incubated at ambient temperature for 10 min. To prepare the cells for imaging, cells were collected and resuspended in 5 µL of 10 mM Na_2HPO_4. The suspension was transferred to a glass slide and imaged using an Olympus IX83 fluorescence microscopy system (Olympus, Center Valley, PA). Propidium iodide (1 $mg \cdot ml^{-1}$; Invitrogen, Waltham, MA) was added immediately before imaging as needed to examine the membrane integrity. Differential interference contrast (DIC), GFP fluorescence, vacuolar stain fluorescence, and/or PI fluorescence images were taken using the automatic process manager of the CellSens Dimension software (Olympus), and images were analyzed using NIH ImageJ software [22].

3.2.4. Quantification of translocation

To prepare the *Candida* cells for quantification by flow cytometry, procedures analogous to those for microscopy were followed. Fresh cells were treated with dilutions of each peptide (1 µM–50 µM) and treated with trypsin after incubation. After washing the cells with 10 mM Na_2HPO_4, the cells were resuspended in 150 µL of 10 mM Na_2HPO_4. Cell suspensions were analyzed for FAM and PI fluorescence using a BD FACSCanto II flow cytometer (BD Biosciences, San Jose, CA). Only single cells were selected for analysis, and the analysis was preformed using FlowJo software (FLOWJO Inc., Ashland, OR).

3.2.5. Antifungal activity assay

In order to assess the antimicrobial activities of the peptides, a microdilution assay was performed. After subculturing cells and growing the culture to OD_{600}=0.5, a 5×10^5 cells/mL cell suspension was prepared in 10 mM Na_2HPO_4. Serial dilutions (20 µL) of the peptides were prepared at 0.2 µM–50 µM in 96-well plates. A control containing 50 µM of free FAM in 10 mM Na_2HPO_4 buffer was used as a control. The cell suspension (20 µL) was then added into each well, and the plate was incubated at 30 °C with vigorous shaking for 60 min. Treated cells were diluted 20-fold in 10 mM Na_2HPO_4 buffer, and 100 µL of diluted cell suspension was added into 100 µL fresh YPD medium in a new 96-well plate. Plates were incubated at 30 °C with vigorous shaking for 16 hours, and the OD_{600} of the wells was measured using a 96-well plate reader (BioTek, Winooski, VT). The percentage of killing was calculated from

$$\text{Killing}\,(\%) = (1\text{-}\frac{\text{OD}_{600,\text{peptide}}}{\text{OD}_{600,\text{control}}})\times 100 \quad (1)$$

Minimal inhibitory concentrations were determined as the minimum concentration resulting in a 50% reduction in cell viability (MIC50).

3.3. Results

3.3.1. Translocation of CPPs in *Candida* species

To study the interaction of CPPs with *Candida* species, we selected peptides representing a variety of structures and native origins to study CPP translocation into *Candida* cells (**Table 3.1**). All peptides were synthesized commercially with an N-terminal 5-carboxyfluorescein label (FAM), which served as the cargo for the CPP and as the reporter to detect translocation. Our set of peptides includes peptides

shown previously to translocate into mammalian cells (all CPPs) or microbial cells, including bacteria and fungi (pVEC, $(KFF)_3K$, penetratin, MAP, PAF26, and TP-10) [13-18]. The CPPs pVEC, $(KFF)_3K$, penetratin, and TP-10 were shown to enter *C. albicans* previously [14, 17]. Some peptides are thought to be transported by energy-dependent endocytic mechanisms (MAP, hCT, TP-10, SynB, PAF26) or macropinocytosis (pVEC and penetratin), while others undergo pore formation (penetratin, MPG and Pep-1) or unknown mechanisms ($(KFF)_3K$) [1-9]. We also included cecropin B, a well-known antimicrobial peptide with antifungal activity, to compare its translocation with peptides previously identified as CPPs. *C. albicans* and *C. glabrata* were selected as target cells, because they are frequently isolated from patients with candidiasis [26].

To screen the CPPs for translocation into *Candida* species, we incubated *C. albicans* and *C. glabrata* cells with each of the CPPs. We identified the CPPs that could cross the barriers of these fungal cells using fluorescence microscopy to visualize the location of the fluorescein-labeled peptides (**Figure 3.1A** and **3.1B**). Cells were treated with trypsin prior to imaging to remove peptide associated with the cell surface [17, 21]. A high level of translocation efficacy was observed in both types of fungal cells for several peptides with a relatively high net charge ($\geq +4$), including penetratin, pVEC, MAP, SynB, $(KFF)_3K$, and MPG. PAF26 and Pep-1, which have a lower net charge ($< +4$), showed limited levels of translocation, while hCT (no net charge) could not be detected entering the *Candida* cells. The antimicrobial peptide cecropin B (+ 9) exhibited a high level of translocation, suggesting cecropin B could function as a CPP in addition to an antimicrobial peptide.

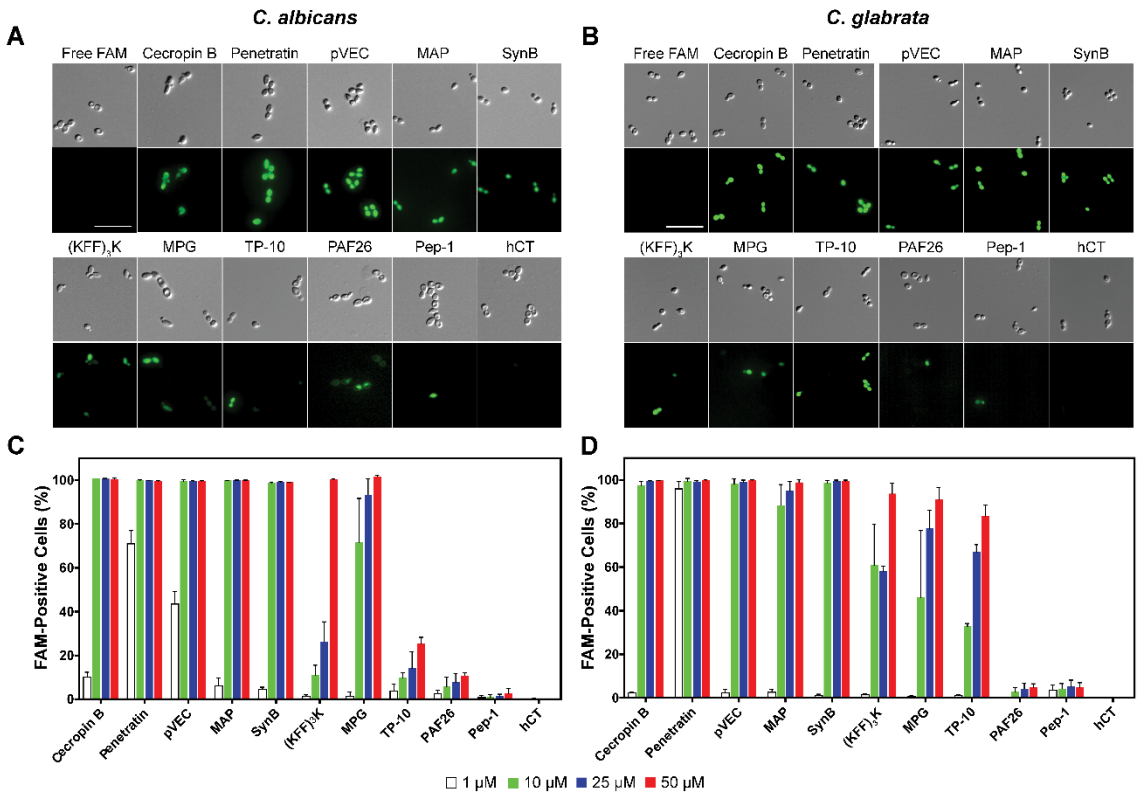

Figure 3.1. Translocation of FAM-labeled CPPs into *Candida* cells. DIC and FAM fluorescence images for translocation into (A) *C. albicans* and (B) *C. glabrata*. Flow cytometry data for translocation into (C) *C. albicans* and (D) *C. glabrata*. Cells were incubated for 1 h at 30 °C with 25 µM peptides for imaging or serial dilutions of peptides (1-50 µM) for flow cytometry. Surface-bound peptides were removed by trypsin prior to imaging or flow cytometry, and controls with free FAM were included. For (A) and (B), scale bar=10 µm. For (C) and (D), error bars represent the standard error of the mean for three separate experiments (*N*=3).

We quantified translocation and the effect of peptide concentration on translocation in *C. albicans* and *C. glabrata* using flow cytometry. Single cells were identified, and the percentage of these cells positive for FAM fluorescence was determined for each species (**Figure 3.1C** and **3.1D**). We detected a dose-dependent fluorescence signal for each of the peptides that showed substantial translocation in the fluorescence microcopy assay. The flow cytometry data confirmed the limited translocation for PAF26 and Pep-1 and the lack of translocation for hCT that we observed by fluorescence microscopy.

For most of the peptides, the behavior in *C. albicans* and *C. glabrata* was very similar. The exception to this was TP-10, which showed significantly enhanced translocation in *C. glabrata* compared to *C. albicans*. Although these two species are closely related, they do have unique characteristics that could affect the interaction of the cells with CPPs. For example, they express different membrane-anchored proteases and other proteins [27, 28], which may alter degradation of CPPs and their interaction with the cell membrane.

3.3.2. Subcellular localization of peptides

To gain insight into the intracellular trafficking of the CPPs, we examined our microscopy images (**Figure 3.1**). In some images, peptides appeared to localize in the vacuole (e.g., see FAM image for PAF26 in **Figure 3.1A**). In other images, the vacuoles that typically are easily visible were no longer present (e.g., see DIC images for MAP and penetratin in **Figure 3.1B**). Yeast vacuoles are very important for maintaining homeostasis, and they are highly involved in transmembrane transport [20]. To better understand the relationship between CPP trafficking, vacuoles, and vacuole loss, we used CellTracker Blue, a yeast vacuole stain, to track the vacuoles during incubation of *C. albicans* cells with the peptide pVEC (**Figure 3.2A**). When cells were incubated with a low concentration of pVEC, they retained their vacuoles and exhibited colocalization of a low level of FAM fluorescence with vacuole stain fluorescence. At higher concentrations of peptide, we observed total loss of vacuole stain fluorescence, an enhancement of FAM fluorescence intensity, and a shift to c ytosolic fluorescence. For cells treated with 10 μM of pVEC, the differential FAM fluorescence was most apparent. Cells retaining their vacuoles showed a brighter

vacuole stain signal but a weaker FAM fluorescence, whereas cells that lost vacuoles had a stronger cytosolic FAM signal and no vacuolar fluorescence. The differential fluorescence intensity arises from the sensitivity of the 5-FAM fluorescein derivative we used. 5-FAM is very sensitive to pH and exhibits higher fluorescence intensity at pH 7.5 and lower intensity at pH 6.6 [29]. Because the cytosolic pH (~7.4) is relatively higher than the one inside vacuoles (~6.2) [30], the fluorescence intensity of the peptides is lower in vacuoles than in the cytosol [31]. Vacuole loss can also be

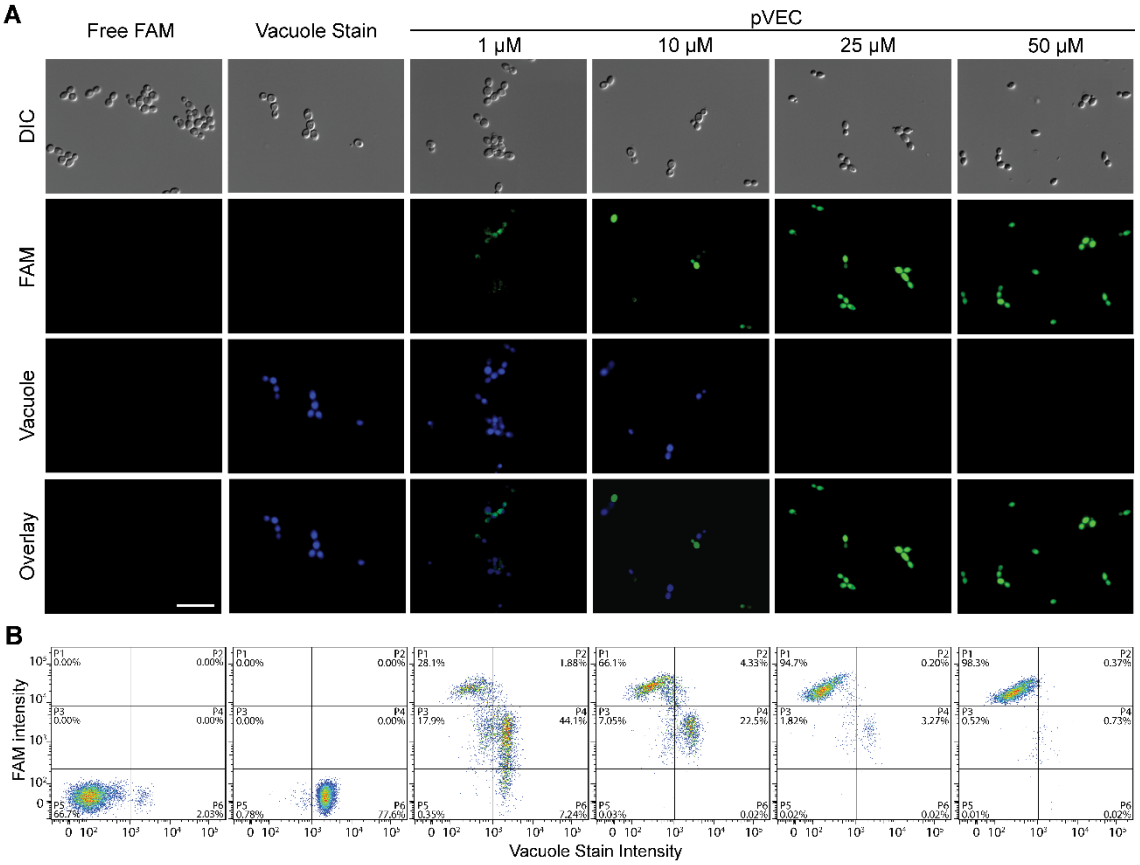

Figure 3.2. Intracellular distribution of pVEC in *C. albicans* at different peptide concentrations. (A) DIC and fluorescence microscopy images showing location of FAM-labeled pVEC and location of vacuoles in cells. (B) Flow cytometry data illustrating shift of FAM and vacuolar fluorescence. Cells were incubated with serial dilutions of pVEC (1-50 μM) at 30 °C for 1 h and treated with trypsin to remove surface-bound peptide. CellTracker Blue vacuolar stain was added, and the samples were incubated at room temperature for 10 min prior to analysis. For (A), scale bar=10 μm.

identified by using flow cytometry to observe the FAM signal shift as the peptides move from the vacuoles to the cytosol at higher concentrations (**Figure 3.2B**). We quantified the cellular localization by gating two distinct populations in the flow cytometry data: one with a stronger FAM intensity but no vacuole stain fluorescence and the other with both vacuole stain fluorescence and lower intensity FAM fluorescence. These data show that vacuole loss is associated with high levels of translocation of pVEC.

Based on the results for pVEC, we used flow cytometry to evaluate the subcellular localization in *C. albicans* and *C. glabrata* for each of the peptides with significant translocation (**Figure 3.3**). Subcellular vacuole localization was observed for each of the CPPs, suggesting vacuoles are generally involved in the translocation mechanism of CPPs for fungal cells. However, the proportion of FAM-positive cells that exhibited vacuole localization was lower for some peptides (e.g., pVEC, penetratin) compared to other peptides (e.g., SynB, MPG, $(KFF)_3K$) (**Figure 3.4**), indicating differences in translocation mechanisms and/or trafficking amongst the peptides.

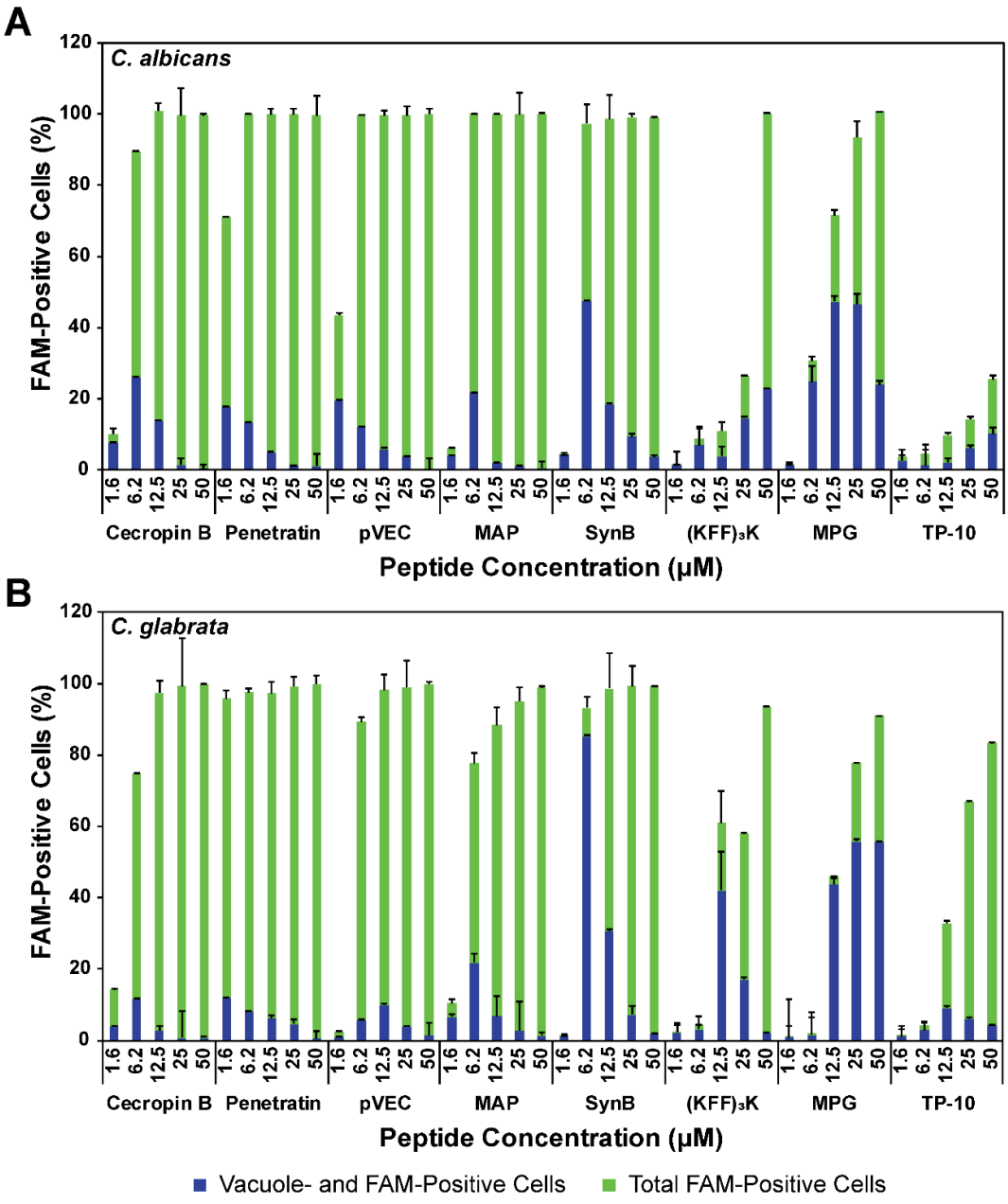

Figure 3.3. Quantification of cellular location of CPPs in (A) *C. albicans* and (B) *C. glabrata*. Cells were incubated with serial dilutions of peptide (1-50 μM) at 30 °C for 1 h, washed with trypsin, and incubated with CellTracker Blue vacuolar stain at room temperature for 10 min. Flow cytometry data were collected for FAM (peptide) fluorescence and vacuolar stain fluorescence. The percentage of cells with FAM fluorescence and with both FAM and vacuolar fluorescence were quantified. Error bars represent the standard error of the mean for three separate experiments (N=3).

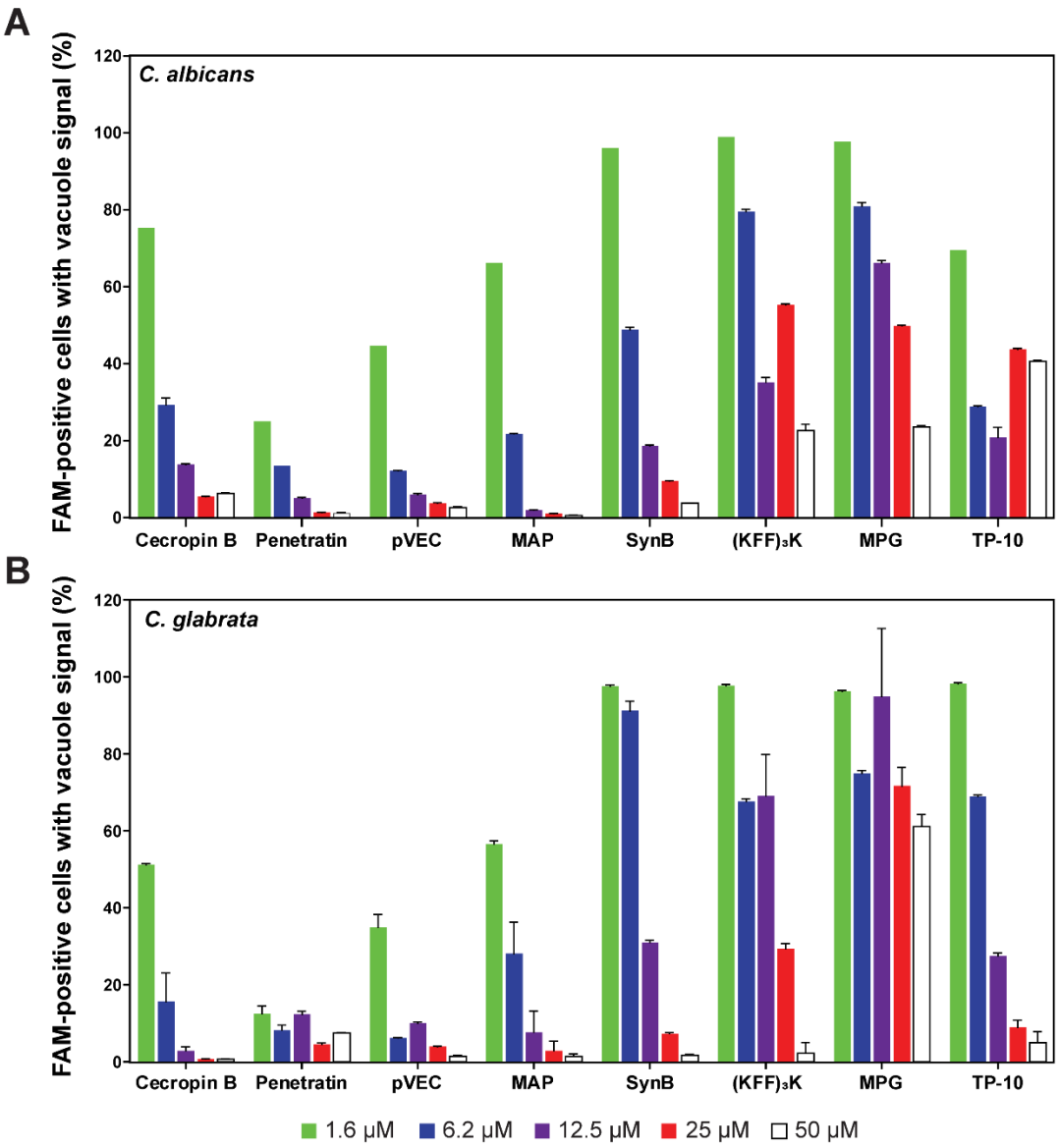

Figure 3.4 Percentage of (A) *C. albicans* and (B) *C. glabrata* cells containing peptide that exhibit fluorescence intensity consistent with vacuolar localization. Following collection of the data in Figure 3, the ratio of vacuole- and FAM-positive cells to the total number of FAM positive cells was calculated. Error bars represent the standard error of the mean for three separate experiments (N=3).

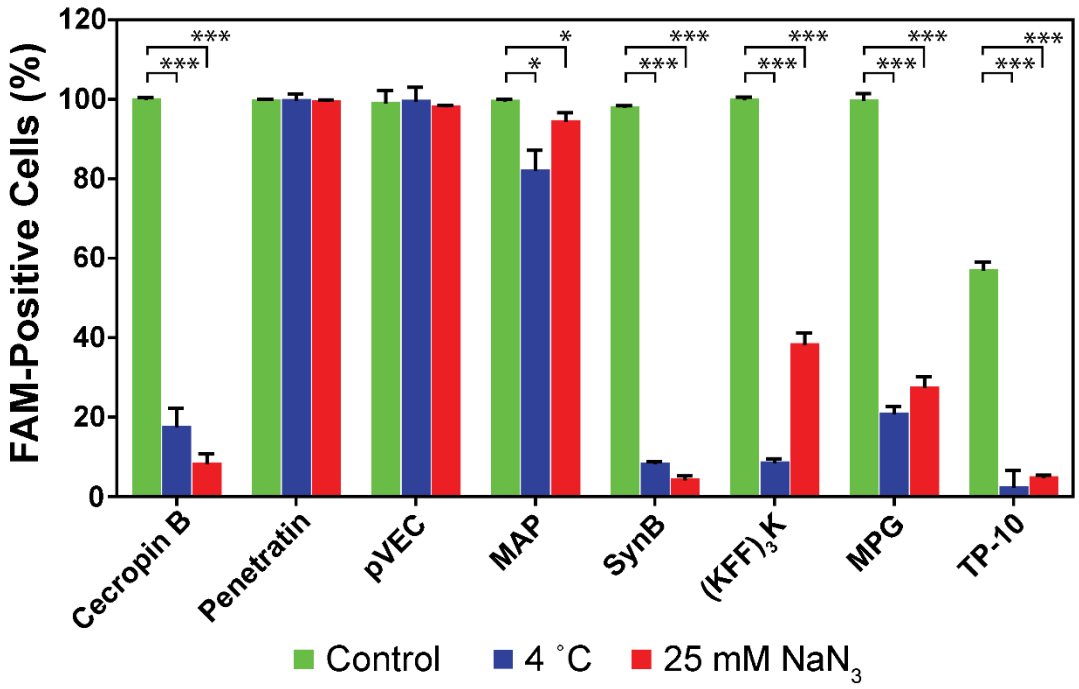

Figure 3.5 CPP translocation into *C. albicans* under conditions that inhibit energy-dependent endocytosis. Cells were incubated with peptides (10 µM) for 1 h. Control samples were incubated at 30 °C. Endocytosis was inhibited by adding 25 mM NaN3 or by changing the incubation temperature to 4 °C. The percentage of cells exhibiting FAM fluorescence was quantified by flow cytometry. Error bars represent the standard error of the mean for three separate experiments (N=3). Statistical significance was analyzed with a one-way ANOVA test (α= 0.05), and the number of asterisks indicates the level of significance (* for $p \leq 0.01$ and *** for $p \leq 0.0001$).

3.3.3. Mechanisms for translocation of CPPs into fungal cells

Our localization experiments revealed the important relationship between vacuoles and translocation. Previous work with yeast vacuoles suggested vacuoles are involved in endocytosis [20, 32], so we next studied endocytosis of the CPPs. To explore whether the mechanisms of translocation in fungal cells involve endotytosis, we first studied the translocation process in *C. albicans* under conditions that inhibit ATP synthesis. Most ATP-dependent processes, including endocytosis, are limited at 4 °C [33]. Sodium azide (NaN_3) also inhibits energy-dependent endocytosis by inhibiting the function of cytochrome-c-oxidase for ATP synthesis [34, 35]. We

observed a significant reduction in translocation for six of the eight peptides (cecropin B, MAP, SynB, MPG, $(KFF)_3K$, and TP-10) in the presence of 25 mM NaN_3 and at low temperature (**Figure 3.5**), suggesting these peptides utilize energy-dependent endocytosis as their translocation mechanisms. pVEC and penetratin were not highly affected by the addition of NaN_3 or the lower temperature, suggesting an energy-independent translocation process.

Membrane destabilization is also involved in the translocation mechanism for some CPPs [4, 5, 25]. To evaluate whether membrane destabilization plays a role in translocation of the peptides in our study, we used propidium iodide (PI) to identify pore formation in the membranes during CPP translocation into *C. albicans* and *C. glabrata*. Cells are normally impermeable to PI, but PI fluorescence can be detected in cells with destabilized membranes, which typically represents cells losing viability [36]. Using fluorescence microscopy, we observed that pVEC, penetratin, MAP, and cecropin B contributed to membrane permeabilization of *C. albicans* at a moderate concentration (10 μM) (**Figure 3.6A**). We confirmed these results by flow cytometry (**Figure 3.6B** and **3.6C**) and found almost all cells incubated with these peptides were both PI- and FAM-positive, indicating translocation of these peptides is correlated to cell permeabilization. In contrast, $(KFF)_3K$, SynB, and MPG showed FAM fluorescence with little to no PI fluorescence, suggesting these CPPs did not lead to general defects in membrane integrity at this concentration.

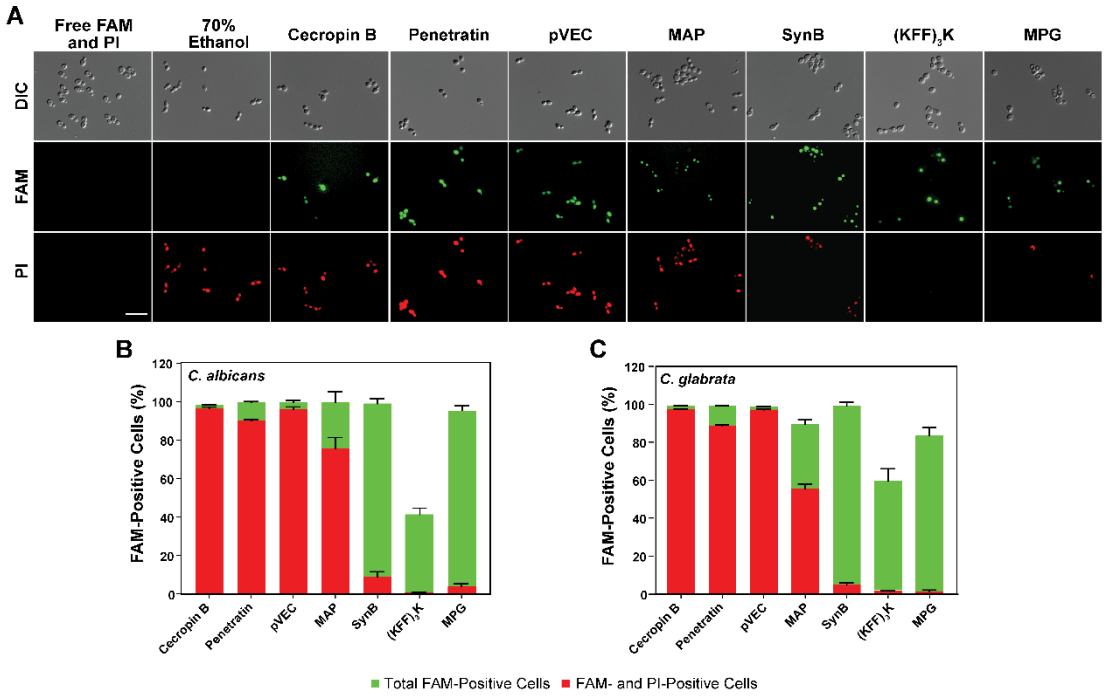

Figure 3.6 Effect of CPPs on integrity of cell membrane. (A) DIC and fluorescence microscopy images showing CPP translocation and PI uptake in *C. albicans*. (B) Flow cytometry data indicating the percentage of cells with CPP translocation (FAM fluorescence) and with PI uptake in *C. albicans*. (C) Flow cytometry data indicating the percentage of cells with CPP translocation and with PI uptake in *C. glabrata*. Following incubation with FAM-labeled CPPs (10 µM), cells were treated with trypsin and then incubated with PI for 1 min immediately prior to imaging or flow cytometry. For (A), scale bar=10 µm. For (B) and (C), error bars represent the standard error of the mean for three separate experiments (N=3).

3.3.4. Toxicity of CPPs towards *Candida* cells

Yeast vacuoles are necessary for cells to maintain homeostasis, so the loss of vacuoles due to CPPs may lead to toxicity toward fungal cells. To examine the

Table 3.2. Antimicrobial activities of peptides

	Minimum Inhibitory Concentration (MIC50, µM)[a]										
	Cecropin B	Penetratin	pVEC	MAP	SynB	$(KFF)_3K$	MPG	TP-10	PAF26	Pep-1	hCT
C. albicans	4	1	2	4	50	50	10	> 50	> 50	> 50	> 50
C. glabrata	25	2	4	8	25	50	50	32	> 50	> 50	> 50

[a] MIC50 values are defined as the minimum concentration of peptide required to reduce growth of cells by 50%. The highest concentration tested was 50 µM.

toxicity of CPPs toward *C. albicans* and *C. glabrata*, we incubated the cells with serial dilutions of the peptides. At high concentrations of peptide, we observed significant toxicity toward both types of *Candida* cells for each peptide that exhibited substantial translocation (**Figure 3.7)**, with minimum inhibitory concentrations (MIC50s) ranging from 1 µM to 50 µM (**Table 3.2**). Little to no antifungal activity could be detected for CPPs that exhibited very low levels of translocation (i.e., Pep-1, PAF26 and hCT in both species and TP-10 in *C. albicans*) (**Figure 3.7**), and MIC50s for these peptides were above 100 µM (**Table 3.2**). Incubation with free FAM did not lead to any viability loss of *Candida* cells compared to the cells incubated with only Na_2HPO_4 buffer (data not shown). Interestingly, the CPPs pVEC, penetratin, and MAP exhibited even stronger antifungal activity than the well-known antimicrobial peptide cecropin B. For many of the peptides the loss of viability could be due to the

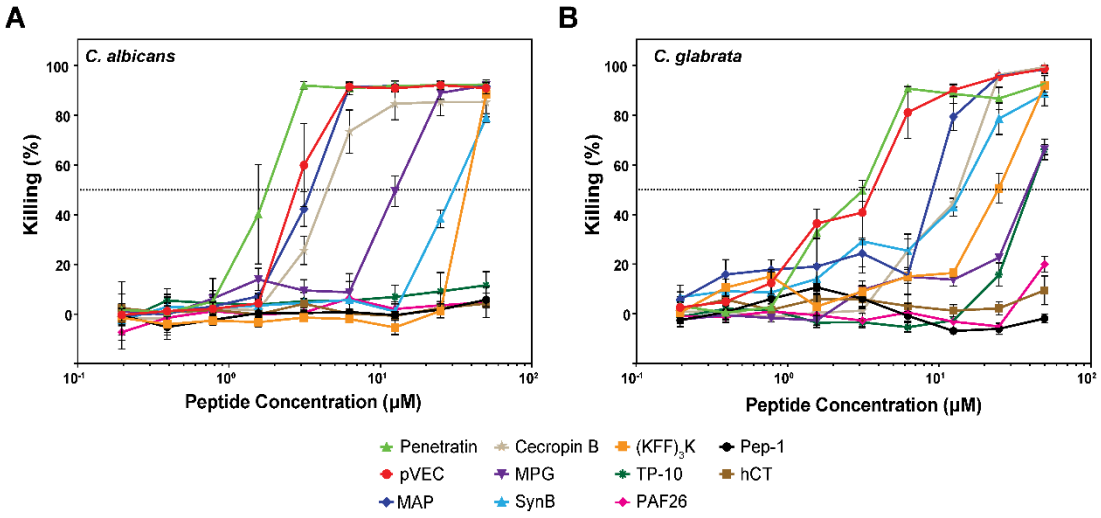

Figure 3.7 Toxicity of CPPs toward (A) *C. albicans* and (B) *C. glabrata*. Cells were incubated with serial dilutions of peptides (0.2-50 µM) for 1 h at 30 °C. Samples were diluted, mixed with YPD medium, and incubated at 30 °C for 16 h. Optical density (OD600) of the cultures was measured and converted to killing percentage. Error bars represent the standard error of the mean for three separate experiments (N=3). Dotted line represents 50% killing, which was used to determine the MIC50 (**Table 3.2**)

vacuole loss we observed in our microscopy and flow cytometry data, since vacuoles are essential for fungal cells in controlling the cellular osmotic pressure, salt balance, and pH [20, 37]. For the peptides that exhibited substantial PI permeability (pVEC, penetratin, and MAP), the loss of viability could also be due to membrane permeabilization, though it is not clear from our data whether the permeabilization is a cause or an effect of cell death. Between the two *Candida* species, *C. glabrata* tended to be less sensitive to toxicity of the peptides compared to *C. albicans*, which is consistent with previous research of antimicrobial peptides and other antifungal agents [38-40]. This difference in toxicity of CPPs and antimicrobial peptides between *Candida* species is not yet fully understood, though work has suggested that it may be due to the different compositions of the cell membranes and the presence of different membrane proteins [38, 40].

3.4. Discussion

Our evaluation of the interaction of CPPs with *Candida* cells provides insight into the biophysical properties that affect translocation, the mechanisms of translocation, and the toxicity of the peptides we studied.

Our data indicate that net charge of the peptides plays a role in translocation, with higher levels of positive charge generally leading to higher levels of translocation. As the phosphate heads of the membrane lipid are negatively charged, positive charged residues in peptides will lead to electrostatic interactions that bring peptide in close contact with the cell membrane. CPPs with higher net charges ($\geq +4$) including pVEC, penetratin, MAP, SynB, $(KFF)_3K$, MPG, TP-10 and Cecropin B would have stronger electrostatic interactions, which enables them to have a stronger

interaction with the cell membrane and explains their higher stronger translocation efficacy. In our experiments, we used a FAM label as the cargo for our peptides. This FAM label has a net negative charge of -3 at the pH of our experiments, which would reduce the overall net charge of the peptide-cargo constructs. Additional studies evaluating other cargo molecules will be important in understanding the impact of the peptide charge alone and in determining whether properties of cargo molecules strongly influence the translocation effects of the peptides.

Although each of the CPPs was previously shown to translocate into mammalian cells [21, 41], only pVEC, $(KFF)_3K$, penetratin, and TP-10 were previously shown to translocate into *Candida* cells [14, 17]. Our results indicate that many of the CPPs that function in mammalian cells do function in *C. albicans* and *C. glabrata*, but translocation into mammalian cells does not guarantee translocation in fungal cells. Three of the peptides tested showed little to no translocation in the two *Candida* species. In the case of Pep-1, association of the peptide with the cell wall contributed to the low level of translocation: when cells incubated with Pep-1 were imaged prior to trypsin treatment, the peptide was observed on the cell surface (**Figure 3.8**). However, for hCT and PAF26, the origin of the difference is less clear, since these peptides did not localize at the cell surface.

Our results for subcellular localization, membrane stability, and endocytic inhibition together provide insight into the translocation mechanisms for the CPPs in fungal cells (**Table 3.3**). The combination of significant vacuolar localization, lack of strong membane destabilization, and inhibition of translocation by NaN_3 and low temperature suggests endocytosis is involved in the translocation of a peptide, and we

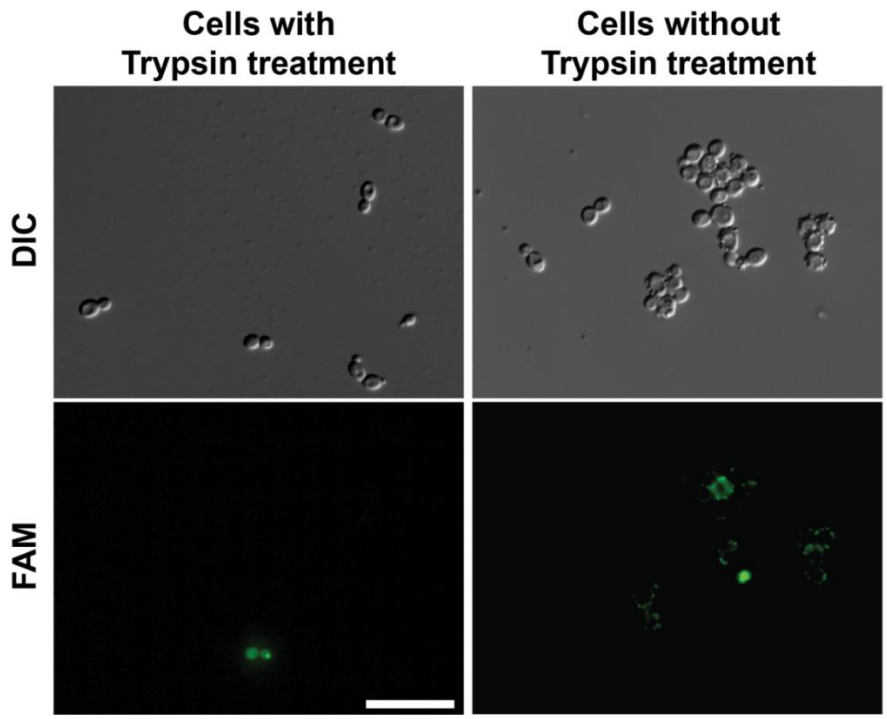

Figure 3.8 Effect of trypsin treatment on localization of Pep-1. *C. albicans* cells were incubated with 25 µM of FAM-labeled Pep-1 at 30 °C for 1 h. A portion of the cells were further treated with trypsin to remove surface-bound peptide, and the samples with and without trypsin treatment were imaged for FAM fluorescence. Scale bar =10 µm.

observed these characteristics for the translocation of SynB and $(KFF)_3K$. Stronger cytosolic localization along with high PI permeability, as we observed at high concentrations for cecropin B, pVEC, penetratin, and MAP, indicates the possibility of direct translocation into the cytosol, though endocytosis might still be possible at concentrations resulting in vacuolar localization.

Interestingly, the data for several of the peptides indicate multiple mechanisms may be involved in their translocation into fungal cells. For example, the NaN_3 and low temperature data for pVEC suggest an energy-independent mechanism, such as macropinocytosis or direct pore formation, which is consistent with the PI data. However, the microscopy images and flow cytometry data (**Figure 3.2**) also indicate vacuolar trafficking, which is more consistent with energy-dependent

endocytosis. The possibility of multiple mechanisms is consistent with prior work with pVEC in mammalian cells. Elmquist *et al*. found that a clathrin-dependent endocytic pathway is involved in the translocation of pVEC, yet they still observed modest translocation at low temperatures to also implicate non-endocytic pathways [42]. Likewise, MAP and cecropin B have high PI permeability consistent with direct translocation, yet they exhibit the energy-dependent translocation and vacuolar trafficking consistent with endocytosis, which could indicate multiple mechanisms are also involved in translocation of these peptides.

For some peptides, our results implicate a translocation mechanism in *Candida* cells that differs from previous studies with mammalian cells. MPG and TP-10 were previously suggested to destabilize and make pores in the membrane of HeLa and melanoma cells, respectively [24, 25]. However, our PI data, NaN_3 assay, and localization images indicate an endocytic process is involved for *Candida* cells. The

Table 3.3. Summary of subcellular localization and potential translocation mechanism of CPPs

	Cecropin B	Penetratin	pVEC	MAP	SynB	$(KFF)_3K$	MPG	TP-10
Vacuolar localization	Low	Low	Low	Low	High	High	High	High
PI permeability[a]	++	++	++	++	+	-	-	-
Endocytosis inhibition	Yes	No	No	Yes	Yes	Yes	Yes	Yes
Potential mechanism[b]	E/D	M/D	E/M	E/D	E	E	E	E
Reported mechanism[b]	E/D[c]	E/D[d]	M[e]	D[f]	E[d]	n/a	D[g]	D[f]

[a] Strong PI permeability is indicated by ++, moderate permeability by +, and no significant permeability by -.
[b] Translocation mechanisms are as follows: endocytosis (E), macropinocytosis (M), direct translocation/pore formation (D), or no data available (n/a)
[c] Reference [23]
[d] Reference [4]
[e] Reference [7]
[f] Reference [24]
[g] Reference [25]

difference in structure of the cell types may help explain this discrepancy. Hallbrink *et al.* and Simeoni *et al.* showed the translocation and pore formation of MPG, Pep-1, and TP-10 was associated with the close interaction between peptides and cell membranes [24, 25]. However, the additional barrier of the cell wall in fungal cells could interfere with this close interaction. This idea is consistent with our observation that Pep-1 associated with the surface and did not translocate into fungal cells (**Figure 3.8**). Additionally, differences in cell-surface properties and proteins could change the overall structure and behavior of CPPs. For example, *Candida* cells could have a receptor that recognizes MPG and TP-10, causing a shift in the translocation mechanism in fungal cells to endocytosis, even though membrane destabilization occurs in mammalian cells.

Our vacuolar localization study and PI uptake investigation also highlighted the potential toxicity of CPPs towards fungal cells. CPPs like pVEC and penetratin, which showed significant intracellular (especially cytosolic) delivery, had a higher level of antifungal activity. The toxicity of these CPPs toward *Candida* pathogens could prove to be a positive feature of CPPs targeted to fungal pathogens, as one motivation for studying CPPs in fungal cells is to use them to deliver antifungal molecules, and the cytotoxicity of the CPP vehicles would potentially increase the therapeutic effects of the cargo being delivered. To function as a delivery vehicle for antifungal therapeutics, toxicity of the CPPs to host cells would need to be minimal. Previous studies suggest TP-10, penetratin, MAP, and cecropin B negatively affect mammalian cell viability [41, 43-46], which would complicate their use in delivery of antifungal therapeutics. In contrast, pVEC and MPG did not significantly reduce

viability of mammalian cells [41, 47], and we observed both strong translocation and strong toxicity toward fungal cells, suggesting these peptides would be promising candidates for delivering antifungal agents or could potentially serve as antifungal agents themselves.

Although toxicity of CPPs may be desirable in the case of delivering antifungal molecules, CPPs also have potential in delivering non-toxic bioactive cargo to study the effect of the cargo on cellular function [48, 49]. In this case, toxicity from CPP vehicles would need to be as low as possible. While most of the peptides we studied would not be suitable for this type of application, SynB is the exception. At a concentration of 10 μM, essentially 100% of *Candida* cells were positive for peptide translocation (**Figure 3.1C**), while the same concentration led to a loss of viability for only 10% of *C. albicans* and 5% of *C. glabrata* cells (**Figure 3.7**). SynB also has a low level of toxicity toward mammalian cells [50], further increasing its potential applications in studying the biology of *Candida* pathogens.

Our data for the toxicity of the CPPs highlight the importance of considering the goal of cargo delivery in selecting a CPP. The level of CPP translocation, along with the toxicity toward the target cells and any other cells that may be present, must be evaluated to identify a CPP with the desired delivery and toxicity profiles.

3.5. Conclusion

We have identified a number of CPPs that are able to translocate into the fungal pathogens *C. albicans* and *C. glabrata*. Our work also explored the intracellular distribution of the CPPs following translocation into fungal cells and found that vacuoles play a significant role in CPP trafficking. Our results suggest that

translocation of CPPs into fungal cells may involve multiple mechanisms and that these mechanisms may lead to the toxicity observed for some peptides. Further work to explore the translocation mechanisms of CPPs could improve their efficacy and toxicity profiles to make CPPs viable therapeutic delivery agents. By increasing the translocation of bioactive cargo using CPPs, effectiveness of antifungal agents could be improved and new classes of molecules that currently lack the ability to cross cell membranes could be explored as antifungal agents.

3.6. Reference

1. Oehlke, J., A. Scheller, B. Wiesner, E. Krause, M. Beyermann, E. Klauschenz, M. Melzig, and M. Bienert, *Cellular uptake of an alpha-helical amphipathic model peptide with the potential to deliver polar compounds into the cell interior non-endocytically.* Biochimica Et Biophysica Acta-Biomembranes, 1998. **1414**(1-2): p. 127-139.
2. Soomets, U., M. Lindgren, X. Gallet, M. Hallbrink, A. Elmquist, L. Balaspiri, M. Zorko, M. Pooga, R. Brasseur, and U. Langel, *Deletion analogues of transportan.* Biochimica et Biophysica Acta, 2000. **1467**(1): p. 165-76.
3. Lopez-Garcia, B., E. Perez-Paya and J.F. Marcos, *Identification of novel hexapeptides bioactive against phytopathogenic fungi through screening of a synthetic peptide combinatorial library.* Applied and Environmental Microbiology, 2002. **68**(5): p. 2453-2460.
4. Drin, G., S. Cottin, E. Blanc, A.R. Rees, and J. Temsamani, *Studies on the internalization mechanism of cationic cell-penetrating peptides.* Journal of Biological Chemistry, 2003. **278**(33): p. 31192-201.
5. Munoz, A., J.F. Marcos and N.D. Read, *Concentration-dependent mechanisms of cell penetration and killing by the de novo designed antifungal hexapeptide PAF26.* Molecular Microbiology, 2012. **85**(1): p. 89-106.
6. Mager, I., E. Eiriksdottir, K. Langel, S. El Andaloussi, and U. Langel, *Assessing the uptake kinetics and internalization mechanisms of cell-penetrating peptides using a quenched fluorescence assay.* Biochimica et Biophysica Acta, 2010. **1798**(3): p. 338-43.
7. Elmquist, A., M. Lindgren, T. Bartfai and U. Langel, *VE-cadherin-derived cell-penetrating peptide, pVEC, with carrier functions.* Exp Cell Res, 2001. **269**(2): p. 237-44.
8. Derossi, D., S. Calvet, A. Trembleau, A. Brunissen, G. Chassaing, and A. Prochiantz, *Cell internalization of the third helix of the antennapedia homeodomain is receptor-independent.* Journal of Biological Chemistry, 1996. **271**(30): p. 18188-18193.
9. Fischer, R., M. Fotin-Mleczek, H. Hufnagel and R. Brock, *Break on through to the other side-biophysics and cell biology shed light on cell-penetrating peptides.* ChemBioChem, 2005. **6**(12): p. 2126-42.
10. Morris, M.C., P. Vidal, L. Chaloin, F. Heitz, and G. Divita, *A new peptide vector for efficient delivery of oligonucleotides into mammalian cells.* Nucleic Acids Research, 1997. **25**(14): p. 2730-2736.
11. Morris, M.C., J. Depollier, J. Mery, F. Heitz, and G. Divita, *A peptide carrier for the delivery of biologically active proteins into mammalian cells.* Nature Biotechnology, 2001. **19**(12): p. 1173-1176.
12. Vaara, M. and M. Porro, *Group of peptides that act synergistically with hydrophobic antibiotics against gram-negative enteric bacteria.* Antimicrobial Agents and Chemotherapy, 1997. **41**(2): p. 496-496.
13. Rajarao, G.K., N. Nekhotiaeva and L. Good, *Peptide-mediated delivery of green fluorescent protein into yeasts and bacteria.* FEMS Microbiol Lett, 2002. **215**(2): p. 267-72.

14. Holm, T., S. Netzereab, M. Hansen, U. Langel, and M. Hallbrink, *Uptake of cell-penetrating peptides in yeasts.* FEBS Lett, 2005. **579**(23): p. 5217-22.
15. Parenteau, J., R. Klinck, L. Good, U. Langel, R.J. Wellinger, and S.A. Elela, *Free uptake of cell-penetrating peptides by fission yeast.* FEBS Lett, 2005. **579**(21): p. 4873-8.
16. Palm, C., S. Netzereab and M. Hallbrink, *Quantitatively determined uptake of cell-penetrating peptides in non-mammalian cells with an evaluation of degradation and antimicrobial effects.* Peptides, 2006. **27**(7): p. 1710-6.
17. Gong, Z., M.T. Walls, A.N. Karley and A.J. Karlsson, *Effect of a flexible linker on recombinant expression of cell-penetrating peptide fusion proteins and their translocation into fungal cells.* Molecular Biotechnology, 2016. **58**(12): p. 838-849.
18. Munoz, A., E. Harries, A. Contreras-Valenzuela, L. Carmona, N.D. Read, and J.F. Marcos, *Two functional motifs define the interaction, internalization and toxicity of the cell-penetrating antifungal peptide PAF26 on fungal cells.* PLoS One, 2013. **8**(1): p. e54813.
19. Bowman, S.M. and S.J. Free, *The structure and synthesis of the fungal cell wall.* BioEssays, 2006. **28**(8): p. 799-808.
20. Klionsky, D.J., P.K. Herman and S.D. Emr, *The fungal vacuole: composition, function, and biogenesis.* Microbiological Reviews, 1990. **54**(3): p. 266-92.
21. Richard, J.P., K. Melikov, E. Vives, C. Ramos, B. Verbeure, M.J. Gait, L.V. Chernomordik, and B. Lebleu, *Cell-penetrating peptides. A reevaluation of the mechanism of cellular uptake.* Journal of Biological Chemistry, 2003. **278**(1): p. 585-90.
22. Schneider, C.A., W.S. Rasband and K.W. Eliceiri, *NIH Image to ImageJ: 25 years of image analysis.* Nature Methods, 2012. **9**(7): p. 671-675.
23. Epand, R.M. and H.J. Vogel, *Diversity of antimicrobial peptides and their mechanisms of action.* Biochimica Et Biophysica Acta-Biomembranes, 1999. **1462**(1-2): p. 11-28.
24. Hallbrink, M., A. Floren, A. Elmquist, M. Pooga, T. Bartfai, and U. Langel, *Cargo delivery kinetics of cell-penetrating peptides.* Biochimica et Biophysica Acta, 2001. **1515**(2): p. 101-9.
25. Simeoni, F., M.C. Morris, F. Heitz and G. Divita, *Insight into the mechanism of the peptide-based gene delivery system MPG: implications for delivery of siRNA into mammalian cells.* Nucleic Acids Res, 2003. **31**(11): p. 2717-24.
26. Paluchowska, P., M. Tokarczyk, B. Bogusz, I. Skiba, and A. Budak, *Molecular epidemiology of Candida albicans and Candida glabrata strains isolated from intensive care unit patients in Poland.* Mem Inst Oswaldo Cruz, 2014. **109**(4): p. 436-41.
27. Meiller, T.F., B. Hube, L. Schild, M.E. Shirtliff, M.A. Scheper, R. Winkler, A. Ton, and M.A. Jabra-Rizk, *A novel immune evasion strategy of candida albicans: proteolytic cleavage of a salivary antimicrobial peptide.* PLoS One, 2009. **4**(4): p. e5039.
28. Sikora, M., M. Dabkowska, E. Swoboda-Kopec, S. Jarzynka, I. Netsvyetayeva, M. Jaworska-Zaremba, M. Pertkiewicz, and G. Mlynarczyk, *Differences in proteolytic activity and gene profiles of fungal strains isolated*

from the total parenteral nutrition patients. Folia Microbiologica, 2011. **56**(2): p. 143-8.
29. Lorenz, J.N. and E. Gruenstein, *A simple, nonradioactive method for evaluating single-nephron filtration rate using FITC-inulin.* American Journal of Physiology, 1999. **276**(1 Pt 2): p. F172-7.
30. Preston, R.A., R.F. Murphy and E.W. Jones, *Assay of vacuolar pH in yeast and identification of acidification-defective mutants.* Proceedings of the National Academy of Sciences of the United States of America, 1989. **86**(18): p. 7027-31.
31. Mochon, A.B. and H. Liu, *The antimicrobial peptide histatin-5 causes a spatially restricted disruption on the Candida albicans surface, allowing rapid entry of the peptide into the cytoplasm.* PLoS Pathogens, 2008. **4**(10): p. e1000190.
32. Li, L. and J. Kaplan, *A mitochondrial-vacuolar signaling pathway in yeast that affects iron and copper metabolism.* J Biol Chem, 2004. **279**(32): p. 33653-61.
33. Jiao, C.Y., D. Delaroche, F. Burlina, I.D. Alves, G. Chassaing, and S. Sagan, *Translocation and Endocytosis for Cell-penetrating Peptide Internalization.* Journal of Biological Chemistry, 2009. **284**(49): p. 33957-33965.
34. Lichstein, H.C. and M.H. Soule, *Studies of the effect of sodium azide on microbic growth and respiration: I. The action of sodium azide on microbic growth.* Journal of Bacteriology, 1944. **47**(3): p. 221-30.
35. Noumi, T., M. Maeda and M. Futai, *Mode of inhibition of sodium azide on H+-ATPase of Escherichia coli.* FEBS Letters, 1987. **213**(2): p. 381-4.
36. Halder, S., K.K. Yadav, R. Sarkar, S. Mukherjee, P. Saha, S. Haldar, S. Karmakar, and T. Sen, *Alteration of Zeta potential and membrane permeability in bacteria: a study with cationic agents.* Springerplus, 2015. **4**: p. 672.
37. Shirahama, K., Y. Yazaki, K. Sakano, Y. Wada, and Y. Ohsumi, *Vacuolar function in the phosphate homeostasis of the yeast Saccharomyces cerevisiae.* Plant and Cell Physiology, 1996. **37**(8): p. 1090-3.
38. Helmerhorst, E.J., C. Venuleo, A. Beri and F.G. Oppenheim, *Candida glabrata is unusual with respect to its resistance to cationic antifungal proteins.* Yeast, 2005. **22**(9): p. 705-14.
39. Pfaller, M.A., S.A. Messer, R.J. Hollis, R.N. Jones, and D.J. Diekema, *In vitro activities of ravuconazole and voriconazole compared with those of four approved systemic antifungal agents against 6,970 clinical isolates of Candida spp.* Antimicrobial Agents and Chemotherapy, 2002. **46**(6): p. 1723-1727.
40. Raman, N., M.R. Lee, D.M. Lynn and S.P. Palecek, *Antifungal activity of 14-helical beta-peptides against planktonic cells and biofilms of Candida species.* Pharmaceuticals (Basel), 2015. **8**(3): p. 483-503.
41. Saar, K., M. Lindgren, M. Hansen, E. Eiriksdottir, Y. Jiang, K. Rosenthal-Aizman, M. Sassian, and U. Langel, *Cell-penetrating peptides: A comparative membrane toxicity study.* Analytical Biochemistry, 2005. **345**(1): p. 55-65.

42. Elmquist, A., M. Hansen and U. Langel, *Structure-activity relationship study of the cell-penetrating peptide pVEC.* Biochim Biophys Acta Biomembr, 2006. **1758**(6): p. 721-9.
43. El-Andaloussi, S., P. Jarver, H.J. Johansson and U. Langel, *Cargo-dependent cytotoxicity and delivery efficacy of cell-penetrating peptides: a comparative study.* Biochemical Journal, 2007. **407**(2): p. 285-92.
44. Dinca, A., W.M. Chien and M.T. Chin, *Intracellular delivery of proteins with cell-penetrating peptides for therapeutic uses in human disease.* International Journal of Molecular Sciences, 2016. **17**(2): p. 263.
45. Suttmann, H., M. Retz, F. Paulsen, J. Harder, U. Zwergel, J. Kamradt, B. Wullich, G. Unteregger, M. Stockle, and J. Lehmann, *Antimicrobial peptides of the cecropin-family show potent antitumor activity against bladder cancer cells.* BMC Urology, 2008. **8**(1): p. 5.
46. Bacalum, M. and M. Radu, *Cationic Antimicrobial Peptides Cytotoxicity on Mammalian Cells: An Analysis Using Therapeutic Index Integrative Concept.* International Journal of Peptide Research and Therapeutics, 2015. **21**(1): p. 47-55.
47. Mussbach, F., R. Pietrucha, B. Schaefer and S. Reissmann, *Internalization of nucleoside phosphates into live cells by complex formation with different CPPs and JBS-nucleoducin.* Methods in Molecular Biology, 2011. **683**: p. 375-89.
48. Alhakamy, N.A., A.S. Nigatu, C.J. Berkland and J.D. Ramsey, *Noncovalently associated cell-penetrating peptides for gene delivery applications.* Ther Deliv, 2013. **4**(6): p. 741-57.
49. Jiang, Q.Y., L.H. Lai, J. Shen, Q.Q. Wang, F.J. Xu, and G.P. Tang, *Gene delivery to tumor cells by cationic polymeric nanovectors coupled to folic acid and the cell-penetrating peptide octaarginine.* Biomaterials, 2011. **32**(29): p. 7253-7262.
50. Tian, X.H., F. Wei, T.X. Wang, P. Wang, X.N. Lin, J. Wang, D. Wang, and L. Ren, *In vitro and in vivo studies on gelatin-siloxane nanoparticles conjugated with SynB peptide to increase drug delivery to the brain.* International Journal of Nanomedicine, 2012. **7**: p. 1031-41.

Chapter 4. Secondary structure of CPPs and the interaction with fungal cells

4.1. Introduction

In Chapter 3, we identified the CPPs that can be applied to fungal pathogens, for either cargo delivery or killing fungal cells and initiated studies of translocation mechanisms of CPPs to better understand the mode of action of the CPPs. In this chapter, we further explore the translocation mechanisms from the molecular level to develop an improved understanding of the reason for translocation and the difference in behavior for different CPPs.

As we discussed in Chapter 3 and as suggested in previous CPPs research in fungal cells, the translocation mechanisms were studied with the help of fluorescently labeled peptides. This allows qualitative and quantitative study of uptake, subcellular localization and even membrane destabilization [1-4]. It also enables understanding of translocation mechanisms from biological perspectives, as energy dependence or membrane integrity can reveal whether the translocation is an endocytic process or direct translocation. However, fluorescent labelling of peptides cannot reveal exactly how these peptides interact with cells at the molecular level and what happens to the peptides upon interaction.

Biophysical studies of CPPs have indicated that the structure of CPPs may be related to the overall translocation processes. Most of the biophysical studies were carried out using direct circular dichroism (CD) of peptides either in different

solvents or in a mixture of lipids or lipopolysaccharides to mimic cell membrane components [2, 5-8]. While CD data of CPPs in solutions provide information about the conformation of the peptides before the interaction happens, they fail in providing structural information while CPPs are very close to or on the cell surface. Model membrane or model lipid vesicles have been used to improve studies of peptide-lipid interactions by mimicking the phosphate lipid bilayers. According to previous studies, many CPPs like pVEC, TP-10, MAP, MPG, Pep-1, and Tat remain in a random conformation in aqueous solutions [6]. However, when lipid vesicles were added into the system, a higher order structure (β-sheet or α-helix) could be observed, and vesicle leakage was detected, which is analogous to membrane leakage for live cells [6]. Similar results were observed while different types of vesicles were added into the peptide solutions [9, 10]. Using lipid vesicles, researchers have proposed several modes of actions for the translocation of CPPs based on the CD spectra [11].

However, cells are very dynamic and complicated systems, and these characteristics extend to the cell membrane and, in the case of fungal cells, the cell wall. *Candida* cell membrane lipids include phosphatidylinositol (PI), phosphatidylserine (PS), phosphatidylglycerol (PG), phosphatidylcholine, phosphatidylethanolamine, and phosphatidylinositol [12], and the lipid composition can vary between azole sensitive and insensitive stains. In addition, a number of anchored proteases such as secreted aspartic proteases (Saps) could potentially affect the interaction of CPPs with membrane as they might degrade the peptides [13, 14]. Model membranes or vesicles enable the understanding of the interaction between lipid bilayers and the peptides due to the electrostatic force or hydrophobic

interaction, yet fail to take these cell-surface embedded proteins into account. In addition, the higher tendency of aggregation of lipid vesicles complicates the structure of the vesicles while interacting with peptides. Hence, model vesicles have some disadvantages in predicting the interaction of CPPs with lipid bilayers.

To address the limitations of using model cell membranes, Concetta *et al.* recently reported using CD spectroscopy to directly study the interaction between antimicrobial peptides, which are similar in structure and function to CPPs, with bacterial cells [15, 16]. Details of the initial interaction of peptides with cells can be resolved by CD measurement in the presence of the whole cells, and the time-lapse measurement provides the long-term conformational change due to the interaction. Using this approach yields molecular-level understanding of the peptide-membrane interaction that can be directly compared to data on CPP translocation.

In this study, we applied the direct CD measurement with whole cells developed by Concetta *et al.* to the fungal pathogen *C. albicans* to not only understand the structure of CPPs in the presence of the cell membrane, but also to determine what causes the conformational transition when CPPs are near the cell surface. In addition, we used Monte Carlo simulation to understand the initial interaction of CPPs with a model lipid layer to gain a residue-level understanding of the mode of action and the conformational transition upon interaction with a lipid membrane for peptides with helical secondary structures. The present study allows us to look closely at the cell surface and discern a biophysical explanation of secondary structure formation and translocation mechanisms of CPPs during their interaction with *C. albicans*

Table 4.1 CPPs tested in this chapter

Peptide	Sequence	MW (Da)	Net Charge[a]
pVEC	LLIILRRRIRKQAHAHSK	2209.7	+8
Penetratin	RQIKIWFQNRRMKWKK	2246.8	+7
MAP	KLALKLALKALKAALKLA	1876.0	+5
Pep-1	KETWWETWWTEWSQPKKKRKV	2848.3	+2
SynB	RGGRLSYSRRRFSTSTGR	2100.3	+6
MPG	GALFLGFLGAAGSTMGAWSQPKKKRKV	2807.4	+5
TP-10	AGYLLGKINLKALAALAKKIL	2182.8	+4
Cecropin B	KWKVFKKIEKMGRNIRNGIVKAGPAIAVLGEA KAL	3835.7	+9

[a] **Includes only charges due to amino acid side chains (pH 7) and not N-terminal FAM (-3)**

4.2. Materials and methods

4.2.1. Peptides

The peptides used in this study (**Table 4.1**) were commercially synthesized with an N-terminal 5-carboxyfluorescein (FAM) and a purity > 90% (Genscript). The lyophilized peptides were reconstituted in either 10mM Na_2HPO_4 buffer, 2, 2, 2-trifluoroethanol (TFE), or a mixture with a buffer/TFE ratio of 1:1 (v/v), depending on the assay.

4.2.2. Strains and culture conditions

The fungal pathogen *C. albicans* SC5314 was purchased from the American Type Culture Collection (ATCC). Cells were first inoculated from a yeast-peptone-dextrose (YPD) agar plate into 5 mL of YPD liquid medium and grown overnight while shaking at 230 rpm. The overnight cell culture was subsequently subcultured into 5 mL of fresh liquid YPD at OD_{600}=0.1. The culture was grown at 30 °C with

shaking to mid-log phase (~4h with an OD_{600}=0.5). Cells were collected by centrifugation at 4,000 × g for 10 min and washed with 10 mM Na_2HPO_4 buffer twice before finally resuspending in 10 mM Na_2HPO_4 buffer with a final OD_{600}=0.2 (~ 4×10^6 CFU/ml) before the assays.

For experiments involving a cell lysate, the lysate was prepared from mid-log phase cells. Subcultured cells were lysed in 10 mM Na_2HPO_4 buffer using a homogenizer (Avestin) and diluted to the equivalent of 4×10^6 CFU/ml.

4.2.3. Circular dichroism

CD spectra were collected at 30 °C using a micro-cuvette quartz cell with a 10 mm path length (Fisher Scientific). The CD spectrometer J-810 (Jasco) was set to scanning mode with a 190-240 nm range, 50 nm/min scanning speed, 1 nm bandwidth, 1.0 nm data pitch, and 3-accumulation mode. For CPPs in solutions, the measurement was performed with 400 µL of 5 µM peptide solution in Na_2HPO_4 buffer, TFE, and a mixture with a buffer/TFE ratio of 1:1 (v/v). The signal was converted to molar ellipticity [θ] using

$$[\theta] = \frac{100\times\theta}{C\times l} \quad \text{(Equation 4.1)}$$

where θ is the ellipticity (degrees), C is the molar concentration (M), and l is the cell pathlength (cm).

For CD with live fungal cells, 200 µL of a prepared cell suspension or cell lysate was mixed with 200 µL of 10 µM peptide solution in Na_2HPO_4 buffer to achieve a final peptide concentration of 5 µM and a final cell concentration of 2×10^6 CFU/ml. Due to the existence of cells, the ellipticity cannot be converted from [mdeg] to molar ellipticity. The mixture was either immediately measured by CD or

incubated for 30 min at 30 °C before CD measurement. All experiments were performed with three replicates.

4.2.4. Membrane depolarization assay

Membrane depolarization was evaluated using 3,3'-dipropylthiadi-carbocyanine iodide ($DiSC_3(5)$). Subcultured *C. albicans* cells were washed twice with 10 mM Na_2HPO_4 buffer and concentrated to a final OD_{600}=1.0. $DiSC_3(5)$ (ThermoFisher) was diluted to a stock concentration of 1 M in DMSO. A volume of 990µL of cell suspension was added to a glass micro-cuvette, and the fluorescence emission was measured using a fluorometer (Molecular Devices; 633 nm excitation and 666 emission filters). This concentrated cell suspension containing no peptide was used to measure the baseline fluorescence level for 60 sec with data collected every 3 sec. The $DiSC_3(5)$ stock solution (1 µL) was added into the suspension and the fluorescence was measured for another 120 sec with 3 sec data pitch until the reading reached a steady level. A volume of 10 µL of 50 g/L glucose stock solution was added into solution to further reduce the fluorescence level for another 120 sec with 3 sec data pitch. A volume of 10 uL of peptides solution (1 M) was added into the solution, and the fluorescence signal was measured for 600 sec. All experiments were performed with three replicates.

4.2.5. Monte Carlo simulation for helical peptides

Monte Carlo simulations of the peptides that can form helical structures were performed using the MCPep server (available online at http://bental.tau.ac.il/MCPep/) [17]. The hydrophobicity of the membrane was represented as a smooth profile of 30 Å width, similar to a fungal cell membrane [8], with the hydrophobic surface at a

distance of 20 Å from the mid-plane. The negative charge was estimated based on the composition of *C. albicans* cell membranes [12], i.e., 20 % phosphatidylinositol + 17 % phosphatidylserine (PS) + 3 % phosphatidylglycerol (PG) = 40% charged lipids. The solution was set to contain 0.01 M monovalent salts. Three independent runs of the simulations were performed with 500,000 MC cycles in each run. The total free energy of membrane association was calculated as the difference between the free energies of the peptide in water and in the membrane. The average distance to the mid-plane and the helical content percentage of each individual residue were also determined in the simulation.

4.3. Results

In Chapter 3, I identified the CPPs that can translocate into *Candida* cells, such as pVEC, SynB, and the antimicrobial peptide cecropin B. In addition, I explored the translocation mode of action of these peptides from a biological perspective by evaluating pore formation and endocytosis. To better understand the translocation and mode of action from the molecular level, this study focused on the biophysical properties of CPPs, in particular the secondary structure, and how these properties affect the membrane association of the peptides, as well as the internalization mechanisms.

4.3.1. CPP structure in solution

Several CPPs have the ability to translocate into the fungal pathogen *C. albicans*. We evaluated the structure of 8 of those peptides (**Table 4.1**) in solution to gauge the solvent effect on secondary structure formation. The CD spectra of these peptides in aqueous solution suggest that all of the peptides, except Pep-1, remain as

random coils in a hydrophilic environment. Pep-1 exhibits a weak minimum at 208/222 nm, which is characteristic of helical structure (**Figure 4.1**). The secondary structures of all these peptides were previously studied in the solutions [5-8], and our results are consistent with those data.

Although the peptides have little to no secondary structure in aqueous solution, the hydrophilic solution does not truly represent the environment of the peptides when they insert into the hydrophobic domain of the membrane's lipid bilayer. Thus, we also examined the structure of these peptides in TFE to mimic this hydrophobic environment and better understand how the peptides behave in membranes (**Figure 4.1**). Consistent with previous research [6], all peptides except SynB showed a conformational transition from random coil (or weak helix, in the case of Pep-1) to α-helix. Unlike the other peptides, SynB showed a β-sheet structure in 50% TFE and switched to a more helical dominant conformation in pure TFE, suggesting that the secondary structure of SynB depending on the degree of hydrophobicity of its environment. Overall, these results suggest that the formation of secondary structure for these peptides requires a hydrophobic environment, such as that of the cell membrane, and that the peptides are unlikely to maintain a helical structure in an aqueous buffer.

4.3.2. Circular dichroism with fungal cells

Previous studies of CPP-membrane interactions were conducted with model lipid vesicles and structure information was measured by CD, but these measurements fail to take the complexity of the cell matrix into account. To account for this complexity, we evaluated the interaction between peptides and *C. albicans* cells by

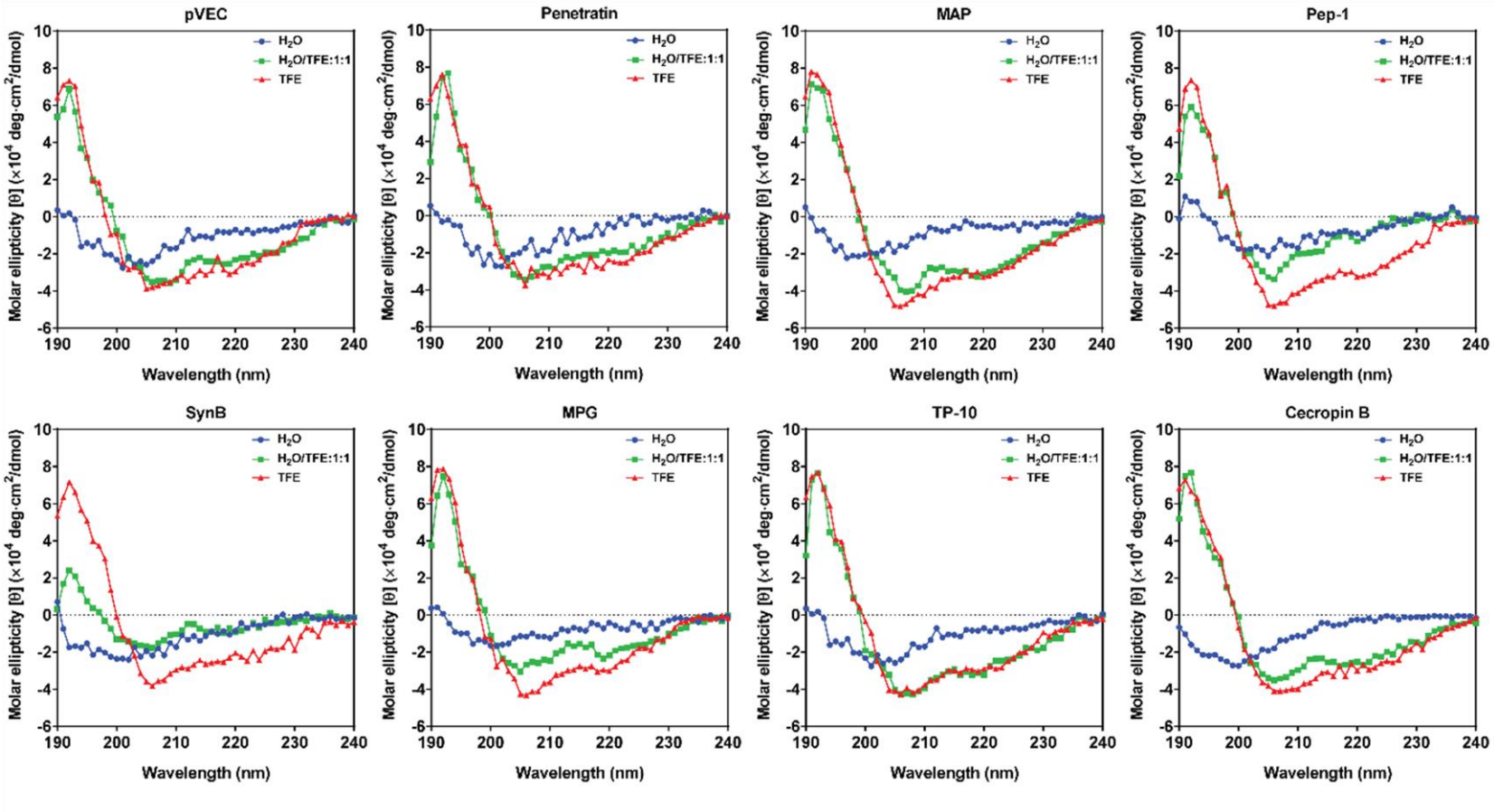

Figure 4.1. CD spectra of CPPs (10 μM) in different solutions. Peptides were suspended in pure buffer (10 mM Na_2HPO_4, blue), pure TFE (red), or in a buffer/TFE mixture solution (50%, v/v). Each data point represents the mean for three separate experiments (*N*=3)

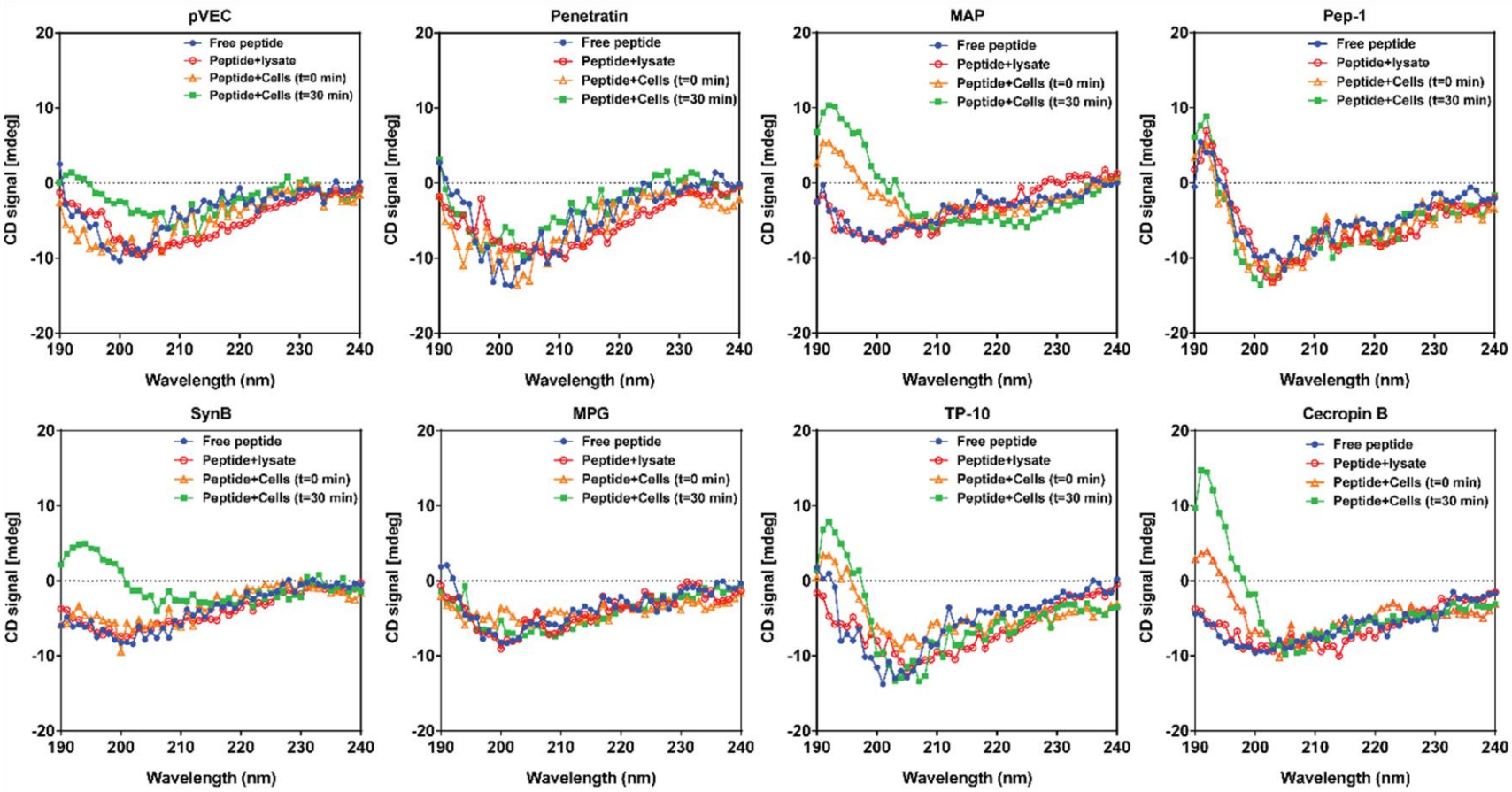

Figure 4.2. CD spectra of CPPs (10 μM) incubated with *C. albicans* cells. A total amount of 1×10^6 *C. albicans* cells was used to incubated with peptides at 30 ºC for 0 min (orange, t=0 min), or for 30 min (green, t=30 min) before CD measurement. Cell lysate was prepared and diluted to a final concentration that equivalent to 1×10^6 cells. Peptides were also incubated with soluble cell lysates (red) or 10 mM Na_2HPO_4 buffer (blue) at 30 ºC for 30 min before CD measurement to get background spectra. Each data point represents the mean for three separate experiments (*N*=3)

using CD (**Figure 4.2**). A suspension of *C. albicans* with no peptide was used to measure the baseline CD spectrum, and this baseline was subtracted from the spectra of peptides in cell suspensions, as suggested by Concetta *et al.* [15, 16]. As the molar concentration of cells cannot be converted to a meaningful molar ellipticity, we report our results in [mdeg]. The far-UV spectrum of each peptide was scanned after the addition of *C. albicans* cells. We did not observe any effects due to the intracellular contents, as there was no observable difference in the spectra for peptides in solution and peptides treated with soluble cell lysates (Figure 4.2). Due to significant noise in the far-UV range, the concentration of peptides cannot be higher than 5 μM. The CD spectra of 5 μM peptides with *C. albicans* cells indicated no conformational change was evident for penetratin, MPG or Pep-1. MPG and penetratin remained as a random coil, and Pep-1 showed an α-helical structure at all tested conditions. In contrast, the remaining peptides exhibited a structural transition. For MAP and cecropin B, the transition was rapid. The random coil structure shifted to an α-helical structure within 30 min of the addition of the cell suspension into the peptide solutions (Figure 4.2). These peptides have a strong amphipathic helical structure with all positively charged residues located on one side of the helix (Figure 4.3), which could promote interaction of the peptides with the negatively charged lipid head groups in the cell membrane. For pVEC and TP-10, the conformational transition to helical structure became apparent after 30 min of incubation with cells, suggesting these peptides respond to the interaction with the membrane in a slower manner, which might be due to the imperfectly aligned charge on the surface compared with a model amphipathic CPP like MAP (Figure 4.3). SynB, on the other hand, formed a β-sheet conformation

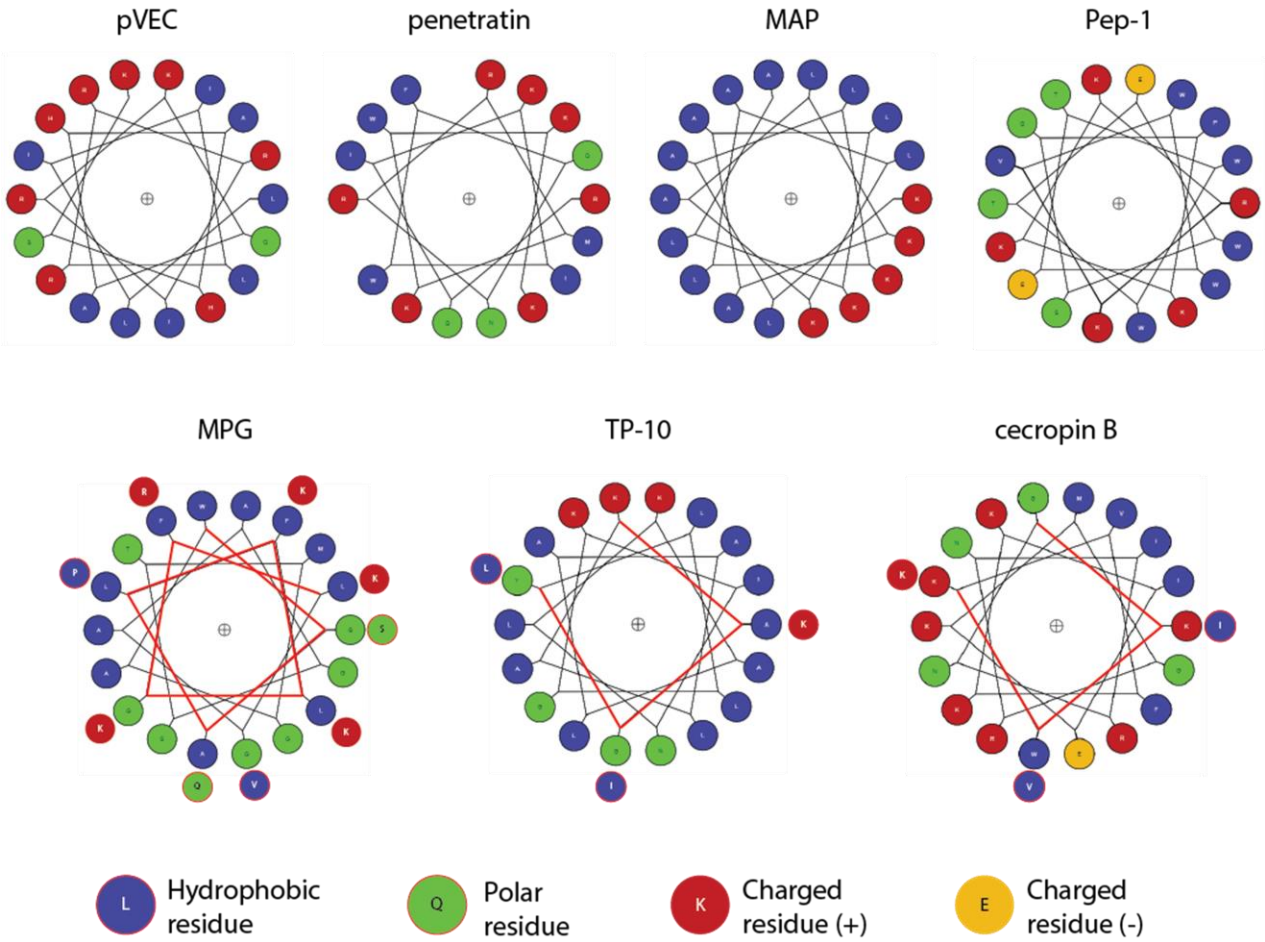

Figure 4.3 Helical wheels of CPPs. The wheels represent the structure of CPPs that showed helical conformations in Figure 4.1. Different types of residue were color-coded. For longer peptides (MPG, TP-10, and cecropin B), the extra residues beyond the inner helices are placed on the outer helices, connected by red line. Cecropin B has two helices and only the first helix is presented. Helical wheels were simulated using server: http://kael.net/helical.htm

instead of a helix, indicating a conformational transition to a different secondary structure than seen for the other peptides, consistent with the 50% TFE solution in the results for peptides in solution.

4.3.3. Simulations of peptide-membrane interactions

Our CD data suggest conformational change when CPPs are near the cell membrane. To help understand this behavior for the peptides that showed helical structures while interacting with cells, we used Monte Carlo (MC) simulations to model the interaction of the helical peptides with the *C. albicans* cell membrane. SynB was not included in the simulation as it formed β-sheet conformation upon interaction with fungal cells, and our simulation approach is not appropriate for peptides that form β-sheets [17]. The membrane was set up based on previous research about *C. albicans* membranes and membrane compositions. The thickness of the membrane was set to 30 Å [8] and the percentage of charged lipid was set to 40% (20 % PI + 17 % PS + 3 % PG based on the average reported lipid composition of *C. albicans* [8, 9]). The solution was assumed to be a buffer with 10 mM of monovalent salts, similar to our cell-based experiments.

One parameter we evaluated was the free energy of membrane association (**Table 4.2**) [17]. For all the peptides, the membrane association free energy was negative, and the electrostatic term (ΔG_{coul}) dominated the free energy, indicating all the peptides spontaneously interact with the membrane due to the electrostatic force between the positively charged peptides and the negatively charged lipid head groups. Interestingly, the free energies of hydrophobic interaction (ΔG_{SIL}) and conformational change (ΔG_{conf}) for pVEC, MAP, TP-10, and cecropin B were significantly negative

compared with penetratin, Pep-1, and MPG. This suggests that, not only can they interact with the hydrophilic domain of the membrane, but also with the hydrophobic domain, resulting in the conformational change. These peptides exhibited a conformational shift in our CD measurement (**Figure 4.2**), which can be explained by this negative ΔG_{conf}. As discussed earlier, hydrophobic interactions are the driving force of the secondary structure formation for all the peptides (**Figure 4.1**). Thus, the negative ΔG_{SIL} is consistent with the shift in CD spectra and the negative ΔG_{conf} for these peptides. For the peptides that did not show the evolution of secondary structure while interacting with *Candida* cells (penetratin, Pep-1, and MPG), the only force that substantially contributed to the membrane association was the ΔG_{coul}, indicating these peptides interact with the surface of the cell membrane and not with the hydrophobic lipid tails deeper within the core of the bilayers.

We also simulated the conformation of the peptides on the surface to seek a biophysical explanation of our observations during the CD measurements (**Figure 4.4**). For the peptides that showed a negative ΔG_{conf} and ΔG_{SIL} (**Table 4.2**), the simulations showed that the peptides either partially inserted (pVEC and TP-10) or fully inserted (MAP and Cecropin B) into the hydrophobic core of the membrane, compared to the peptides that remained on the surface of membrane and did not show

Table 4.2 Membrane association free energy calculation from Monte Carlo simulation

Peptides	ΔG_{Total}[a] (kT)	ΔG_{conf}[b] (kT)	ΔG_{SIL}[c] (kT)	ΔG_{coul}[d] (kT)	ΔG_{def}[e] (kT)
pVEC	-28.58	-2.09	-9.95	-16.79	0.25
Penetratin	-16.46	0.16	1.07	-17.95	0.25
MAP	-27.25	-1.20	-10.3	-16.53	0.25
Pep-1	-11.28	-0.60	0.90	-11.69	0.25
MPG	-17.57	-1.68	-2.74	-13.40	0.24
TP-10	-22.88	-1.37	-9.54	-12.22	0.26
Cecropin B	-36.41	-7.29	-8.39	-20.97	0.25

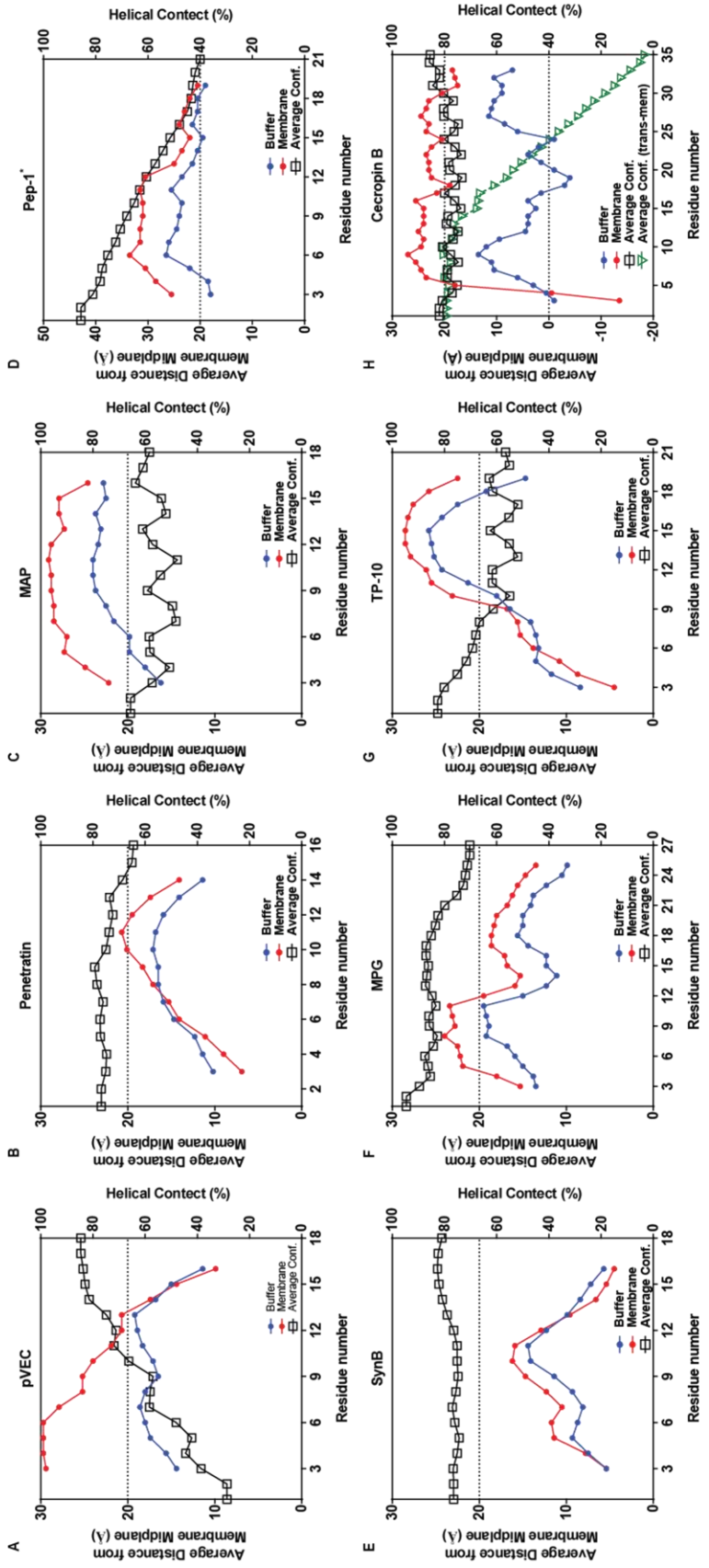

Figure 4.4 Monte Carlo simulation (MC) of the interaction between CPPs and phosphate lipid membrane. The membrane was assumed to be 30 Å with 40% charged lipids to mimic fungal cell membranes, and the monovalent salts concentration was set to be 10 mM. Three independent MC simulation was run with a 50000 MC cycle in each independent run. The average of three runs was plotted against the residue number of the peptides. The helical content percentage of peptides in buffer (Blue circle) or in contact with membrane (Red circle) was plotted on the right y-axis. The average position of each residue (Black square, green triangle for cecropin B transmembrane case) was plotted on the left axis. The dash line represents the location of the phosphate group of the lipids polar heads. Pep-1 all simulation indicated the peptide would extend vertically away from the membrane mid-plane. 1 out of 3 MC simulation of cecropin B suggested that cecropin B could adopt a vertically extended transmembrane helical structure.

a conformational transition in the CD spectra (penetratin, Pep-1, and MPG). Furthermore, the inserted residues showed an increase in helical content, suggesting a stronger preference for formation of α-helical secondary structure. Surprisingly, MPG and Pep-1, which did not show a structural transition in the CD experiment with cells but did show an energetically favorable structural transition in free energy calculations, exhibited increased helical content. This could be explained by the difference in cells and the simulated membrane. The simulation relies on direct interaction with the membrane, which could be affected by the existence of the cell wall in live-cell experiments with these peptides.

Overall, our MC calculations and simulations successfully explain the experimental data and help us build the connection between the membrane association and structure of CPPs.

4.3.4. Membrane depolarization assay

As we observed from our simulation results, interaction with the membrane core is possible for some CPPs. These close interactions with the core may potentially affect the integrity of the membrane [1]. To understand the biophysical interaction of these peptides with the membrane and the biological effect on the cells, we used a membrane depolarization assay with DiSC3(5), a dye that is sensitive to membrane potential. A total of 1×10^7 *C. albicans* cells was suspended in 1 mL of 10 mM Na_2HPO_4 buffer. The cell suspension was used to measure the baseline fluorescence, and the release of $DiSC_3(5)$ was measured for 600 sec (**Figure 4.5**). pVEC, penetratin, and cecropin B, which showed the potential for direct translation in our

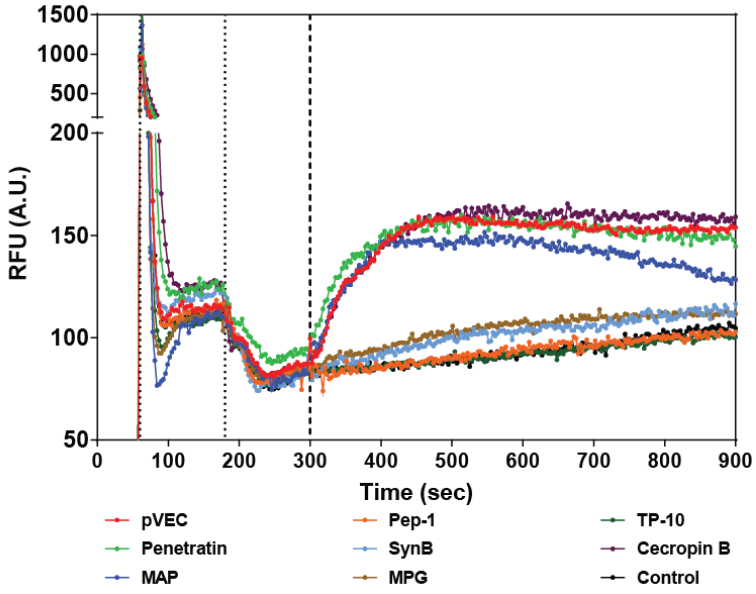

Figure 4.5. Evaluation of membrane depolarization. The fluorimeter was set with a 633 nm excitation and 666 nm emission. A total of 1×10^7 *C. albicans* cells suspended in 1 mL of 10 mM Na_2HPO_4 buffer was added in the cuvette and used to measure the base line of fluorescence level. The base line was measured for 60 sec before $DiSC_3(5)$ (3,3'-Dipropylthiadicarbocyanine Iodide, 1 mM) was added into the cuvette. The maximum uptake of $DiSC_3(5)$ was observed at 180 sec. 10 µL of 20% glucose was added to further decrease the fluorescence level until 300 sec. Peptides were added into the cuvette to a final concentration of 10 µM and the release of fluorescence was monitored for 600 sec with a 3 sec measurement integral. The data represents the average of three separated experiments.

previous work with *C. albicans* [1], exhibited significant membrane depolarization within the first 100 sec after adding peptide to the cells. MAP exhibited a different behavior, where it depolarized the membrane rapidly, indicating strong membrane binding and interaction, likely due to its high amphiphilicity and high net charge. However, a hyperpolarization was observed after 700 sec. This has been observed for peptides in other studies [21-23], though the explanation is not clear. One possible cause could be internalization of the peptides, as internalization would reduce the amount of surface-bound peptide that is able to depolarize the membrane. SynB, MPG, Pep-1 and TP-10 showed results very similar to the control, suggesting

minimal membrane depolarization is involved during their interaction with membrane.

4.4. Discussion

As indicated in previous research, many well-known CPPs remain in a random conformation in aqueous solutions [5, 18-20]. Our results support this observation and also suggest that peptides in the vicinity of the cell membrane, but not inserted into the membrane, remain in a random coil conformation (**Figure 4.1**). The observation of secondary structure under the hydrophobic solution suggests these peptides are capable of forming secondary structures, but that the conformation shift does not happen unless the peptides are in a hydrophobic environment, such as the core of the bilayers.

Previous attempts to understand the interactions of CPPs with membranes were focused on gaining structural information through interactions with model membrane or vesicles or in hydrophobic solvents. However, neither approach reflects the real situation on the surface of cells. The cell surface with proteins, glycans, and the cell wall is complex and is likely to affect the interaction between the peptides and the membrane. Experimental methods that can take these into account need to be developed to give a more accurate representation of the membrane association. Our CD measurements along with our MC simulations provide a comprehensive understanding of secondary structure formation during the interaction of peptides with cells. The primary sequence of the peptides and the amphipathicity subsequently affect the extent of interaction. Those peptides showing a CD signal shift and negative confirmation free energy (**Figure 4.2, 4.4, Table 4.2**) were previously

shown to use a more aggressive direct translocation mechanism, which relies on the interaction of the peptides with the hydrophobic core of bilayers [1], which is consistent with our current observation. Membrane penetration allows access to the hydrophobic tail of membrane lipids, driving the formation of secondary structure, as we observed in this study (**Figure 4.1, Table 4.2**).

In addition, our membrane depolarization data, along with CD and simulation data, enable a more detailed understanding of the translocation mechanisms. We previously found that Pep-1, SynB, and MPG use an endocytic pathway to gain intracellular access without affecting membrane integrity or the viability of cells [1]. This would require only brief interaction with the membrane. In this study, these peptides showed no secondary structure formation during interactions with cells and no significant membrane depolarization, suggesting the interaction between the peptides and cells stays on the top layer of the membrane, which is consistent with endocytosis. On the other hand, aggressively penetrating peptides like pVEC, MAP, and cecropin B deeply inserted into the membrane, showed structural transition and membrane depolarization, consistent with our previous work [1] that shows damage to membrane integrity to allow the translocation.

Our CD and MC simulation methods provide a great platform for understanding the structure-function relationships of helical CPPs. Given that MC simulation can predict how the peptides interact with membranes and how the interaction is related to the translocation mechanism, cell-specific, rational peptides design can be achieved by simulating the peptides to select best candidates prior to cell-based experiments.

4.5. Conclusion

Our results show for the first time that we can use CD to detect secondary structure transitions for CPPs during their interaction with the fungal pathogen *C. albicans*. Although CPPs may remain unstructured in aqueous solution, CD spectra and MC simulations, combine to indicate that, while electrostatic forces dominate the surface interaction between the helical peptides and the membrane, a closer interaction with the hydrophobic domain of the bilayers promotes a structural transition and leads to insertion and membrane disruption. These data from each of our approaches strongly correlate with each other, as well as previous CPP research in fungal cells. Our methods provide a platform for understanding the structure-function relationships of CPPs and for predicting the behavior of CPPs at the molecular level, which will aid in the design of peptides with specific properties and functions.

4.6. Reference

1. Gong Z., K.A., *Translocation of cell-penetrating peptides into Candida fungal pathogens.* Protein Science, 2017. **(Accepted)**.
2. Mochon, A.B. and H.P. Liu, *The Antimicrobial Peptide Histatin-5 Causes a Spatially Restricted Disruption on the Candida albicans Surface, Allowing Rapid Entry of the Peptide into the Cytoplasm.* Plos Pathogens, 2008. **4**(10).
3. Richard, J.P., et al., *Cell-penetrating peptides: a re-evaluation of the mechanism of cellular uptake.* Biophysical Journal, 2003. **84**(2): p. 212a-212a.
4. Holm, T., et al., *Uptake of cell-penetrating peptides in yeasts.* Febs Letters, 2005. **579**(23): p. 5217-5222.
5. Bahnsen, J.S., et al., *Antimicrobial and cell-penetrating properties of penetratin analogs: effect of sequence and secondary structure.* Biochim Biophys Acta, 2013. **1828**(2): p. 223-32.
6. Magzoub, M., et al., *Interaction and structure induction of cell-penetrating peptides in the presence of phospholipid vesicles.* Biochimica et Biophysica Acta (BBA) - Biomembranes, 2001. **1512**(1): p. 77-89.
7. Magzoub, M., L.E.G. Eriksson, and A. Gräslund, *Comparison of the interaction, positioning, structure induction and membrane perturbation of cell-penetrating peptides and non-translocating variants with phospholipid vesicles.* Biophysical Chemistry, 2003. **103**(3): p. 271-288.
8. Deshayes, S., et al., *Primary Amphipathic Cell-Penetrating Peptides: Structural Requirements and Interactions with Model Membranes.* Biochemistry, 2004. **43**(24): p. 7698-7706.
9. Ruzza, P., et al., *Cell-Penetrating Peptides: A Comparative Study on Lipid Affinity and Cargo Delivery Properties.* Pharmaceuticals (Basel), 2010. **3**(4): p. 1045-1062.
10. Yang, S.-T., et al., *Cell-Penetrating Peptide Induces Leaky Fusion of Liposomes Containing Late Endosome-Specific Anionic Lipid.* Biophysical Journal, 2010. **99**(8): p. 2525-2533.
11. Heitz, F., M.C. Morris, and G. Divita, *Twenty years of cell-penetrating peptides: from molecular mechanisms to therapeutics.* British Journal of Pharmacology, 2009. **157**(2): p. 195-206.
12. Hitchcock, C.A., K.J. Barrett-Bee, and N.J. Russell, *The lipid composition of azole-sensitive and azole-resistant strains of Candida albicans.* J Gen Microbiol, 1986. **132**(9): p. 2421-31.
13. Chaffin, W.L., *Candida albicans cell wall proteins.* Microbiol Mol Biol Rev, 2008. **72**(3): p. 495-544.
14. Hube, B., *Candida albicans secreted aspartyl proteinases.* Current topics in medical mycology, 1996. **7**(1): p. 55-69.
15. Malgieri, G., et al., *Structural Basis of a Temporin 1b Analogue Antimicrobial Activity against Gram Negative Bacteria Determined by CD and NMR Techniques in Cellular Environment.* ACS Chemical Biology, 2015. **10**(4): p. 965-969.

16. Avitabile, C., L.D. D'Andrea, and A. Romanelli, *Circular Dichroism studies on the interactions of antimicrobial peptides with bacterial cells.* Scientific Reports, 2014. **4**: p. 4293.
17. Gofman, Y., T. Haliloglu, and N. Ben-Tal, *Monte Carlo simulations of peptide-membrane interactions with the MCPep web server.* Nucleic Acids Res, 2012. **40**(Web Server issue): p. W358-63.
18. Zelezetsky, I. and A. Tossi, *Alpha-helical antimicrobial peptides--using a sequence template to guide structure-activity relationship studies.* Biochim Biophys Acta, 2006. **1758**(9): p. 1436-49.
19. Xie, J., et al., *Antimicrobial activities and action mechanism studies of transportan 10 and its analogues against multidrug-resistant bacteria.* J Pept Sci, 2015. **21**(7): p. 599-607.
20. Fischer, R., et al., *Break on through to the other side - Biophysics and cell biology shed light on cell-penetrating peptides.* Chembiochem, 2005. **6**(12): p. 2126-2142.
21. Singh, J., Joshi, et al. *Enhanced cationic charge is a key factor in promoting staphylocidal activity of alpha]-melanocyte stimulating hormone via selective lipid affinity*. Scientific Reports, 2016, 6, 31492.
22. Scheinpflug, K., et al. *Antimicrobial peptide cWFW kills by combining lipid phase separation with autolysis*. Scientific Reports, 2017, 7, 44332.
23. Murugan, et al. *De novo design and synthesis of ultra-short peptidomimetic antibiotics having dual antimicrobial and anti-inflammatory activities*. PLoS One, , 2013, 8(11), e80025.

Chapter 5. Rational engineering of CPPs for fungal pathogens

5.1. Introduction

In Chapter 3, I identified the CPPs that can be applied to target fungal pathogens. I validated the idea of utilizing CPPs for cargo delivery and treating fungal infections caused by *C. albicans*, even though the peptides were initially discovered or designed for mammalian cell studies. However, not all the peptides we screened can translocate into fungal cells, suggesting that CPPs can be specific for different species, suggesting additional study of the properties of CPPs that affect the translocation mechanisms and specificities.

In Chapter 4, we explored the mechanisms of membrane association and related that to our translocation studies to seek a molecular explanation for cell entry of CPPs. The charge and the hydrophobicity play important roles in determining the translocation mechanisms. As previous work suggested, peptide-cell interactions and toxicity are directly related to charge and hydrophobicity [1, 2]. Rationally designed peptides with a higher net charge affected the cell viability more significantly [1, 2]. Karagiannis *et al.* also suggested that the net charge of short peptides does not only affect the membrane association, but also could facilitate deeper membrane interaction of the hydrophobic residues [3]. Thus, net charge and hydrophobicity of the peptides should be carefully studied to understand and specify CPP-cell interactions.

Understanding the structure-function relationship will also benefit the rational design of CPPs for specific cell types, such as only targeting fungal cells without attacking host mammalian cells. Previous work with antimicrobial peptides showed that the properties of peptides affect the selectivity of the peptides for *C. albicans* and human red blood cells [2], indicating the potential in modulating peptide properties to modulate specificity. pVEC was previously shown to only affect the viability of microbial cells [4-8], without reducing the viability of mammalian cell lines [5, 9], making it a promising candidate for further engineering to enhance targeting of fungal cells. SynB was also studied as a "safe" cargo delivery vehicle for both mammalian cells and *C. albicans.* This provides another opportunity to engineer CPPs for specificity [8, 10] and allow cargo delivery without toxicity.

In this study, we designed new CPPs based on the two well-studied peptides, pVEC and SynB, to understand the structure-function relationship and to improve the specificity and efficacy of CPPs towards a fungal pathogen. Our data indicate that net charge of peptides positively correlates with the translocation efficacy and the antifungal activity of the peptides. CPPs with high net charges tend to enter cells via direct translocation and traffic to the cytosol, which is promoted by a close interaction with the membrane. The hydrophobicity does not directly affect the translocation efficacy; however, it alters the membrane association pattern and affects the translocation mechanisms. Our newly designed peptides do not significantly affect the viability of mammalian cell lines, suggesting a promising opportunity to apply them for directly killing fungal pathogens around normal host tissues. Overall, our rational design of CPPs helps build understanding of CPPs to predict their behaviors

against both fungal cells and mammalian cells and to design them for desired interactions.

5.2. Materials and methods

5.2.1. Peptides

The peptides listed in **Table 5.1** were commercially synthesized at >95% purity with an N-terminal 5-carboxyfluorescein (FAM) (Genscript, Piscataway, NJ). The lyophilized peptides were reconstituted in sterile, ultrapure H_2O and diluted to a final concentration of 10 mM Na_2HPO_4 buffer.

Table 5.1 Rationally designed peptides for studying the property-function relationship[a]

	Sequence																		Net Charges[a]	% Hydrophobic Residues	Purpose
	1	2	3	4	5	6	7	8	9	10	11	12	13	14	15	16	17	18			
pVEC	L	L	I	I	L	R	R	R	I	R	K	Q	A	H	A	H	S	K	+8	44%	Original
1	L	L	I	I	L	R	R	R	I	R	K	R	A	H	A	H	R	K	+10	44%	Increase charge
2	L	L	I	I	L	R	R	S	I	R	K	Q	A	H	A	S	S	K	+6	44%	Decrease charge
3	L	L	I	I	L	S	R	R	I	R	K	Q	A	S	A	H	S	K	+6	44%	Decrease charge
4	L	L	I	I	L	R	R	R	I	R	K	L	A	H	A	H	L	K	+8	56%	Increase Hydrophobicity
5	L	L	I	I	L	R	R	R	I	R	K	Q	S	H	S	H	S	K	+8	33%	Decrease Hydrophobicity
6	L	S	I	I	S	R	R	R	I	R	K	Q	A	H	A	H	S	K	+8	33%	Decrease Hydrophobicity
SynB	R	G	G	R	L	S	Y	S	R	R	R	F	S	T	S	T	G	R	+6	16%	Original
1	R	G	G	R	L	K	Y	R	R	R	R	F	S	T	S	T	G	R	+8	16%	Increase charge
2	R	G	G	R	L	S	Y	S	R	R	R	F	K	T	R	T	G	R	+8	16%	Increase charge
3	R	G	G	S	L	S	Y	S	R	R	R	F	S	T	S	T	G	S	+4	16%	Decrease charge
4	R	G	G	R	L	S	Y	S	S	R	S	F	S	T	S	T	G	R	+4	16%	Decrease charge
5	R	G	W	R	L	A	Y	A	R	R	R	F	S	T	S	T	G	R	+6	39%	Increase Hydrophobicity
6	R	G	L	R	L	L	Y	S	R	R	R	F	S	T	L	T	G	R	+6	39%	Increase Hydrophobicity
7	R	G	G	R	S	S	S	S	R	R	R	F	S	T	S	T	G	R	+6	6%	Decrease Hydrophobicity
8	R	G	G	R	S	S	S	S	R	R	R	F	K	T	R	T	G	R	+8	6%	Decrease Hydrophobicity Increase charge

[a] Includes only charge due to amino acid side chains and not N-terminal free amine

5.2.2. *Candida* strains and culture conditions

C. albicans strain SC5314 was purchased from American Type Culture Collection (ATCC, Manassas, VA). *Candida* cells were inoculated from yeast-

peptone-dextrose (YPD) agar plates (1% w/v yeast extract), 2% w/v peptone, 2% w/v glucose, and 2% w/v agar) into 5 mL of liquid YPD medium (1% w/v yeast extract, 2% w/v peptone, and 2% w/v glucose) and grown overnight at 30 °C while shaking at 230 rpm. The cells in the overnight culture were subcultured into 5 mL of fresh YPD medium at OD_{600}=0.1 (equivalent to ~2×10^6 CFU/mL). The culture was then grown at 30 °C to OD_{600}=0.5 (equivalent to ~1×10^7 CFU/mL) while shaking. Cells were harvested by centrifugation at 4,000 × g for 10 min and washed twice with 10 mM Na_2HPO_4 buffer before use in downstream assays.

5.2.3. Quantification of translocation

For each peptide, 100 µL of peptide solution (2–100 µM), depending on the experiment) was prepared in 10 mM Na_2HPO_4 buffer, mixed with 100 µL of fungal cell suspension containing 5×10^5 cells in 10 mM Na_2HPO_4 and incubated at 30 °C for 30 or 60 min. Cells were collected by centrifugation at 5,000 ×g for 10 min at 4 °C and washed once with 10 mM Na_2HPO_4. The cell pellet was then incubated with 200 µL of 0.025% trypsin (Invitrogen, Waltham, MA) at 37 °C for 5 min to remove surface-bound peptide [11]. Cells were collected and washed again with 10 mM Na_2HPO_4. For yeast vacuole staining, CellTracker Blue CMAC (Invitrogen Molecular Probes, Waltham, MA) was added into the washed cell suspension at 1 µM and incubated at ambient temperature for 10 min. Propidium iodide (PI, 1 $mg\cdot ml^{-1}$; Invitrogen, Waltham, MA) was added at 0.2 $mg\cdot ml^{-1}$ immediately before imaging as needed to examine the membrane integrity. For quantification of translocation, the cells were resuspended in 150 µL of 10 mM Na_2HPO_4 after trypsin treatment and the final wash. Cell suspensions were analyzed for FAM and PI fluorescence using a BD

FACSCanto II flow cytometer (BD Biosciences, San Jose, CA). Only single cells were selected for analysis, and the analysis was preformed using FlowJo software (FLOWJO Inc., Ashland, OR).

5.2.4. Antifungal activity assay

In order to assess the antimicrobial activity of the peptides, a microdilution assay was performed. After subculturing cells and growing the culture to OD_{600}=0.5, a 5×10^5 cells/mL cell suspension was prepared in 10 mM Na_2HPO_4. Serial dilutions (20 µL) of the peptides were prepared at 0.2 µM–100 µM in 96-well plates, and the cell suspension (20 µL) was then added into each well. A control well containing 50 µM free FAM in 10 mM Na_2HPO_4 buffer was used as a control. The plate was incubated at 30 °C with vigorous shaking at 400 rpm for 60 min. Treated cells were diluted 20-fold in 10 mM Na_2HPO_4 buffer, and 100 µL of diluted cell suspension was added into 100 µL fresh YPD medium in a new 96-well plate. Plates were incubated at 30 °C with vigorous shaking for 16 hours, and the OD_{600} of the wells was measured using a 96-well plate reader (BioTek, Winooski, VT). The percentage of killing was calculated from

$$\text{Killing}\ (\%) = (1 - \frac{\text{OD}_{600,\text{peptide}}}{\text{OD}_{600,\text{control}}})\times 100 \qquad (1)$$

Minimal inhibitory concentrations were determined as the minimum concentration resulting in a 50% reduction in cell viability (MIC50).

5.2.5. Membrane depolarization assay

Membrane depolarization was evaluated using 3,3'-dipropylthiadi-carbocyanine iodide ($DiSC_3(5)$). Subcultured *C. albicans* cells were washed twice with 10 mM Na_2HPO_4 buffer and concentrated to a final OD_{600}=1.0. $DiSC_3(5)$

(ThermoFisher) was diluted to a stock concentration of 1 M. A Volume of 990 µL of cell suspension was added to a glass micro-cuvette, and the fluorescence emission was measured using a fluorometer (Molecular Devices; 633 nm excitation and 666 emission filters). This concentrated cell suspension containing no peptide was used to measure the baseline fluorescence level for 60 sec with data collected every 3 sec. The $DiSC_3(5)$ stock solution (1 µL) was added into the suspension and the fluorescence was measured for another 120 sec until the reading reached a steady level. A volume of 1 µL of 50 g/L glucose stock solution was added into solution to further reduce the fluorescence level for another 120 sec. A volume of 10 uL of peptides solution was added into the solution and the fluorescence signal was measured for 600 sec. All experiments were performed with three replicates.

5.2.6. Monte Carlo simulation

To understand the main force field of peptide-membrane interaction, we used a Monte Carlo simulation model to simulate membrane binding for peptides with potential helical structures upon interactions. MC simulations of the peptides were performed using the MCPep server (available online at http://bental.tau.ac.il/MCPep/) [12]. The hydrophobicity of the membrane was represented as a smooth profile of 30 Å width, similar to a fungal cell membrane [13], with the hydrophobic surface at a distance of 20 Å from the mid-plane. The negative charge was estimated based on the composition of *C. albicans* cell membranes [13], i.e., 20 % phosphatidylinositol + 17 % (PS) + 3 % (PG) = 40% charged lipid. The solution was set with 0.01 M monovalent salts. The MC simulation was performed with 3 independent runs with 500,000 MC cycles in each run. The total free energy of membrane association was

calculated as the difference between the free energies of the peptide in water and in the membrane. The average distance to the mid plane and the helical content percentage of each individual residue were simulated.

5.2.7. Mammalian cells uptake and toxicity

Human embryonic kidney cells (HEK293T) were purchased from ATCC (Manassas, VA, USA). Cells were cultured in media composed of Dulbecco's Modified Eagle's Medium with high glucose and L-glutamine (ThermoFisher, Waltham, MA, USA), 10% fetal bovine serum (FBS) (ThermoFisher), and 1% penicillin-streptomycin 10,000 U/mL (ThermoFisher). Cells were passaged at 70% to 90% confluency. Cells were washed with phosphate-buffered saline (PBS; VWR, Radnor, PA, USA), and detached with 0.025% trypsin-ethylenediaminetetraacetic acid (EDTA, Invitrogen). All cells were cultured at 37 °C, 50% humidity, and 5% CO_2:95% air.

For evaluating the translocation efficacy of CPPs in mammalian cells and their effect on viability of mammalian cells, HEK293T cells were cultured in a 12-well tissue culture treated polystyrene plate, such that cells were 90% to 100% confluent for the translocation experiment. Culture media was changed to FBS-free media the night prior to the uptake experiment. Cells were rinsed with PBS, then each well received 1 mL of peptide solution (10 μM) for experimental wells or 10 mM sodium phosphate buffer for control wells. Cells were incubated with the peptide solution or control buffer for 30 min at 37 °C. The peptide solution was subsequently removed, and cells were washed with PBS. Next, 0.25% trypsin-EDTA was added to each well, and cells were incubated for 5 min at 37 °C to facilitate cell detachment

from the well and peptide detachment from the cells. Cells were then washed with PBS, resuspended in 250 μL of PBS, and transferred to the respective flow cytometer tubes, with 1 μL of 1 mg/ml propidium iodide added right before sample testing.

5.3. Results

5.3.1. Quantification of translocation

To study the effect of the charge and hydrophobicity of CPPs on translocation, we designed new peptides by systematically varying the amino acids to change the properties of the peptides (**Table 5.1**). All peptides were commercially synthesized with an N-terminal FAM fluorescent label, serving as the intracellular reporter and vacuolar localization indicator [8].

To evaluate the translocation efficacy and localization pattern with *C. albicans*, we incubated cells with each of the peptides and quantified the translocation using flow cytometry (**Figure 5.1**). Compared with the parent peptides, the derivatives with a higher net charge (+2 higher) had a stronger translocation efficacy (pVEC 1, SynB 1, SynB 2 and SynB 8). pVEC 2, pVEC 3, SynB 3 and SynB 4, which have a lower net charge (-2 lower), showed reduced cellular uptake or even complete loss of penetration for SynB 3. Meanwhile, altering the hydrophobicity of peptides did not significantly affect the cellular entry efficacy (pVEC 4-6 and SynB 5-7). By combining the higher net charge and reduced hydrophobicity, we were still able to achieve an enhanced translocation (SynB 8). These results suggest that net charge positively affects the level of uptake.

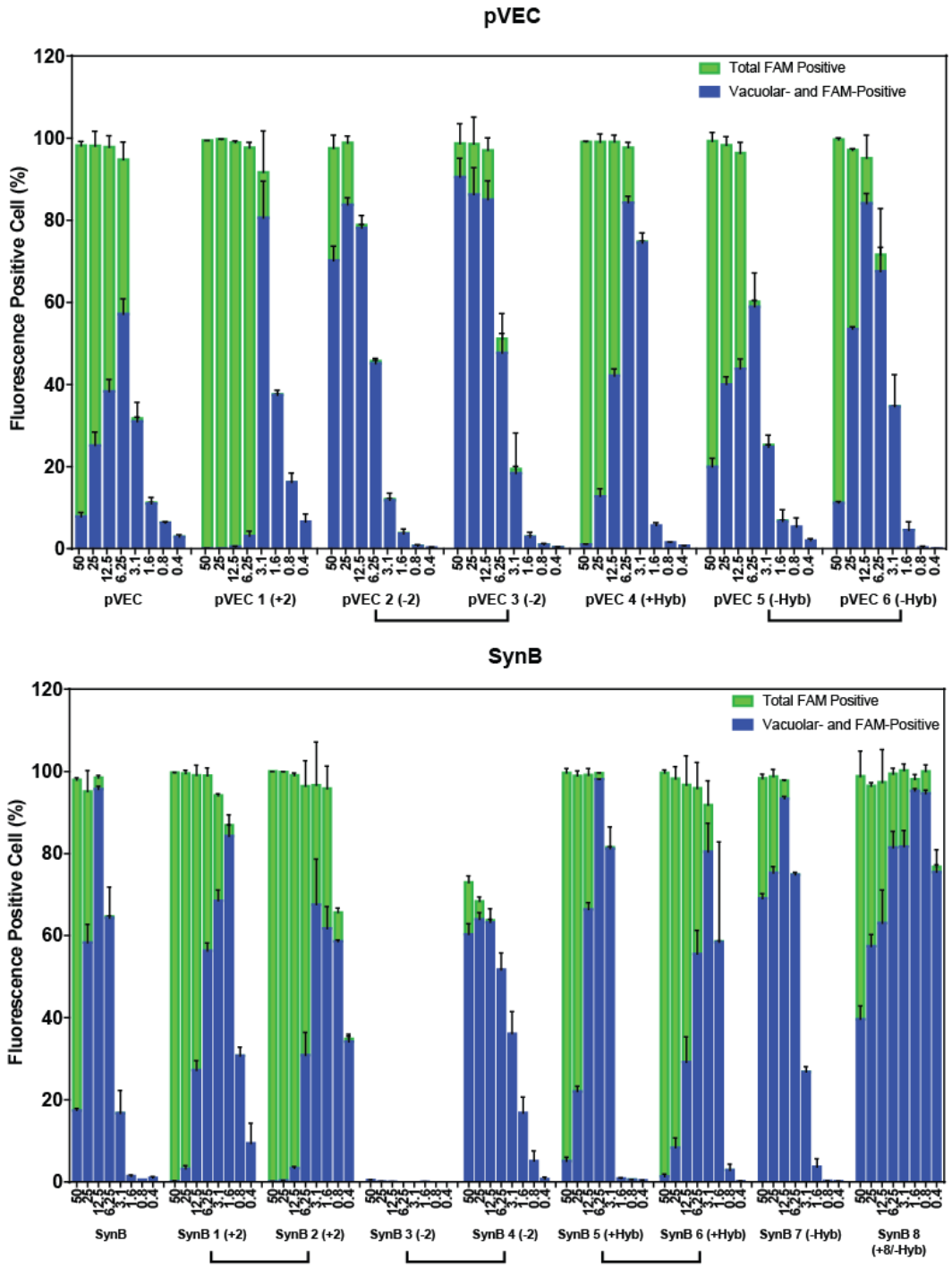

Figure 5.1 Quantification of cellular location of CPPs in *C. albicans*. Cells were incubated with serial dilutions of peptide (1-50 µM) at 30 °C for 1 h, washed with trypsin, and incubated with CellTracker Blue vacuolar stain at room temperature for 10 min. Flow cytometry data were collected for FAM (peptide) fluorescence and vacuolar stain fluorescence. The percentage of cells with FAM fluorescence and with both FAM and vacuolar fluorescence were quantified. Error bars represent the standard error of the mean for three separate experiments (*N*=3).

In addition, we also evaluated whether these changes were due to the amino acids changes or to the specific location of the modifications. Except SynB 3 and SynB4, the derivatives with same amino acid mutations but at different locations did not show a significant change in the behavior of peptides (for example, compare pVEC 2/pVEC 3 or SynB 1/SynB 2). The complete loss of translocation of SynB 3 might be due to loss of a critical residue, as the R→S modifications did not cause a loss of efficacy for the SynB 4 variant.

5.3.2. Translocation mechanism

Our translocation study not only quantified the effects of modifications on the efficacy of translocation, but also revealed the effect of these changes on the translocation mechanism. As our previous studied suggested, FAM and yeast vacuolar stains can be used to evaluate the uptake mechanism as yeast vacuoles are involved in the cellular trafficking process [8]. The higher extent of cytosolic peptide at low concentration is consistent with a higher degree of direct translocation, and endocytosis is more involved for peptides trafficked through vacuoles. Peptides appeared to be present more in the cytosol when the surface net charges were increased (pVEC 1, SynB 1, SynB 2, and SynB 8, **Figure 5.1**). A slightly stronger cytosolic tendency was observed for derivatives with a higher hydrophobicity (pVEC4, SynB 5 and SynB 6). By reducing the net charge or the hydrophobicity, we were able to observe more intracellular trafficking through vacuoles for both groups of peptides. When we combined the high net charge and reduction of hydrophobicity, we were able to achieve high uptake efficacy and a high level of vacuolar trafficking (correlated to low toxicity towards *C. albicans* as discussed in Chapter 3) with the

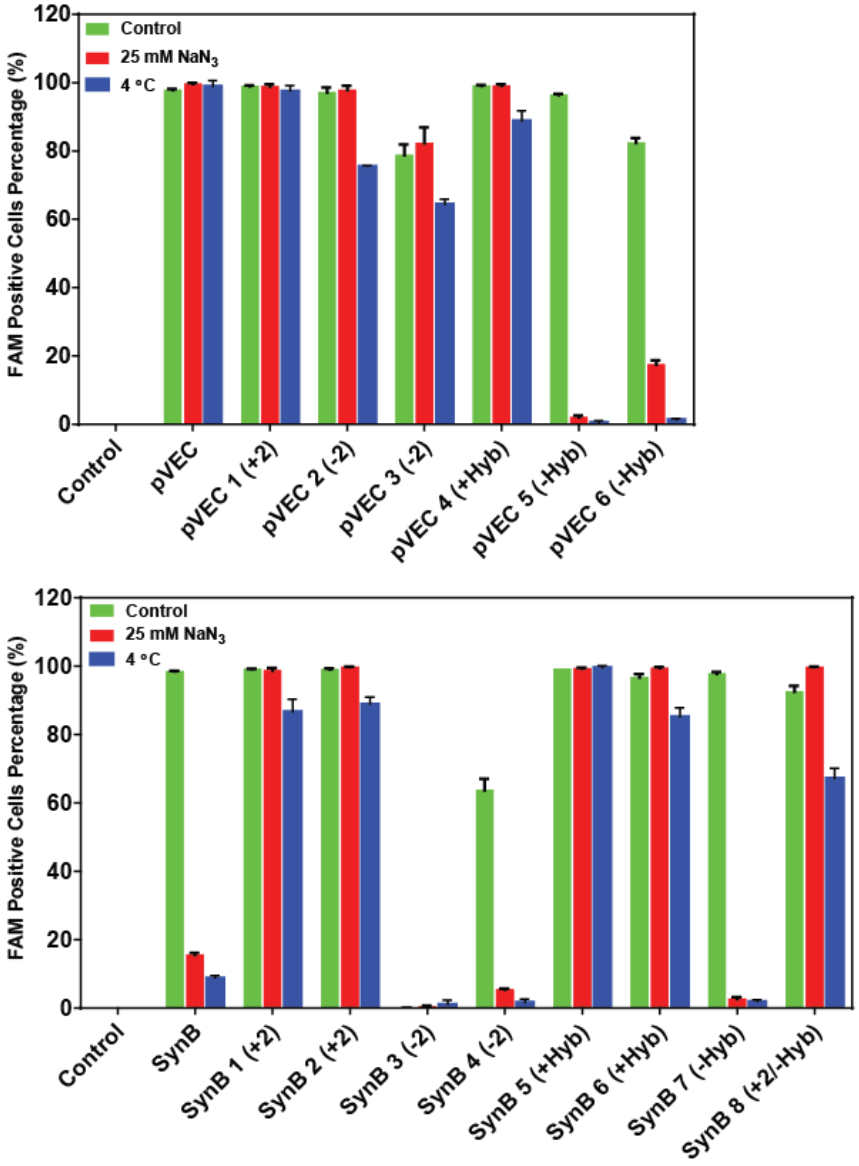

Figure 5.2 CPP translocation into *C. albicans* under conditions that inhibit energy-dependent endocytosis. Cells were incubated with peptides (10 µM) for 1 h. Control samples were incubated at 30 °C. Endocytosis was inhibited by adding 25 mM NaN3 or by changing the incubation temperature to 4 °C. The percentage of cells exhibiting FAM fluorescence was quantified by flow cytometry. Error bars represent the standard error of the mean for three separate experiments (N=3).

same peptide (SynB 8). Most importantly, our work suggests that we can alter the translocation mechanisms by changing the properties of peptides. The parent SynB has a higher tendency of translocation through vacuoles indicating an endocytic translocation, but the extra net charge led to data more consistent with direct

translocation related process at low concentration, where more cytosolic peptide was detected.

To further confirm our observation, we studied endocytosis of the peptides at low temperature and in the presence of NaN_3, conditions that inhibit energy-dependent endocytosis (**Figure 5.2**). The parent pVEC peptide used an energy-independent process to penetrate into cells, where the uptake of SynB was energy dependent. A higher net charge (pVEC 1, SynB 1, SynB 2, and SynB 8) maintained the translocation efficacy under ATP-inhibition conditions, indicating energy-independent translocation. A similar effect was observed as we increased the number of hydrophobic residues of the peptides (pVEC 4, SynB 5 and SynB 6). Reduced charge or hydrophobicity resulted in a more energy-dependent mechanism. Our localization and endocytosis studies together helps us to understand how the properties of peptides affect and change the translocation mechanisms.

In addition to endocytosis, direct translocation, which would potentially affect the membrane integrity, has been widely proposed as an uptake mechanisms for many CPPs. To evaluate whether membrane destabilization plays a role in translocation of the peptides in our study, we used PI and $DiSC_3(5)$ to identify pore formation in the membranes during CPP translocation into *C. albicans* (**Figure 5.3**). Overall, pVEC affected the membrane integrity more significantly than SynB for all peptide variants. pVEC has been proposed to enter the cells partially via direct translocation [8], while SynB entered cells through endocytosis (Chapter 3). Reducing charge and hydrophobicity significantly reduced the membrane damage for both peptides, except pVEC 3 showed moderate membrane depolarization at early time points (**Figure 5.3**

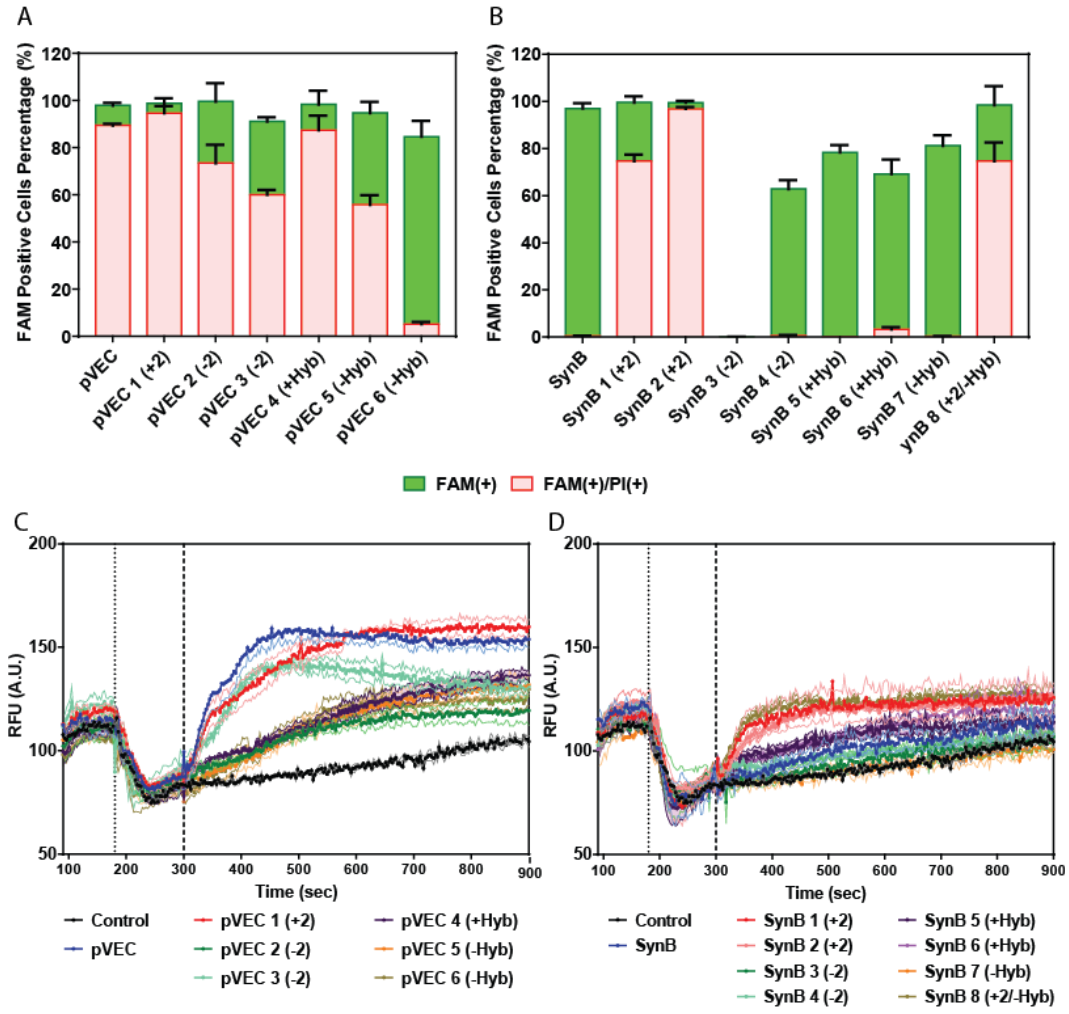

Figure 5.3 Effect of CPPs on integrity of cell membrane. Flow cytometry data indicating the percentage of cells with CPP translocation (FAM fluorescence) and with PI uptake in *C. albicans* in the presence of 10 µM pVEC/pVEC derivatives (A) or SynB/SynB derivatives (B). Membrane depolarization was evaluated by the release of DiSC3(5) into the solution and the increment of the fluorescence. At 60 sec, DiSC3(5) probe was added into cell suspension and reference fluorescence level was measured after 90 sec. At 180 sec,10% glucose was added to further reduce the background. A volume of 10 µL of 1 mM stock solution of pVEC peptides (C) and SynB peptides (D) was added to evaluate the fluorescence release due to the membrane depolarization. For (A) and (B), error bars represent the standard error of the mean for three separate experiments (N=3). For (C) and (D), each data point represents the average of three replicates with lines of a lighter shade indicating the standard error (N=3).

C). The charge played a more important role in membrane damage, as the derivatives with higher charge always showed a higher PI permeability and depolarized membrane potential, and the extra charge overcame the effect from the reduction of

hydrophobicity (SynB 7 vs. SynB 8). However, reducing hydrophobicity could potentially reduce the membrane damage, as deep interaction with the bilayer core may be more limited (pVEC vs. pVEC 6, and SynB 3 vs. SynB 8).

5.3.3. Antifungal activity

The PI stain could potentially indicate cell death due to a permeabilized membrane. Thus, our observation of propidium iodide permeability (**Figure 5.3**) could indicate that the CPP derivatives kill fungal cells. To examine the toxicity of CPPs toward *C. albicans*, we incubated the cells with serial dilutions of the peptides. At high concentrations of peptide, we observed significant toxicity for all peptides (**Figure 5.4**). For the peptides with more cytosolic localization (**Figure 5.1**) and more PI permeability (**Figure 5.3**), which includes those with a higher net charge/hydrophobicity (pVEC1, pVEC 4, SynB 1, SynB 2, and SynB 8), the

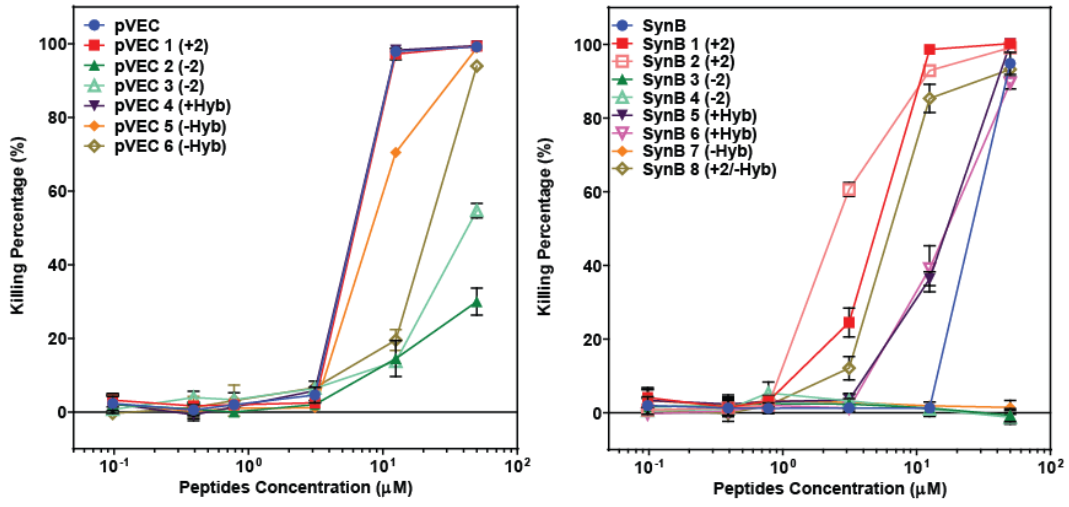

Figure 5.4 Toxicity of CPPs and the derivatives toward *C. albicans*. Cells were incubated with serial dilutions of peptides (0.2-100 μM) for 1 h at 30 °C. Samples were diluted, mixed with YPD medium, and incubated at 30 °C for 16 h. Optical density (OD_{600}) of the cultures was measured and converted to killing percentage. Error bars represent the standard error of the mean for three separate experiments (*N*=3).

antifungal activity was higher than for the ones with a lower net charge/hydrophobicity. The net charge has a higher impact on toxicity than hydrophobicity, as the derivatives with different charges always showed more significant changes in the antifungal activities compared to those with altered hydrophobicity.

Our antifungal activity assays can also serve as a gauge to evaluate the effect of peptide properties on the activities. By tuning the charge and hydrophobicity of the peptides, we can design peptides with stronger or weaker antifungal activities.

5.3.4. Simulations of peptide-membrane interactions

To gain insight into the membrane association process for the peptides, we used a Monte Carlo simulation to understand the peptide-membrane interactions at the molecular level [12]. This model is dedicated to simulation of peptides with potential α-helical conformations upon membrane binding and insertion. Although the data in in Chapter 4 suggests that the parent SynB does not form a helical structure while interacting with cells and membranes, we still included the SynB derivatives in these studies to explore potential shifts in the biophysical characteristics of SynB derivatives.

The free energy calculation provided a detailed analysis of the membrane association process (**Table 5.2**). For all peptides, the membrane association was thermodynamically favorable, as indicated by the negative free energy for the peptides in solution to bind the membrane (ΔG_{Total}). The major contribution to the membrane association was always the electrostatic force (ΔG_{coul}) due to the opposite charge states of the membranes (-) and the peptides (+). As the net charge of the

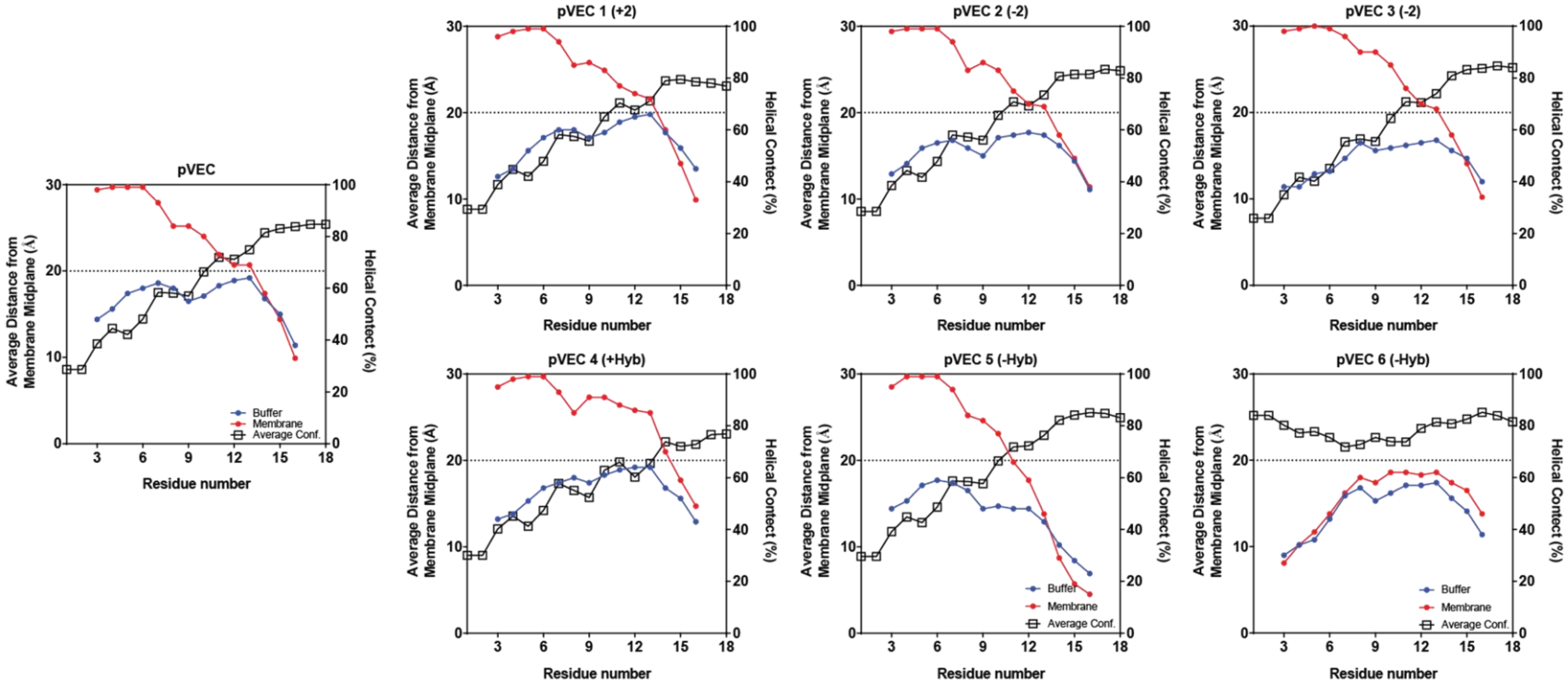

Figure 5.5 Monte Carlo simulation (MC) of the interaction between pVEC/pVEC derivatives and phosphate lipid membrane. The membrane was assumed to be 30 Å with 40% charged lipids to mimic fungal cell membranes, and the monovalent salts concentration was set to be 10 mM. Three independent MC simulation was run with a 50000 MC cycle in each independent run. The average of three runs was plotted against the residue number of the peptides. The helical content percentage of peptides in buffer (Blue circle) or in contact with membrane (Red circle) was plotted on the right y-axis. The average position of each residue (Black square, green triangle for cecropin B transmembrane case) was plotted on the left axis. The dash line represents the location of the phosphate group of the lipids polar heads.

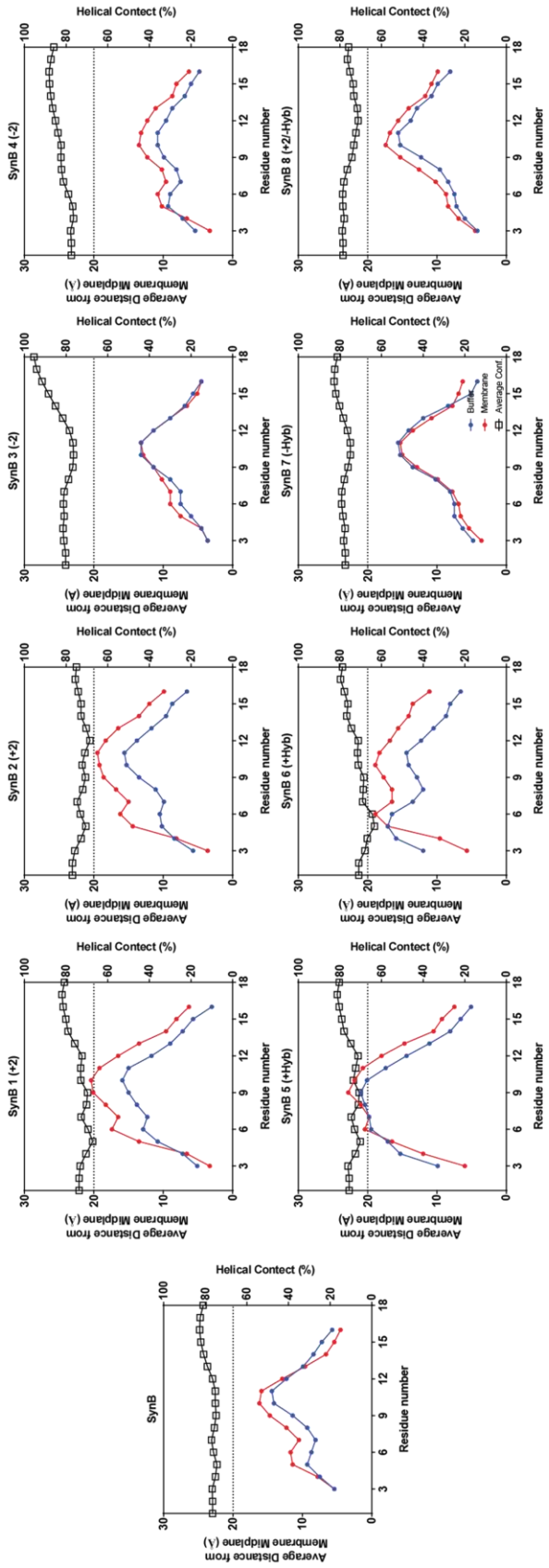

Figure 5.6 Monte Carlo simulation (MC) of the interaction between SynB/SynB derivatives and phosphate lipid membrane. The membrane was assumed to be 30 Å with 40% charged lipids to mimic fungal cell membranes, and the monovalent salts concentration was set to be 10 mM. Three independent MC simulation was run with a 50000 MC cycle in each independent run. The average of three runs was plotted against the residue number of the peptides. The helical content percentage of peptides in buffer (Blue circle) or in contact with membrane (Red circle) was plotted on the right y-axis. The average position of each residue (Black square, green triangle for cecropin B transmembrane case) was plotted on the left axis. The dash line represents the location of the phosphate group of the lipids polar heads.

Table 5.2 Membrane association free energy calculation from Monte Carlo simulation

Peptides	ΔG_{Total}[a] (kT)	ΔG_{conf}[b] (kT)	ΔG_{SIL}[c] (kT)	ΔG_{coul}[d] (kT)	ΔG_{def}[e] (kT)
pVEC	-28.58	-2.09	-9.95	-16.79	0.25
pVEC 1 (+2)	-32.95	-4.55	-9.73	-22.56	0.25
pVEC 2 (-2)	-26.77	-3.04	-9.84	-13.85	0.26
pVEC 3 (-2)	-26.84	-3.33	-9.93	-13.82	0.25
pVEC 4 (+Hyb)	-32.59	-2.98	-12.29	-17.67	0.25
pVEC 5 (-Hyb)	-29.20	-2.86	-9.74	-16.84	0.25
pVEC 6 (-Hyb)	-14.54	0.02	0.59	-15.41	0.25
SynB	-13.65	0.17	0.66	-14.75	0.26
SynB 1 (+2)	-21.81	-1.74	0.54	-20.85	0.25
SynB 2 (+2)	-21.48	-1.74	0.81	-20.76	0.25
SynB 3 (-2)	-8.81	0.09	0.47	-9.63	0.25
SynB 4 (-2)	-9.06	-0.57	0.36	-9.11	0.26
SynB 5 (+Hyb)	-14.27	0.36	0.27	-15.15	0.26
SynB 6 (+Hyb)	-17.57	0.26	-1.58	-15.81	0.25
SynB 7 (-Hyb)	-13.72	-0.45	1.08	-14.60	0.25
SynB 8 (+2/-Hyb)	-19.4	-0.72	1.40	-20.32	0.25

a. ΔG_{Total}, total free energy difference between the peptide in solution and with the membrane
b. ΔG_{conf}, free energy change due to membrane-induced conformational changes in the peptide
c. ΔG_{SIL}, free energy change due to the hydrophobic interaction with the core of bilayer
d. ΔG_{coul}, free energy change due to the electrostatic interactions between titratable residues of the peptide and membrane surface charge
e. ΔG_{def}, free energy penalty associated with fluctuations of the membrane width

peptides increased, this electrostatic force was stronger, such as was seen for pVEC 1, SynB 1, SynB 2, and SynB 8. Peptides with a lower net charge exhibited a lower electrostatic force contribution, including pVEC 2, pVEC 3, SynB 3 and SynB 4. The energy for membrane association was lowest for SynB 3, which showed almost no intracellular uptake. The hydrophobicity did not significantly affect this energy contribution. Compared to SynB, the derivatives SynB 1, SynB 2, and SynB 8 showed significant free energy for conformational transition, indicating structural shift upon membrane association. These calculations show that the electrostatic force plays a strong role in membrane association, so changing the charge of a peptide has an impact on this membrane association. However, these results must be viewed vary

cautiously, as the experimental secondary structure for the derivatives have not been determined and the MC simulations are only intended to be used for helical peptides.

Previous mechanistic studies in Chapter 3 suggested that pVEC enters cells via direct translocation and macropinocytosis and that the translocation of SynB is endocytosis-related [8]. In Chapter 4, I correlated the translocation with MC simulation, showing how free energy calculation can be used to explain and predict the translocation mode. The negative value of ΔG_{conf} and ΔG_{SIL} (representing free energy due to membrane association induced conformation changes and free energy due to hydrophobic interactions, respectively) along with the PI stain assay and endocytosis assay, could indicate deeper membrane interaction and membrane disruption. Except pVEC 6, all pVEC derivatives showed negative values for these two types of energy. As discussed above, pVEC peptides other than pVEC 6 also showed higher PI permeability (**Figure 5.3 A**), whereas pVEC 6 exhibited little intracellular PI staining. For SynB, none of the peptides showed significant negative values for structural transition and hydrophobic interaction, consistent with an endocytosis-dependent translocation and our experimental studies of endocytosis and membrane permeabilization (**Figures 5.2 and 5.3**). Importantly, the hydrophobicity of the peptides affected the value of ΔG_{conf} and ΔG_{SIL} more significantly than the charges, suggesting the deeper membrane interaction and translocation mechanism are more directly related to the hydrophobicity of the peptides.

To further investigate the peptide-membrane interaction and trans-membrane processes for the pVEC derivatives, we also used MC simulation to predict the peptide location in relation to the membrane bilayer (**Figure 5.5 and 5.6**). For pVEC

and the derivatives other than pVEC 6, all the peptides showed a partial insertion into the membrane. The inserted portion exhibited a higher helical content percentage, indicating a stronger tendency of forming an α-helical structure (**Figure 5.5**). This insertion can also be explained by our calculations from the simulations, as they showed a higher energy for structural transition and hydrophobic interaction (ΔG_{conf} and ΔG_{SIL}, **Table 5.2**). In contrast, pVEC 6 had a lower calculated energy of ΔG_{conf} and ΔG_{SIL}, the membrane insertion could no longer be observed and the helical content percentage was much lower.

For SynB and its derivatives, no significant free energy for conformational change and hydrophobic interaction was observed in our calculation, and we did not see significant membrane insertion for any peptides (Figure 5.6). Peptides with higher net charges or higher hydrophobicity showed ΔG_{Total} and closer interaction with the hydrophobic interface, including SynB 1, SynB 2, SynB 5 and SynB 6 (**Figure 5.6**). These peptides showed energy-independent translocation mechanisms (**Figure 5.2**) and high PI permeability (**Figure 5.3 B**). Although no significant helical structures were observed for any SynB peptides, these results can still aid the understanding of the relationship between the secondary structure of the peptides, the properties of the peptides, and the translocation mechanism. Obtaining experimental data on the secondary structures of the SynB derivatives will provide additional data and determine the level of trust that can be placed in these simulations.

5.3.5. Mammalian cell study

Our ultimate goal is to design optimal CPPs that can be applied to treat fungal infections. I observed toxicity towards fungal cells in this study, yet the effects on

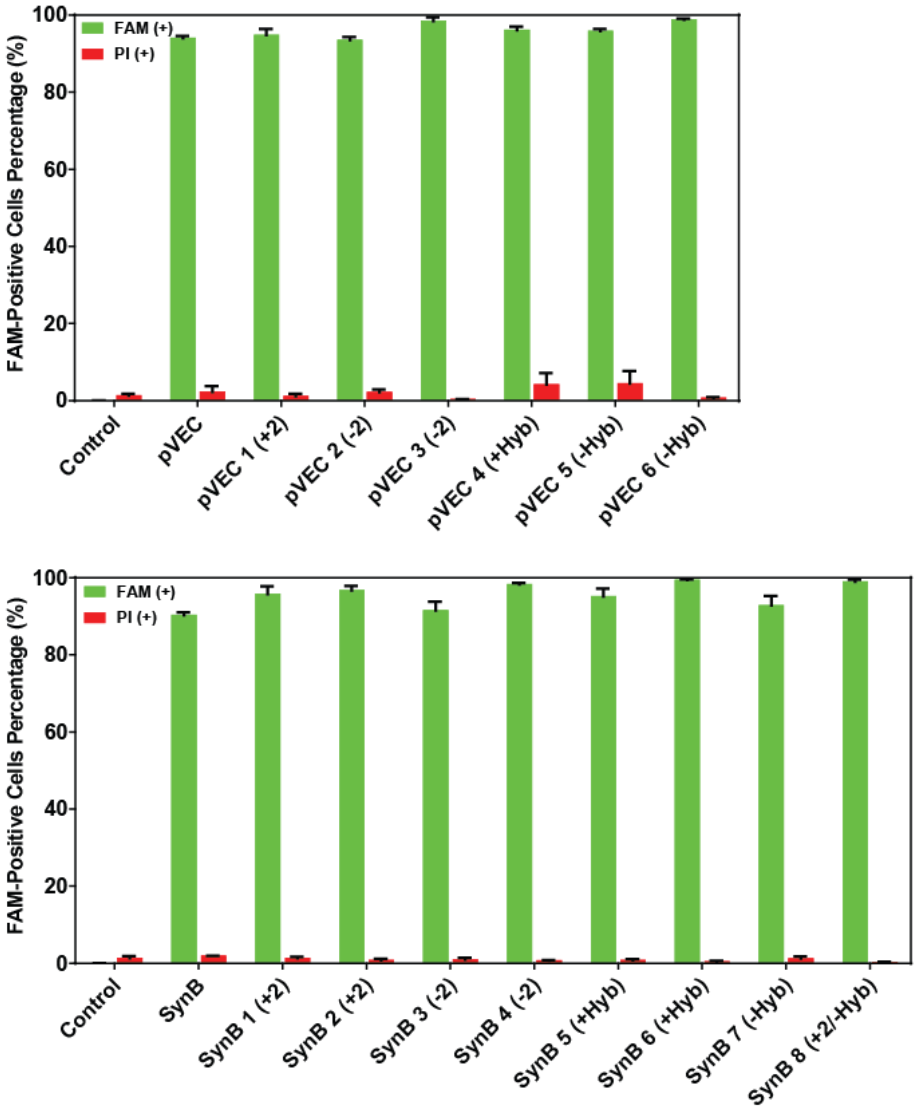

Figure 5.7 Evaluation of the translocation and cytotoxicity of CPPs and their derivatives towards HEK293T. A total count of 2×10^5 of cells were seeded and put into serum-free media a day for experiment. Cells were treated with 10 mM sodium phosphate buffer (Control) or 10 μM of peptide solution in 10 mM sodium buffer for 30 min at 37°C. Cells were carefully washed and trypsin treated to remove surface bounded peptides. PI was added prior to the flow cytometry measurement of the percentage of FAM-positive cells and the ones with PI uptake among these cells. Error bars represent the standard error of the mean for three separate experiments (N=3).

mammalian cell viability are also important. I evaluated the translocation of the CPPs into the mammalian cell line, HEK293T, as well as the effect of the CPPs on the viability of the mammalian cells (**Figure 5.7**). All peptides showed significant translocation at 10 μM, even SynB3, which completely lost the ability to translocate

into fungal cells. More importantly, although a high net charge or high hydrophobicity significantly enhanced the cytotoxicity towards *C. albicans*, we did not observe any viability loss for mammalian cells with any of the peptides. Our modification of CPPs did not directly affect the viability of mammalian cells, indicating the specificity of the peptides between two types of cells in terms of toxicity.

5.4. Discussion

Cell penetrating peptides (CPPs) have great potential in drug delivery and therapeutic application. Currently, the majority of CPPs studies have been performed in mammalian cells, with limited understanding of their interaction with microbial cells. In addition, most of the CPPs in the previous studies did not show the cell specificity required for developing CPPs as disease-specific drug delivery methods. In this study, we used a rational design approach to correlate the properties of the CPPs to their function and translocation mechanisms. This enables us to understand the structure-function relationship of the CPPs. We can also use our experiments to investigate the peptide-cell interaction and the mode of action and to improve the specificity of CPPs by tuning the properties of the peptides.

Since the peptides have an opposite charge compared to cell membranes, the net charge of peptides has been shown to play an important role in the translocation process of CPPs [3, 8, 14, 15]. We observed that a high net charge in CPPs strongly promoted intracellular delivery of the peptides. In addition to the higher translocation efficacy, it also led to a stronger tendency for cytosolic delivery (**Figure 5.1**) and a higher cytotoxicity (**Figure 5.4**). Direct translocation (**Figure 5.2 and 5.3**) and a

closer and stronger membrane interaction (**Figure 5.5 and 5.6**) is also associated with increased net charge. Our data indicate that a high net charge results in stronger membrane association and a more aggressive direct translocation mechanism, regardless of the original mode of action, as we modulated the translocation method of SynB from endocytosis to direct translocation by increasing the net charge.

After membrane association, the next step of the membrane interaction is related to the hydrophobicity, as the core of the bilayer is hydrophobic. By tuning the hydrophobicity, we can also control the efficacy of the uptake and the translocation mechanisms. While the hydrophobicity did not significantly affect the translocation efficacy (**Figure 5.1**), the intracellular trafficking, translocation mechanism, and membrane insertion are closely related to the number of hydrophobic residues on the peptides. We reduced the hydrophobicity to achieve a more energy-dependent uptake mechanism, lower disruption of the membrane integrity, and a lower toxicity towards fungal cells. This will enable us to develop CPPs as a "safer" vehicle for delivering cargo with biological activity without damaging the host cells.

To use CPPs as therapeutic tools for drug delivery or as antifungal agents, a low level of toxicity to mammalian cell lines is very important to ensure the safety of the treatment. We selected pVEC and SynB as peptides to study, because they have been reported to exhibit little effect on the viability of multiple mammalian cell lines [5, 6, 10, 16, 17]. Although we have observed significant toxicity towards fungal pathogens, we observed no significant loss of viability in HEK293T cells. This suggests that our newly engineered peptides can all be used for cargo delivery or to kill fungal cells without damaging mammalian cells that may also be present.

Interestingly, SynB 3, which showed no translocation into fungal cells, can significantly enter the mammalian cell line, indicating the strong specificity of this peptide and the impact of different membrane compositions on translocation into these two types of cells.

5.5. Conclusion

We have developed a series of novel CPPs based on two well-studied peptides. We were able to tune the translocation, toxicity, and mode of translocation by altering the net charge and hydrophobicity of the peptides. Our study provides data on the structure-function relationships for CPPs to improve understanding of the peptides and aid in the development of CPPs as novel therapeutic tools for treating fungal infections.

5.6. Reference

1. Karlsson, A.J., et al., *Antifungal activity from 14-helical beta-peptides.* J Am Chem Soc, 2006. **128**(39): p. 12630-12631.
2. Karlsson, A.J., et al., *Effect of sequence and structural properties on 14-helical beta-peptide activity against Candida albicans planktonic cells and biofilms.* ACS Chem Biol, 2009. **4**(7): p. 567-79.
3. Karagiannis, E.D., et al., *Rational Design of a Biomimetic Cell Penetrating Peptide Library.* ACS Nano, 2013. **7**(10): p. 8616-8626.
4. Palm, C., S. Netzerea, and M. Hallbrink, *Quantitatively determined uptake of cell-penetrating peptides in non-mammalian cells with an evaluation of degradation and antimicrobial effects.* Peptides, 2006. **27**(7): p. 1710-1716.
5. Elmquist, A., M. Hansen, and U. Langel, *Structure-activity relationship study of the cell-penetrating peptide pVEC.* Biochim Biophys Acta, 2006. **1758**(6): p. 721-9.
6. Elmquist, A., et al., *VE-cadherin-derived cell-penetrating peptide, pVEC, with carrier functions.* Experimental Cell Research, 2001. **269**(2): p. 237-244.
7. Gong Z., W., MT., Karley AN., Karlsson AJ., *Effect of a flexible linker on recombinant expression of cell-penetrating peptide fusion proteins and their translocation into fungal cells.* Mol Biotechnol, 2016.
8. Gong Z., K.A., *Translocation of cell-penetrating peptides into Candida fungal pathogens.* Protein Science, 2017. **(Accepted)**.
9. Saalik, P., et al., *Protein cargo delivery properties of cell-penetrating peptides. A comparative study.* Bioconjugate Chemistry, 2004. **15**(6): p. 1246-1253.
10. Tian, X.H., et al., *In vitro and in vivo studies on gelatin-siloxane nanoparticles conjugated with SynB peptide to increase drug delivery to the brain.* Int J Nanomedicine, 2012. **7**: p. 1031-41.
11. Richard, J.P., et al., *Cell-penetrating peptides. A reevaluation of the mechanism of cellular uptake.* Journal of Biological Chemistry, 2003. **278**(1): p. 585-90.
12. Gofman, Y., T. Haliloglu, and N. Ben-Tal, *Monte Carlo simulations of peptide-membrane interactions with the MCPep web server.* Nucleic Acids Res, 2012. **40**(Web Server issue): p. W358-63.
13. Hitchcock, C.A., K.J. Barrett-Bee, and N.J. Russell, *The lipid composition of azole-sensitive and azole-resistant strains of Candida albicans.* J Gen Microbiol, 1986. **132**(9): p. 2421-31.
14. Horn, M., et al., *Tuning the properties of a novel short cell-penetrating peptide by intramolecular cyclization with a triazole bridge.* Chemical Communications, 2016. **52**(11): p. 2261-2264.
15. Mickan, A., et al., *Rational design of CPP-based drug delivery systems: considerations from pharmacokinetics.* Curr Pharm Biotechnol, 2014. **15**(3): p. 200-9.
16. Rousselle, C., et al., *New advances in the transport of doxorubicin through the blood-brain barrier by a peptide vector-mediated strategy.* Molecular Pharmacology, 2000. **57**(4): p. 679-686.

17. Saar, K., et al., *Cell-penetrating peptides: A comparative membrane toxicity study.* Analytical Biochemistry, 2005. **345**(1): p. 55-65.

Chapter 6. Effect of a flexible linker on recombinant expression of CPP fusion proteins and their translocation into fungal cells[2]

6.1. Introduction

Although CPPs are capable of carrying protein cargo into cells, the recombinant production of CPP fusions to protein cargo can be challenging. The CPP-cargo protein fusion can exhibit low levels of expression or be found in inclusion bodies when produced in *Escherichia coli* cells, as has been observed for fusions of various cargos to the TAT peptide and a poly-arginine peptide [1-5]. Even if fusions can be produced and purified, the CPP-cargo fusion production may be substantially lower than the cargo protein alone [6], the solubility of the fusion may not be sufficient in a biological buffer [7], or the fusion may not successfully enter cells [2]. Finding methods to improve the recombinant expression and solubility of CPP fusions will aid in the development of CPPs as vehicles for carrying protein cargo into cells. One approach to improving the production of peptide-protein fusions is to incorporate a flexible peptide linker between the peptide and its fusion partner. One commonly used flexible linker is the glycine-serine linker $(G_4S)n$, which has

[2] This chapter has been published in the Molecular Biotechnology Journal and appears in this thesis with the journal`s permission:

Gong Z, Walls MT, Karley AN, Karlsson AJ
Effect of a Flexible Linker on Recombinant Expression of Cell-Penetrating Peptide Fusion Proteins and Their Translocation into Fungal Cells.
Mol Biotechnol. 2016 Dec;58(12):838-849.

been used to improve the expression of a number of proteins fusions [8-11]. $(G_4S)n$ linkers have also been used to improve the biological activity of antibody fragments, bifunctional enzymes, and many other proteins and protein fusions [12-17]. Although linkers have been used to enhance expression of many fusion constructs, their effect on expression of CPP fusions and on cellular uptake of CPPs, especially for fungal cells, has not been studied.

To improve the understanding of the effect a (G_4S) linker has on CPP expression, we genetically fused pVEC and NPFSD to green fluorescent protein (GFP) with and without the linker. We recombinantly produced the fusions containing each peptide in *E. coli*, purified the constructs, and evaluated their translocation into *C. albicans* cells. Our results show that the flexible linker improves the recombinant production of the CPP-GFP fusions, while having either a positive or neutral impact on uptake by the fungal cells.

Table 6.1 Primers used in this chapter

Primer name	Sequence (5' to 3')
SacI-ATG-GFP-F	gcgatggagctcatgagtaaaggagaagaacttttc
EcoRI-NPFSD-SacI-GFP	ttcggaattcaatggtgctgaccaacgaaaacccgttttctgatccggagctcagtaaaggagaagaa ctttc
EcoRI-NPFSD-G_4S-SacI-GFP	ttcggaattcaatggtgctgaccaacgaaaacccgttttctgatccgggaggcggtggaagcgagctc gagctcagtaaaggagaagaacttttc
pVEC-1-F	aattcaatgctgttgatcatcctgcgccgc
pVEC-1-R	tgcggcggcgcaggatgatcaacagcattg
pVEC-2-F	cgcatccgtaagcaggcccacgcgcatagtaaagagct
pVEC-2-R	ctttactatgcgcgtgggcctgcttacgga
pVEC-G_4S-F	cgcatccgtaagcaggcccacgcgcatagtaaaggaggcggtggaagcgagct
pVEC-G_4S-R	cgcttccaccgcctcctttactatgcgcgtgggcctgcttacgga

6.2. Materials and methods

6.2.1. Plasmid construction

Plasmids containing GFP and genetic fusions of NPFSD and pVEC to GFP were constructed using the pET21a(+) (Novagen) plasmid, which contains a C-

terminal hexahistidine tag (6XHis). All primers are provided in **Table 6.1**. To construct the plasmid containing GFP only, the DNA encoding GFP was amplified by PCR from a template plasmid in our lab stock using the primers SacI-ATG-GFP-F and GFP-NotI-R and inserted between the SacI and NotI sites of pET21a(+), resulting in pET21-GFP. To construct the plasmids containing genetic fusions of GFP to the NPFSD peptide, the DNA encoding GFP with an N-terminal NPFSD peptide was amplified using a forward PCR primer containing the NPFSD sequence with or without a C-terminal G_4S peptide linker (EcoRI-NPFSD-G4S-SacI-GFP-F and EcoRI-NPFSD-SacI-GFP-F, respectively) and the reverse primer GFP-NotI-R. The PCR products were then inserted between the EocRI and NotI sites of pET21a(+), resulting in pET21-NPFSD-G_4S-GFP and pET21-NPFSD-GFP. Plasmids containing genetic fusions of pVEC to GFP were constructed using annealed primers. For pET21-pVEC-GFP, the primer pair pVEC-1-top and pVEC-1-bottom and the primer pair pVEC-2-top and pVEC-2-bottom were 5' phosphorylated and then annealed to create the primer dimer pairs pVEC-1 and pVEC-2, respectively. The annealed pVEC1 had an EcoRI sticky end, and the annealed pVEC2 had a SacI sticky end; pVEC1 and pVEC2 also had complementary sticky ends, allowing them to anneal to each other. The two primer dimer pairs were then inserted between EcoRI and SacI of pET21-NPFSD to replace the DNA encoding NPFSD with the DNA encoding pVEC. Similarly, inserts constructed with the pVEC-G_4S-2-top and pVEC-G_4S-2-bottom primer pair and the pVEC-1-top and pVEC-1-bottom primer pair were inserted between EcoRI and SacI of pET21-NPFSD-GFP to generate pET21-pVEC-G4S-GFP. All plasmids were sequenced to confirm the constructs were correct.

6.2.2. Protein expression and purification

Plasmids containing the GFP and fusion protein constructs were transformed into E. coli BL21(DE3) electrocompetent cells for protein production. For most experiments, overnight cultures of BL21(DE3) cells were subcultured into fresh Luria-Bertani (LB) medium with ampicillin (100 μg/ml) at an optical density of OD600=0.05 and grown at 37 °C for 3 h while shaking at 225 rpm. Expression was then induced by adding 0.05 mM isopropyl β D 1 thiogalactopyranoside (IPTG, Fisher BioReagents), and the cultures were shaken at 37 °C for an additional 8 h. Cells were then pelleted by centrifugation at 4,300× g for 15 min and lysed with BugBuster Master Mix (EMD Millipore) following the manufacturer's protocol. Following centrifugation of the whole cell lysate at 11,000× g for 40 min at 4 °C, the supernatant was taken as the soluble fraction. For the experiments to evaluate protein expression at different induction conditions, analogous procedures were followed, except the induction of expression was done with different temperatures (20 °C, 30 °C, and 37 °C), induction times (2 h, 4 h, and 8 h), and IPTG concentrations (0.05 mM, 0.1 mM, and 0.5 mM).

The GFP and CPP-GFP fusions were purified from the soluble fraction of the cell lysate using immobilized metal affinity chromatography (IMAC). The soluble fractions of the lysates were passed through a 0.2 μm filter and applied to an IMAC Profinity column (Bio-Rad) attached to an NGC liquid chromatography system (Bio-Rad) to bind the C-terminal 6XHis tag to the column. Proteins were eluted in a buffer containing 300 mM KCl, 30 mM KH_2SO_4 and 500 mM imidazole. The eluate was dialyzed against 20 mM imidazole and applied to an Enrich-Q anion-exchange

column (Bio-Rad). The CPP-GFP fusion proteins were eluted from the anion-exchange column by increasing the concentration of NaCl in a stepwise manner from 250 mM to 400 mM. The purified proteins were stored at 4 °C after dialysis against 0.1× PBS. The concentration of each protein was measured on a NanoDrop instrument (Thermo Scientific) using the ε/1000 method, which measures the absorbance at 280 nm and uses Beer's Law to determine the molar concentration. The extinction coefficient (ε) for each protein was estimated based on the amino acid sequence using the ProtParam tool on the ExPASy website [18]. For quantifying the yield of purified protein, three biological replicates (three separate cultures) were prepared on separate days. Protein yields were compared with a paired t-test using a p-value of $p<0.1$ as significant.

Western blotting and SDS-PAGE were used to evaluate protein expression and purity. Western blotting was used to compare the amount of the protein constructs present in the crude soluble cell lysates. Samples were normalized by culture volume and separated on Any kD Mini-PROTEAN TGX gels (Bio-Rad). After transferring to a polyvinyl difluoride (PVDF) membrane, the GFP and CPP-GFP fusions were detected using an anti-GFP (Mouse) primary antibody (Abcam) and a horseradish peroxidase (HRP)-conjugated anti-mouse (Rabbit) secondary antibody (Abcam). The blot was incubated with Clarity Western ECL substrate (Bio-Rad), and chemiluminescence was imaged on a ChemiDoc MP documentation system (Bio-Rad). To follow the progress of the purification, the elution fractions from the IMAC and ion-exchange columns were normalized by volume and separated on Any kD Mini-PROTEAN TGX gels (Bio-Rad). The proteins were then stained with Bio-

Safe Coomassie stain (Bio-Rad) and imaged. The purity of the proteins was assessed from images of the Coomassie-stained gels using densitometry analysis in ImageLab software (Bio-Rad). Images were taken for each batch of purification (three replicates), and results were similar in each case.

6.2.3. Strains and culture conditions

C. albicans strain SC5314 (American Type Culture Collection) was first inoculated from yeast-peptone-dextrose (YPD) agar (1% yeast extract, 2% peptone, 2% glucose, and 2% agar) into 5 mL of fresh YPD medium (1% yeast extract, 2% peptone and 2% glucose) and grown overnight at 30 °C while shaking at 230 rpm. The cells in the overnight culture were subcultured into 25 mL of fresh YPD medium with an OD_{600}=0.1 (about 2×10^6 CFU/mL). The culture was then grown at 30 °C to OD_{600}=0.5 (about 1×10^7 CFU/mL) while shaking. Cells were harvested by centrifugation at 4,000 g for 15 min at 4 °C and washed twice with 0.1× PBS.

6.2.4. Cellular uptake analysis by fluorescence imaging

Translocation of CPP-GFP constructs was analyzed using fluorescence microscopy. A total of 5×10^5 *C. albicans* cells in 100 µL of 0.1× PBS was prepared as described above. For each GFP or CPP-GFP construct, 100 µL of a 1.0 µM protein solution in 0.1× PBS was prepared. The cell suspension and protein solution were mixed and incubated at 30 °C with vigorous shaking for 10 or 60 min. Cells were collected by centrifugation at 4,500× g for 10 min at 4 °C and washed twice with 0.1× PBS. The cell pellet was then incubated with 200 µL of 0.025% trypsin (Invitrogen) at 37 °C for 5 min to remove surface-bound protein [19]. After trypsin treatment, cells were again washed with 0.1× PBS and resuspended in 10 µL of 0.1× PBS. An

aliquot of 5 µL of the cell suspension was transferred to a glass slide and imaged using an Olympus IX83 fluorescence microscopy system. Differential interference contrast (DIC) and GFP fluorescence images were taken using the automatic process manager of the CellSens Dimension software (Olympus), and images were analyzed using NIH ImageJ software [20]. Cells in the DIC and GFP images were counted separately to quantify the percentage of cells with GFP uptake. For each of three biological replicates, three DIC and three GFP images were taken to determine a percentage of cells with uptake for each replicate. Statistical comparisons of uptake data were performed using t-tests with a 90% confidence level.

6.2.5. Cell viability

To evaluate the toxicity of the CPP-GFP constructs towards *C. albicans*, the viability of *C. albicans* following incubation with the fusion proteins was measured. GFP and CPP fusions to GFP were prepared as serial dilutions (0-5 µM) in 0.1× PBS, with a final volume of 100 µL. Control wells containing 100 µL of 10 µg/µL nourseothricin (NTC; Jena Bioscience) in 0.1× PBS and 100 µL of 0.1× PBS alone were included as controls for complete inhibition of viability and no inhibition of viability, respectively. An overnight culture of *C. albicans* was diluted to OD_{600}=0.1 with YPD medium, and 100 µL of the cell suspension was added to each well. The plate was incubated at 30 °C with vigorous shaking. The OD_{600} of the wells was measured every 2 h for 8 h using a microplate reader (Bio-Tek). Replicates of the experiment were performed on three separate days.

6.3. Results

6.3.1. Expression and purification of fusion constructs

In order to better understand the interaction of CPPs with *C. albicans*, we chose to study two CPPs previously shown to enter *C. albicans*, NPFSD and pVEC. The proposed mechanism of entry for these peptides is different, along with their physical properties. pVEC is a highly positively charged peptide that enters cells through a non-endocytic process [21]. NPFSD is a slightly negatively charged peptide that is proposed to enter cells via clathrin-mediated endocytosis [22]. Our goal was to evaluate the recombinant production and cell-penetration of the two peptides as genetic fusions to GFP with and without a flexible peptide linker separating the CPP and cargo. GFP is an ideal choice of protein cargo for the CPPs, because its fluorescence makes detection of translocation straightforward by fluorescence microscopy and because it is easily expressed recombinantly in *E. coli* [23]. We chose a linker composed of glycine and serine residues (G_4S), because a G_4S linker

Figure 6.1 Genetic constructs used to produce CPP-GFP fusion proteins. CPPs were fused to GFP, with or without a glycine-serine (G_4S) linker

has been widely used to increase production and stability of recombinant proteins in *E. coli* [24-28].

To study the effect of the linker on expression of CPP-cargo protein fusions, we separately fused the DNA encoding each of the CPPs (NPFSD and pVEC) to the DNA encoding GFP with and without the G_4S linker between the CPP and GFP (**Figure 6.1**). We expressed the proteins in *E. coli* BL21(DE3) cells and compared the expression of each of the protein constructs (**Figure 6.2**). The expression of GFP without fusion to a CPP was much higher than the expression of the CPP-GFP

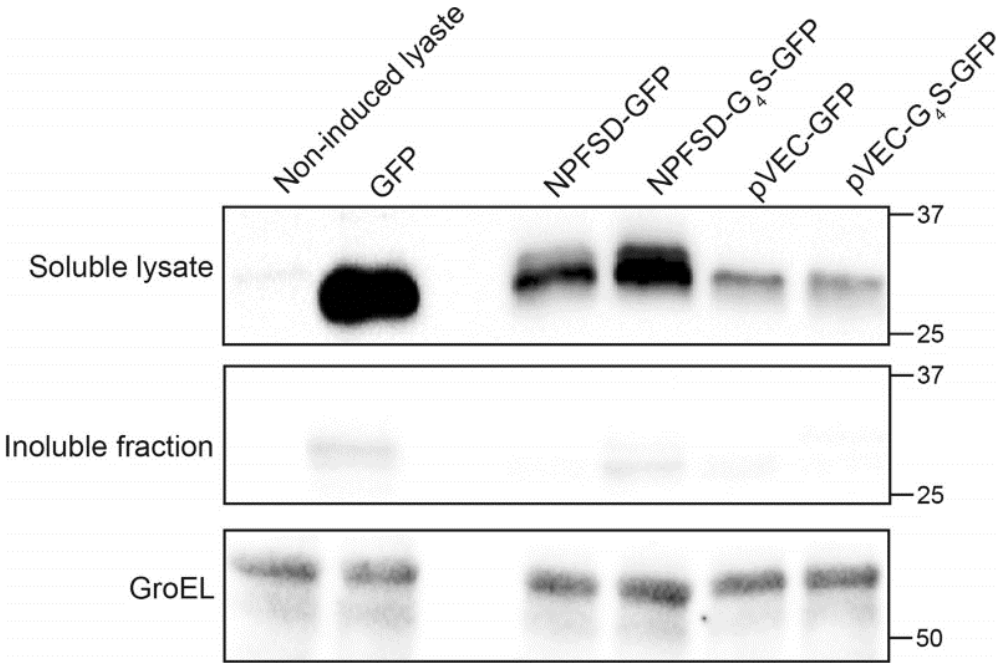

Figure 6.2 Expression of fusion proteins. CPP fusions to GFP were expressed in BL21(DE3) cells at 37 C for 8 h with 0.05 mM IPTG. The soluble cell lysates and insoluble fractions were analyzed by Western blotting, with samples normalized by culture volume. The Western blot was probed using an anti-GFP (mouse) primary antibody and an HRP-conjugated anti-mouse secondary antibody. The soluble and insoluble fractions were imaged simultaneously on the same Western blot. GroEL (60 kDa) was used as an internal loading control and was probed by an anti-GroEL (rabbit) primary antibody and an HRP-conjugated anti-rabbit secondary antibody

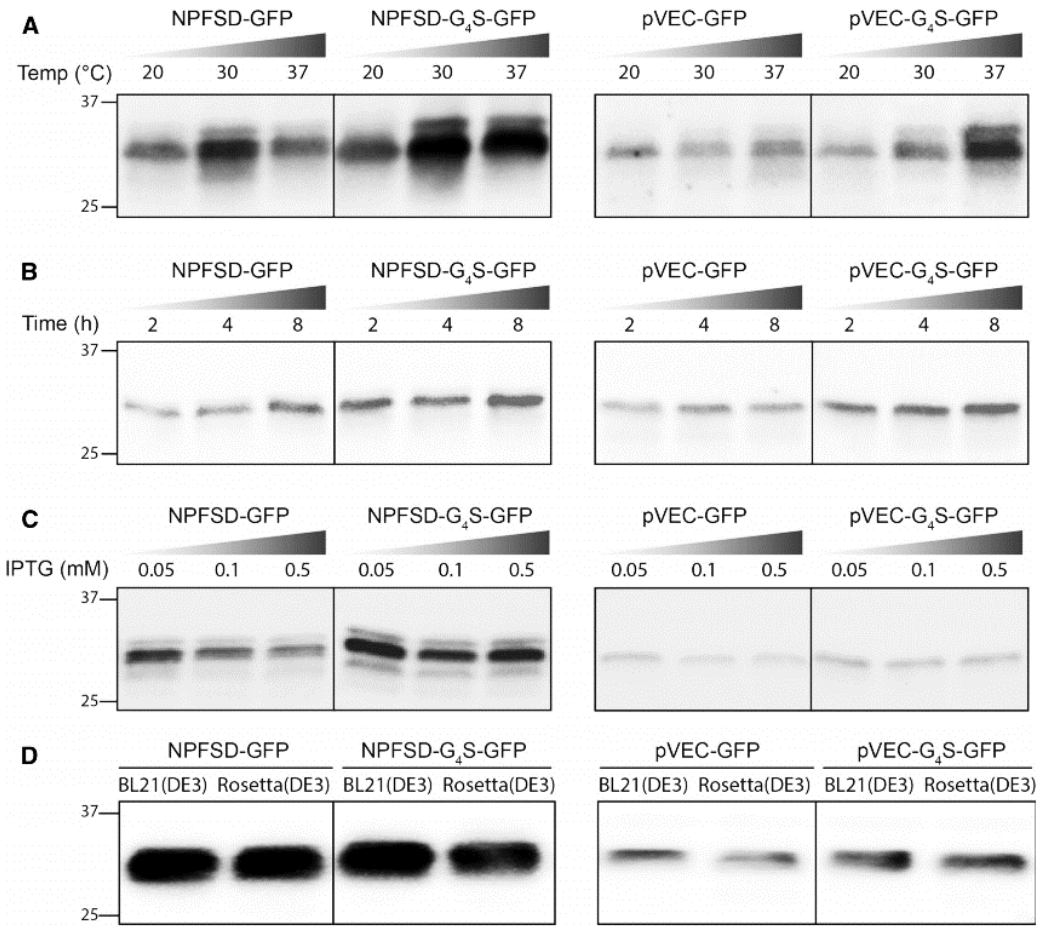

Figure 6.3 Expression of CPP–GFP fusion proteins under different induction conditions and in different strains. **A** The effect of temperature was evaluated by inducing expression at 20, 30, and 37 C for 8 h with 0.1 mM IPTG. **B** The effect of induction time was evaluated by inducing expression at 37 C for 2, 4, and 8 h with 0.1 mM IPTG. **C** The effect of inducer concentration was evaluated by inducing expression at 37 C for 8 h at 0.05, 0.1, and 0.5 mM IPTG. **D** To compare expression in BL21(DE3) and Rosetta(DE3) strains, cultures were induced at 37 C for 8 h with 0.05 mM IPTG

fusions, indicating that the CPPs substantially reduce the amount of soluble GFP produced in *E. coli*, as reported previously for CPP-cargo protein fusions [29]. The reduction in expression was more pronounced for the pVEC constructs than for the NPFSD constructs, potentially due to the antimicrobial activity of the pVEC peptide, which has been shown previously to kill *E. coli* cells [30]. Importantly, for both peptides, the addition of the G_4S linker between the CPP and GFP clearly increased the expression level of the protein fusions. This was a consistent phenomenon for

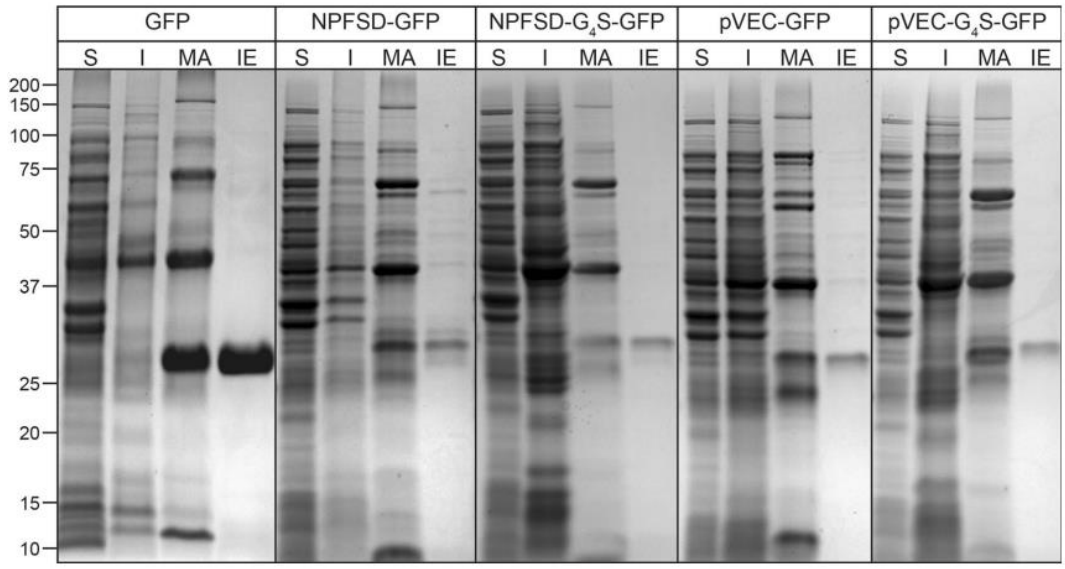

Figure 6.4 Purification of fusion proteins. Coomassie staining was used to evaluate the purification progress and the purity of the fusion proteins. The crude soluble lysates, resolubilized insoluble fractions, and elutions from immobilized metal affinity (MA) chromatography and anion-exchange (IE) chromatography are shown. The expected sizes of the proteins are 27.9 kDa for GFP, 29.0 kDa for NPFSDGFP, 29.3 kDa for NPFSD-G4S-GFP, 30.1 kDa for pVEC-GFP, and 30.4 kDa for pVEC-G4S-GFP. These data are intended to illustrate the quality of the purification and should not be compared for yield of the proteins (yields are found in **Table 6.2**)

these constructs under various expression conditions (**Figure 6.3**). While temperature and induction time did have some effect on expression, these effects varied between the constructs, and the linker improved expression of the fusion proteins under all conditions. The linker provides a more robust method to enhance the expression of the CPP fusions to cargo proteins than varying expression conditions.

We purified the fusion proteins to quantify the effect of the linker on yields of purified protein and better gauge the impact of the linker. The proteins were first purified via their C-terminal 6XHis tag using an IMAC column. Following IMAC, all protein constructs still contained substantial impurities (**Figure 6.4**). For the CPP-fused constructs, the Coomassie staining shows that the impurities were more

abundant than the desired protein constructs. Hence, we performed ion-exchange chromatography with an anion-exchange resin to further purify each of the proteins. The purity of each protein was above 90% following anion-exchange chromatography (**Figure 6.4, Table 6.2**). Consistent with the difference in expression, GFP with no CPP was purified with a much higher yield than the CPP fusions, and a higher yield of protein was obtained for the NPFSD constructs than for the pVEC constructs. Likewise, the addition of the linker to the CPP-GFP constructs led to an increase in the purified protein yield, with an increase of 24.5% for the NPFSD fusion (p=0.003) and an increase of 50.0% for the pVEC fusion (p=0.086). Although the linker was not able to recover the level of purified protein to the level of GFP alone, it did produce a significant improvement in yield, which will be beneficial when producing CPP fusions for future experiments.

Table 6.2 Purification yield of different CPP-GFP fusion proteins

Protein	Yield (mg protein/L of culture)[a]	Purity (%)[a]
GFP	0.795±0.093	97.0±1.5
NPFSD-GFP	0.212±0.013	92.4±5.6
NPFSD-G_4S-GFP	0.264±0.013	95.2±1.5
pVEC-GFP	0.106±0.013	98.4±1.6
pVEC-G_4S-GFP	0.159±0.053	97.2±2.6

[a] The yield and the purity are shown as the average of three separate cultures with standard error.

6.3.2. Cellular uptake efficiency of fusion proteins

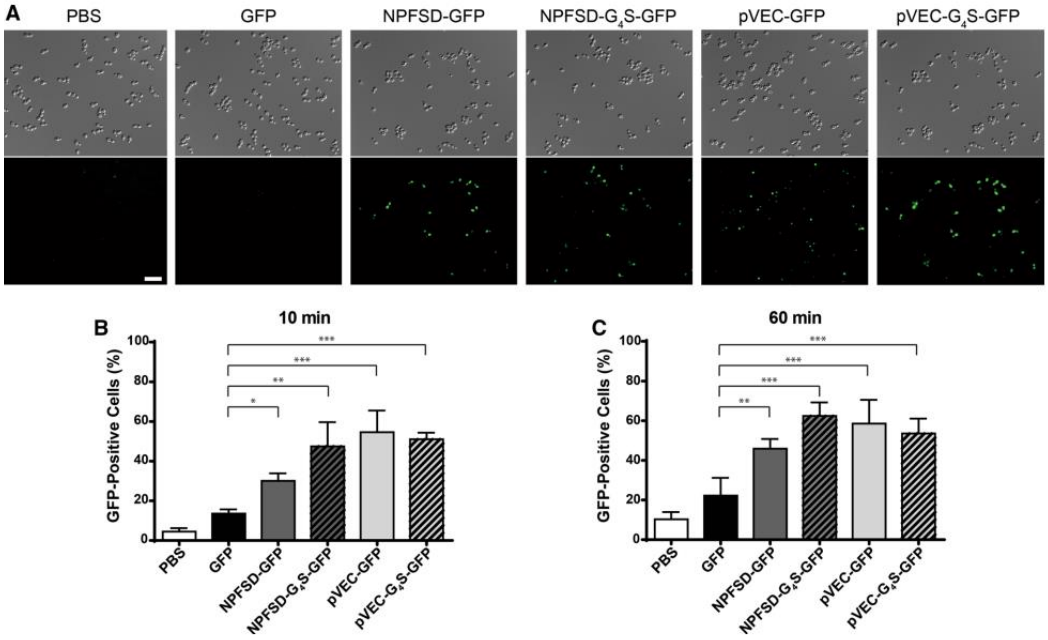

Figure 6.5 Cellular uptake of CPP fusions. **A** Microscopy images of *C. albicans* cells after incubation with fusion proteins for 10 min. Scale bar is 20 µm. **B** Uptake efficiency of CPP fusions (final concentration of 0.5 µM) after 10 min of incubation with cells. **C** Uptake efficiency of CPP fusions (final concentration of 0.5 µM) after 60 min of incubation with cells. For b and c, the number of cells in DIC and GFP images was counted separately after the indicated incubation time to calculate the percentage of GFP-positive cells. Error bars represent the standard error of three separate experiments. Statistical significance was analyzed with a one-way ANOVA test (a = 0.1), and the number of asterisks indicates the level of significance (* for $p \leq 0.05$, ** for $p \leq 0.01$, and *** for $p \leq 0.001$)

As previous research has shown, NPFSD and pVEC have the capacity to translocate into *C. albicans* cells [31, 32]. After showing that the G_4S linker enhanced the recombinant expression of CPP-GFP fusions in *E. coli*, we next evaluated whether the linker affected this translocation. Cells were incubated with 0.5 µM of each protein construct for 10 min, treated briefly with trypsin to remove any fluorescent protein bound to the cell surface, and then examined by fluorescence microscopy to detect GFP. All four fusion proteins were observed intracellularly, whereas GFP lacking a CPP and a negative control with only PBS exhibited almost no fluorescent

cells (**Figure 6.5A**). The GFP constructs were found in the cytoplasm of the cells under the conditions we evaluated, with no difference in the localization observed based on the CPP or on the presence of the linker. These results were confirmed by quantifying the percentage of fluorescence-positive cells (**Figure 6.5B**). The low level of positive cells in the samples with GFP and with no protein is at least partially explained by autofluorescence, which has been observed in yeast previously [33]. It is also possible that a small amount of GFP can be taken into the cells, even in the absence of a CPP. However, samples treated with the four fusion proteins for 10 min had significantly more GFP-positive cells than the samples with PBS only or GFP with no CPP. Translocation of NPFSD-GFP led to 1.2 times as many GFP-positive cells compared to GFP only, while translocation of pVEC-GFP led to 3.0 times as many GFP-positive cells. For constructs containing the NPFSD peptide, the addition of the G_4S linker led to an improvement of translocation, with the NPFSD-G_4S-GFP protein leading to 58% more GFP-positive cells compared to the construct lacking the linker (p=0.093) and improving the translocation to a level similar to pVEC-GFP. In contrast, the linker had little effect on the fusion proteins containing pVEC, with no statistical difference between the levels of GFP-positive cells for pVEC-GFP and pVEC-G_4S-GFP (p=0.70). These results indicate that the linker does not diminish the ability of a CPP-cargo fusion to penetrate cells and has the ability to actually improve the translocation.

CPPs have been frequently shown to enter cells within 15 min, but longer times can lead to a higher number of cells showing uptake [21, 34]. To evaluate whether longer time periods also lead to improved translocation of our constructs, we

increased the incubation time with the CPP fusions from 10 min to 60 min. Microscopy showed the results at 60 min were qualitatively similar to results at 10 min, with the translocated constructs found in the cytoplasm of the *C. albicans* cells (data not shown). The uptake of both NPFSD fusions was significantly higher for 60 min of incubation compared to 10 min (34.5% for NPFSD, p=0.049; 23.9% for NPFSD-G_4S-GFP, p=0.090) (**Figure 6.5B and Figure 6.5C**), while there was no significant increase for the pVEC fusions with additional time. After 60 min of incubation, we observed statistically similar uptake for all four of the CPP fusions. Our results suggest that pVEC enters cells at a higher rate than NPFSD, but that the difference in the translocation rate can be overcome by incubating the CPP constructs for a longer time. However, incubating for a longer time also increases the background fluorescence and non-CPP-mediated translocation of GFP, which may impact the incubation time.

6.3.3. Cell viability after uptake

The goal of using CPPs is to deliver cargo into cells, and the ability to deliver cargo without affecting the viability of cells would broaden the range of applications of CPPs in biological studies. To examine the cytotoxicity of the CPP-GFP fusions, we monitored the cell growth of *C. albicans* in the presence of the CPP fusions and compared this growth to the growth in the presence of GFP (**Figure 6.6**). Incubation of *C. albicans* cells with GFP at concentrations of up to 5 μM of GFP did not lead to a difference in viability compared to cells incubated with no protein (data not shown). We observed a very minor loss of viability for cells incubated with NPFSD and

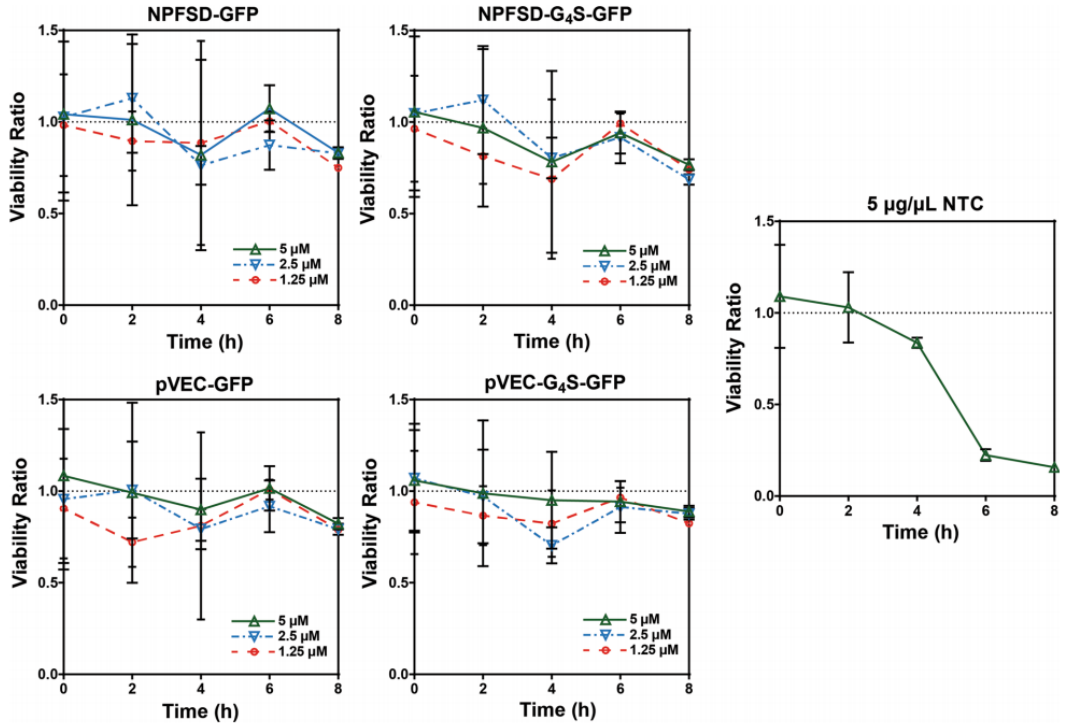

Figure 6.6 Viability of *C. albicans* cells incubated with fusions of CPPs to GFP. *C. albicans* strain SC5314 cells were incubated with the indicated concentrations of pVEC-GFP, pVEC-G_4S-GFP, NPFSD-GFP, and NPFSD-G_4S-GFP in YPD medium, and the OD_{600} was monitored over time. The data are plotted as the ratio of the cell density (OD_{600}) for samples with each fusion protein to the OD_{600} for samples incubated with GFP at the same molar concentration for the same period of time. A control containing 5 µg/µL nourseothricin (NTC), an antifungal agent, was included, and those data are shown relative to 5 µM GFP. Data represent the average of three replicates, and error bars show the standard error, which was propagated through the calculations

pVEC constructs, which is apparent from viability ratios below one for most data points after 0 h. However, the loss of viability due to the CPP constructs is relatively consistent over the course of the experiment, in contrast to the data for the antifungal agent nourseothricin, which continues to see a viability reduction beyond 6 h and is known to constantly inhibit *C. albicans* growth [35]. Our results for the toxicity of the CPP constructs are consistent with previous work that showed no toxicity of NPFSD towards yeast cells [22]. pVEC has been shown to exhibit antimicrobial activity towards some fungal cells [36] , but not *C. albicans* (consistent with our results) and

no toxicity to multiple mammalian cell lines [37]. The linker between the CPPs and GFP does not show an effect on the viability of cells incubated with the CPP fusions, indicating the linker can be included without adverse effects on cells. The relatively low toxicity of the CPP fusions overall indicates that these constructs could be used as tools for delivering cargo to cells and studying the biological impact of the cargo.

6.4. Discussion

Genetic fusion techniques allow the production of recombinant proteins containing different domains with different functions, for example a CPP for cell penetration and a cargo protein with an intracellular function. However, different domains of fusion proteins may interfere with each other, resulting in poor expression. Rachel *et al.* reported that when a polypeptide is directly fused to different fusion partners, some peptides decrease the solubility of the fusion proteins [1, 2, 38]. A flexible linker not only separates the different domains to allow better function of each domain, but it also helps to enhance the recombinant expression [10, 11, 39-41]. In this study, we successfully increased the expression of CPPs fused to GFP by using a glycine-serine linker, leading to a higher yield of the purified fusion proteins for cellular assays. Although the CPP fusion proteins were still expressed at significantly lower levels than GFP without a CPP attached, the linker reliably improved expression of CPP fusions under a variety of different temperatures and induction times.

More importantly, the presence of the linker did not negatively affect the function of either domain of the fusion proteins. The G_4S linker enhanced the translocation of NPFSD-GFP fusions significantly, whereas the translocation capacity

of pVEC-GFP fusions was unaffected. This result may be due to the different mechanisms of uptake for the two peptides. Previous work reported that NPFSD is translocated into cells through clathrin-mediated endocytosis [22], while pVEC enters cells through macropinocytosis (a non-receptor-based mechanism) [21]. Clathrin-mediated endocytosis is the process cells use to take up molecules targeting specific receptors. If the structure of an endocytosed peptide like NPFSD is affected by attachment to a cargo protein, the interaction with the receptor could potentially be changed, altering the translocation capacity of the peptide. Inclusion of the flexible linker as a spacer between NPFSD and GFP could prevent disruption of this interaction with the receptor, leading to improved translocation of the construct containing the linker compared to the construct without the linker. Comparing with clathrin-mediated endocytosis, macropinocytosis is not specific for the molecule being translocated. As pVEC is translocated by macropinocytosis, the uptake of pVEC may be less affected by any structural changes due to fusion to the cargo protein; thus, inclusion of a linker may not as significantly affect the uptake of pVEC constructs.

CPPs are being explored as novel drug delivery vehicles for delivering various molecules intracellularly. In order to use CPPs to explore the biological function of cargo inside cells, cell viability will be important for CPP-mediated delivery systems. Previous studies suggested that pVEC could be considered a “safe” CPP, since it does not significantly affect the viability of mammalian cells [37, 42]. No cytotoxicity data for NPFSD had been reported prior to our work. We observed only a very small decrease in viability due to either pVEC or NPFSD, suggesting both pVEC and

NPFSD could serve as a delivery system for *C. albicans* cells when maintaining cell viability is important. Furthermore, the G_4S linker did not affect cytotoxicity, so its benefits to expression and uptake can be obtained with no negative impact on cell viability.

6.5. Conclusion

Using a glycine-serine linker, we were able to improve the expression and purification of CPPs fused to GFP without negatively impacting the cellular uptake efficiency and without substantial cytotoxicity toward *C. albicans*. These results suggest that future studies with additional CPPs and cargo could benefit from the inclusion of a linker between the CPP and the cargo. Additionally, exploring additional linkers would provide further insight into the mechanism by which the linker is able to improve expression and, in some cases, uptake.

6.6. Reference

1. Mueller, N.H., D.A. Ammar and J.M. Petrash, *Cell Penetration Peptides for Enhanced Entry of alpha B-Crystallin into Lens Cells.* IOVS, 2013. **54**(1): p. 2-8.
2. Liu, J., T. Gaj, J.T. Patterson, S.J. Sirk, and C.F. Barbas, *Cell-penetrating peptide-mediated delivery of TALEN proteins via bioconjugation for genome engineering.* Plos One, 2014. **9**(1).
3. Zhou, H., S. Wu, J.Y. Joo, S. Zhu, D.W. Han, T. Lin, S. Trauger, G. Bien, S. Yao, Y. Zhu, G. Siuzdak, H.R. Scholer, L. Duan, and S. Ding, *Generation of induced pluripotent stem cells using recombinant proteins.* Cell Stem Cell, 2009. **4**(5): p. 381-4.
4. Vargas, N., S. Álvarez-Cubela, J.A. Giraldo, M. Nieto, N.M. Fort, S. Cechin, E. García, P. Espino-Grosso, C.A. Fraker, C. Ricordi, L. Inverardi, R.L. Pastori, and J. Domínguez-Bendala, *TAT-Mediated Transduction of MafA Protein In Utero Results in Enhanced Pancreatic Insulin Expression and Changes in Islet Morphology.* PLOS ONE, 2011. **6**(8): p. e22364.
5. Shokolenko, I.N., M.F. Alexeyev, S.P. LeDoux and G.L. Wilson, *TAT-mediated protein transduction and targeted delivery of fusion proteins into mitochondria of breast cancer cells.* DNA Repair, 2005. **4**(4): p. 511-518.
6. Marchione, R., D. Dayde, J.L. Lenormand and M. Cornet, *ZEBRA cell-penetrating peptide as an efficient delivery system in Candida albicans.* Biotechnology Journal, 2014. **9**(8): p. 1088-1094.
7. Michiue, H., K. Tomizawa, F.Y. Wei, M. Matsushita, Y.F. Lu, T. Ichikawa, T. Tamiya, I. Date, and H. Matsui, *The NH2 terminus of influenza virus hemagglutinin-2 subunit peptides enhances the antitumor potency of polyarginine-mediated p53 protein transduction.* J Biol Chem, 2005. **280**(9): p. 8285-9.
8. Skosyrev, V.S., N.V. Rudenko, A.V. Yakhnin, V.E. Zagranichny, L.I. Popova, M.V. Zakharov, A.Y. Gorokhovatsky, and L.M. Vinokurov, *EGFP as a fusion partner for the expression and organic extraction of small polypeptides.* Protein Expression and Purification, 2003. **27**(1): p. 55-62.
9. Guo, W.H., L. Cao, Z.J. Jia, G. Wu, T. Li, F.X. Lu, and Z.X. Lu, *High level soluble production of functional ribonuclease inhibitor in Escherichia coli by fusing it to soluble partners.* Protein Expression and Purification, 2011. **77**(2): p. 185-192.
10. Rizk, M., G. Antranikian and S. Elleuche, *Influence of linker length variations on the biomass-degrading performance of heat-active enzyme chimeras.* Mol Biotechnol, 2016. **58**(4): p. 268-279.
11. Chen, X.Y., J.L. Zaro and W.C. Shen, *Fusion protein linkers: Property, design and functionality.* Adv Drug Delivery Rev, 2013. **65**(10): p. 1357-1369.
12. Lu, P. and M.G. Feng, *Bifunctional enhancement of a beta-glucanase-xylanase fusion enzyme by optimization of peptide linkers.* Appl Microbiol Biotechnol, 2008. **79**(4): p. 579-87.

13. Huston, J.S., D. Levinson, M. Mudgetthunter, M.S. Tai, J. Novotny, M.N. Margolies, R.J. Ridge, R.E. Bruccoleri, E. Haber, R. Crea, and H. Oppermann, *Protein engineering of antibody-binding sites - recovery of specific activity in an anti-digoxin single-chain fv analog produced in Escherichia coli.* P Natl Acad Sci USA, 1988. **85**(16): p. 5879-5883.
14. Bai, Y. and W.C. Shen, *Improving the oral efficacy of recombinant granulocyte colony-stimulating factor and transferrin fusion protein by spacer optimization.* Pharm Res, 2006. **23**(9): p. 2116-21.
15. Bergeron, L.M., L. Gomez, T.A. Whitehead and D.S. Clark, *Self-renaturing enzymes: design of an enzyme-chaperone chimera as a new approach to enzyme stabilization.* Biotechnol Bioeng, 2009. **102**(5): p. 1316-22.
16. Zhao, H.L., X.Q. Yao, C. Xue, Y. Wang, X.H. Xiong, and Z.M. Liu, *Increasing the homogeneity, stability and activity of human serum albumin and interferon-alpha 2b fusion protein by linker engineering.* Protein Expression and Purification, 2008. **61**(1): p. 73-77.
17. Hu, W., F. Li, X. Yang, Z. Li, H. Xia, G. Li, Y. Wang, and Z. Zhang, *A flexible peptide linker enhances the immunoreactivity of two copies HBsAg preS1 (21-47) fusion protein.* J Biotechnol, 2004. **107**(1): p. 83-90.
18. Gasteiger, E., Hoogland, C., Gattiker, A., Duvaud, S., Wilkins, M. R., Appel, R. D. & Bairoch, A., *The Proteomics Protocols Handbook.* 2005, Humana Press. 36.
19. Richard, J.P., K. Melikov, E. Vives, C. Ramos, B. Verbeure, M.J. Gait, L.V. Chernomordik, and B. Lebleu, *Cell-penetrating peptides - A reevaluation of the mechanism of cellular uptake.* J Biol Chem, 2003. **278**(1): p. 585-590.
20. Schneider, C.A., W.S. Rasband and K.W. Eliceiri, *NIH Image to ImageJ: 25 years of image analysis.* Nat Methods, 2012. **9**(7): p. 671-675.
21. Mager, I., E. Eiriksdottir, K. Langel, S.E.L. Andaloussi, and U. Langel, *Assessing the uptake kinetics and internalization mechanisms of cell-penetrating peptides using a quenched fluorescence assay.* BBBA-Biomembranes, 2010. **1798**(3): p. 338-343.
22. Rajarao, G.K., N. Nekhotiaeva and L. Good, *The signal peptide NPFSD fused to ricin A chain enhances cell uptake and cytotoxicity in Candida albicans.* Biochem Bioph Res Co, 2003. **301**(2): p. 529-534.
23. Chalfie, M., Y. Tu, G. Euskirchen, W.W. Ward, and D.C. Prasher, *Green fluorescent protein as a marker for gene-expression.* Science, 1994. **263**(5148): p. 802-805.
24. Trinh, R., B. Gurbaxani, S.L. Morrison and M. Seyfzadeh, *Optimization of codon pair use within the (GGGGS)(3) linker sequence results in enhanced protein expression.* Mol Immunol, 2004. **40**(10): p. 717-722.
25. Ueda, M., Y. Manabe and M. Mukai, *The high performance of 3XFLAG for target purification of a bioactive metabolite: A tag combined with a highly effective linker structure.* Bioorg Med Chem Lett, 2011. **21**(5): p. 1359-1362.
26. Argos, P., *An investigation of oligopeptides linking domains in protein tertiary structures and possible candidates for general gene fusion.* J Mol Biol, 1990. **211**(4): p. 943-958.

27. Silacci, M., N. Baenziger-Tobler, W. Lembke, W.J. Zha, S. Batey, J. Bertschinger, and D. Grabulovski, *Linker length matters, fynomer-fc fusion with an optimized linker displaying picomolar il-17a inhibition potency.* J Biol Chem, 2014. **289**(20): p. 14392-14398.
28. Neuner, P., P. Gallo, L. Orsatti, L. Fontana, and P. Monaci, *An efficient and versatile synthesis of bisPNA-peptide conjugates based on chemoselective oxime formation.* Bioconjug Chem, 2003. **14**(2): p. 276-81.
29. Marchione, R., D. Dayde, J.L. Lenormand and M. Cornet, *ZEBRA cell-penetrating peptide as an efficient delivery system in Candida albicans.* Biotechnol J, 2014. **9**(8): p. 1088-1094.
30. Palm, C., S. Netzerea and M. Hallbrink, *Quantitatively determined uptake of cell-penetrating peptides in non-mammalian cells with an evaluation of degradation and antimicrobial effects.* Peptides, 2006. **27**(7): p. 1710-1716.
31. Rajarao, G.K., N. Nekhotiaeva and L. Good, *Peptide-mediated delivery of green fluorescent protein into yeasts and bacteria.* Fems Microbiol Lett, 2002. **215**(2): p. 267-272.
32. Holm, T., S. Netzereab, M. Hansen, U. Langel, and M. Hallbrink, *Uptake of cell-penetrating peptides in yeasts.* FEBS Lett, 2005. **579**(23): p. 5217-22.
33. Bar-Even, A., J. Paulsson, N. Maheshri, M. Carmi, E. O'Shea, Y. Pilpel, and N. Barkai, *Noise in protein expression scales with natural protein abundance.* Nay Genet, 2006. **38**(6): p. 636-643.
34. Mager, I., K. Langel, T. Lehto, E. Eiriksdottir, and U. Langel, *The role of endocytosis on the uptake kinetics of luciferin-conjugated cell-penetrating peptides.* BBA-Biomembranes, 2012. **1818**(3): p. 502-511.
35. Vaara, M., *Agents that increase the permeability of the outer-membrane.* Microbiol Rev, 1992. **56**(3): p. 395-411.
36. Lindgren, M. and Ü. Langel, *Classes and prediction of cell-penetrating peptides,* in *Cell-Penetrating Peptides: Methods and Protocols*, Ü. Langel, Editor. 2011, Humana Press: Totowa, NJ. p. 3-19.
37. Saar, K., M. Lindgren, M. Hansen, E. Eiriksdottir, Y. Jiang, K. Rosenthal-Aizman, M. Sassian, and U. Langel, *Cell-penetrating peptides: A comparative membrane toxicity study.* Anal Biochemi, 2005. **345**(1): p. 55-65.
38. Kapust, R.B. and D.S. Waugh, *Controlled intracellular processing of fusion proteins by TEV protease.* Protein Expr Purif, 2000. **19**(2): p. 312-318.
39. Wriggers, W., S. Chakravarty and P.A. Jennings, *Control of protein functional dynamics by peptide linkers.* Biopolymers, 2005. **80**(6): p. 736-746.
40. Skosyrev, V.S., N.V. Rudenko, A.V. Yakhnin, V.E. Zagranichny, L.I. Popova, M.V. Zakharov, A.Y. Gorokhovatsky, and L.M. Vinokurov, *EGFP as a fusion partner for the expression and organic extraction of small polypeptides.* Protein Expr Purif, 2003. **27**(1): p. 55-62.
41. Guo, W.H., L. Cao, Z.J. Jia, G. Wu, T. Li, F.X. Lu, and Z.X. Lu, *High level soluble production of functional ribonuclease inhibitor in Escherichia coli by fusing it to soluble partners.* Protein Expr Purif, 2011. **77**(2): p. 185-192.
42. Zorko, M. and U. Langel, *Cell-penetrating peptides: mechanism and kinetics of cargo delivery.* Adv Drug Delivery Rev, 2005. **57**(4): p. 529-545.

Chapter 7. Conclusion and future work

In Chapter 3 and 4, we demonstrated that CPPs can be functional towards the fungal pathogen *Candida*. Our initial screening and biophysical characterization of CPPs with *Candida* cells help us to understand how and why peptide internalization occurs and how the structure of CPPs is related to the translocation mechanism. I further investigated the structure-function relationship by using rational design of peptides in Chapter 5. The charge and the hydrophobicity of the peptides directly affected the translocation efficacy, mode of action, as well as the toxicity of the peptides. In Chapter 6, we showed that we can use pVEC to deliver the protein cargo GFP into *C. albicans*, validating the idea of developing CPPs as cargo delivery vehicles for fungal cells. Our work has significant impact for understanding CPPs in fungal pathogens and provides the motivation for additional work to further explore the application of CPPs for cargo delivery into fungal pathogens.

7.1. Intracellular delivery of antifungal agents by CPP

In Chapter 3, 5 and 6, I used CPPs to deliver both a small molecule (FAM) and a larger biomolecule (GFP) into *C. albicans*, indicating the feasibility of using CPPs to deliver bioactive molecular cargos into *Candida* pathogens. Our goal is to use CPPs to resolve the challenges in treating fungal infections, thus delivering antifungal agents and enhancing therapeutic effects need to be explored.

Fluconazole has been widely used as the first-line antifungal drugs to treat fungal infections caused by *C. albicans* [1, 2]. Through an unknown mechanism,

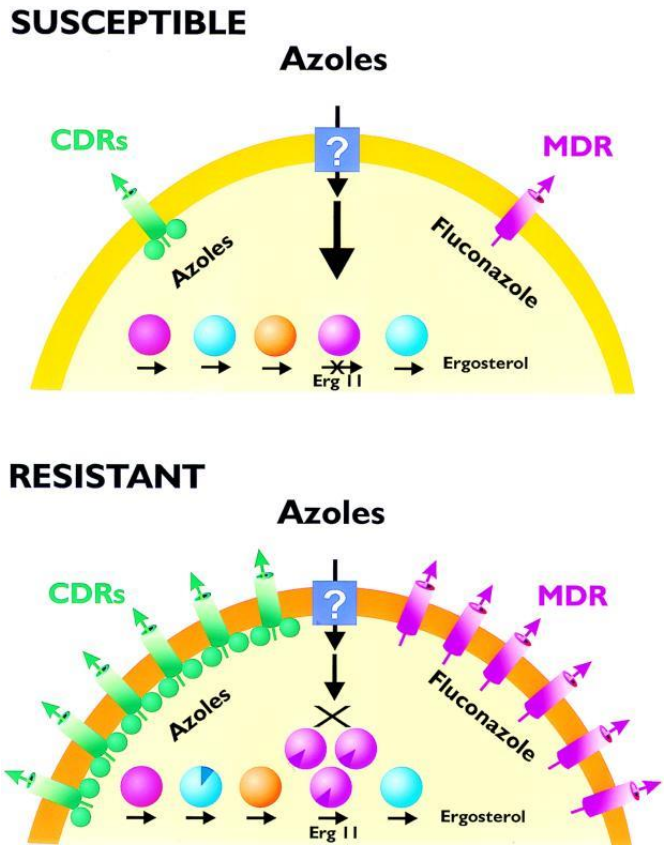

Figure 7.1 Azole drug resistance mechanisms of *C. albicans*. Figure from [2]

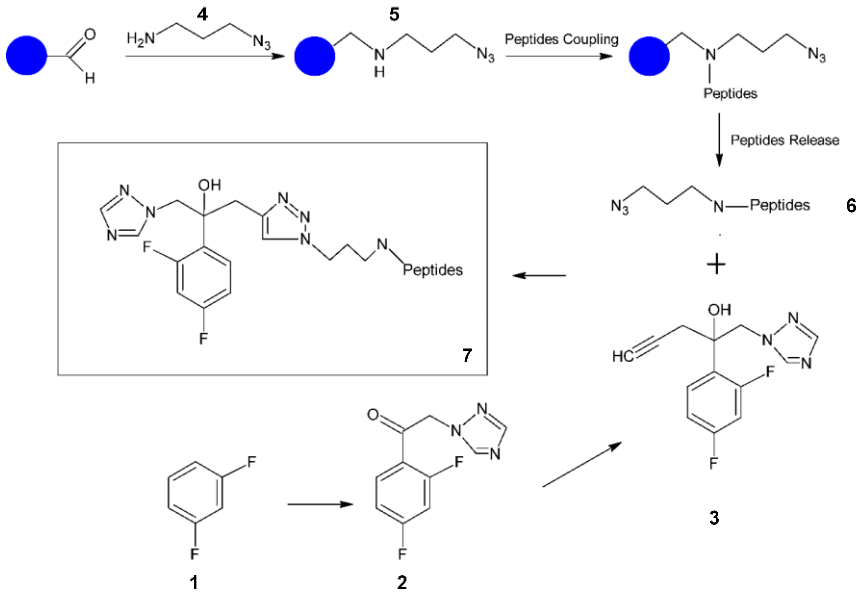

Figure 7.2 Scheme of synthesis pathway for CPP-fluconazole. Peptide will be commercially synthesized with C-terminal azide modification and N-terminal FAM label. Compound (**3**) will be synthesized following procedure mentioned in [3].

fluconazole enters the cells, blocking the synthesis of ergosterol by silencing the ERG11 gene. In order to maintain the inhibition of the ERG11 gene, a cross-membrane azole gradient should be maintained. Hence, the dosage of the azole drug is often high to keep the azole concentration gradient high. However, this higher dosage and long-term treatment promote the development of drug resistance from *C. albicans* [2]. As more azole enters the cells, some drug can still the synthesis of ergosterol, but two major genes, CDR and MDR1, are upregulated, resulting in overexpression of two membrane proteins that actively pump fluconazole out of the cells and reduce the therapeutic effects (**Figure 7.1** [2]). Therefore, developing a highly efficient, safe delivery methods such as CPP will eliminate the high-dosage, long-term treating requirement, and enable better translocation of azole drugs with clear internalization mechanisms.

The challenge for using CPPs to deliver fluconazole is the way to conjugate drugs to the peptides without affecting the properties of both the delivery vehicle and the molecular cargo. One of the most powerful, yet gentle, bioconjugation reactions is the Huisgen cycloadditions reaction [4], known as “click chemistry”, which requires an azide and alkyne residue in the chemicals, and it allows us to covalently link CPPs to drugs. I could modify peptides with an N-terminal azide functional group and fluconazole with an alkyne functional group as fluconazole has been successfully modified with an alkyne moiety to allow bioconjugation [3] (**Figure 7.2**). Starting from 1,3-difluorobenzene (**1**), Pore *et al*. were able to synthesize 2-(2,4-difluorophenyl)-1-(1H-1,2,4-triazol-1-yl)pent-4-yn-2-ol (**3**), which has the alkyne group. With the help of click chemistry, the compound (**3**) can be turned into an

active fluconazole-similar. Meanwhile, solid-phase synthesis of peptides allows us to modify the C-terminus of the peptides. Previous research has shown the modification of peptides with both azide and alkyne modification [5]. As I propose to have fluconazole modified with alkyne group, I could have the peptides commercially synthesized with C-terminally azide label and N-terminally 5-FAM label. As commonly used chemicals for synthesis of pharmaceutical drug candidates, 3-aminopropyl azide (**4**) can be attached to the carboxyl group of the first amino acid attached to the solid-phase beads using a reductive amination reaction. Modified peptides (**6**) could be commercially synthesized and used to react with the compound (**3**) to get the final product (**7**). Previous study of conjugation of fluconazole showed similar antifungal activity to the native drug [3], so I expect the CPP-fluconazole complex would validate the idea of using CPPs for small-molecule cargo intracellular delivery. The final drug product could be purified by reverse phase liquid chromatography and checked by mass spectrometry.

As observed in Chapter 3, 4, and 5, some CPPs can directly affect the viability of *C. albicans* while delivering cargos into cells, such as pVEC and penetratin. They have an MIC50 value lower than 2 μM, and they can lead to at least 50% internalization at 1.5 μM. Meanwhile, although the MIC50 of fluconazole varies between different isolates, the average MIC50 value is 0.5 mg/L [6], which equals to 1.6 μM. If the conjugation does not affect the efficacy of the peptides and the drug effects, the effective concentration of the conjugates should not be higher than 1.5 μM. In addition, I observed pore formation in *C. albicans* when treated with these peptides, which would promote the translocation of the conjugates. A synergistic

effect would reduce the MIC values and enhance the therapeutic efficacy of the new conjugates. In such way, I could reduce the overall dosage to prevent adaptive resistance due to the high-concentration induced pump activation.

7.2. Enhanced *in vitro* CPP-protein fusion production

Chemical synthesis of peptides can ensure the accuracy of the sequence and allow many kinds of chemical medication. However, it has some disadvantages such as the high cost and the long processing time. Alternatively, peptides can be produced by biological systems. I demonstrated I can use recombinant expression technology to product CPP-GFP fusion proteins with the ability to translocate (Chapter 6). Due to the potential toxicity of the peptides, the overall recombinant expression yield is significantly lower than the cargo protein without CPPs. Innovative expression and production methods beyond the limitation of live cells need to be widely explored to increase the yield and efficiency of CPP-cargo fusion protein production.

7.2.1. Cell-free protein synthesis

The idea of using bacteria or yeast to produce recombinant proteins depends on the biological machinery inside cells. Cells have all the required enzymes to convert DNA into mature protein based on the central dogma. To remove the constraint of the cell membrane and the toxicity of the protein to the host cells, an *in vitro* new protein synthesis method, cell-free protein synthesis (CFPS) was developed. CFPS uses extracts from cells. The recovered cell extracts along with other essential components can be added into a tube to allow the direct access and control of the expression process. These essential components of

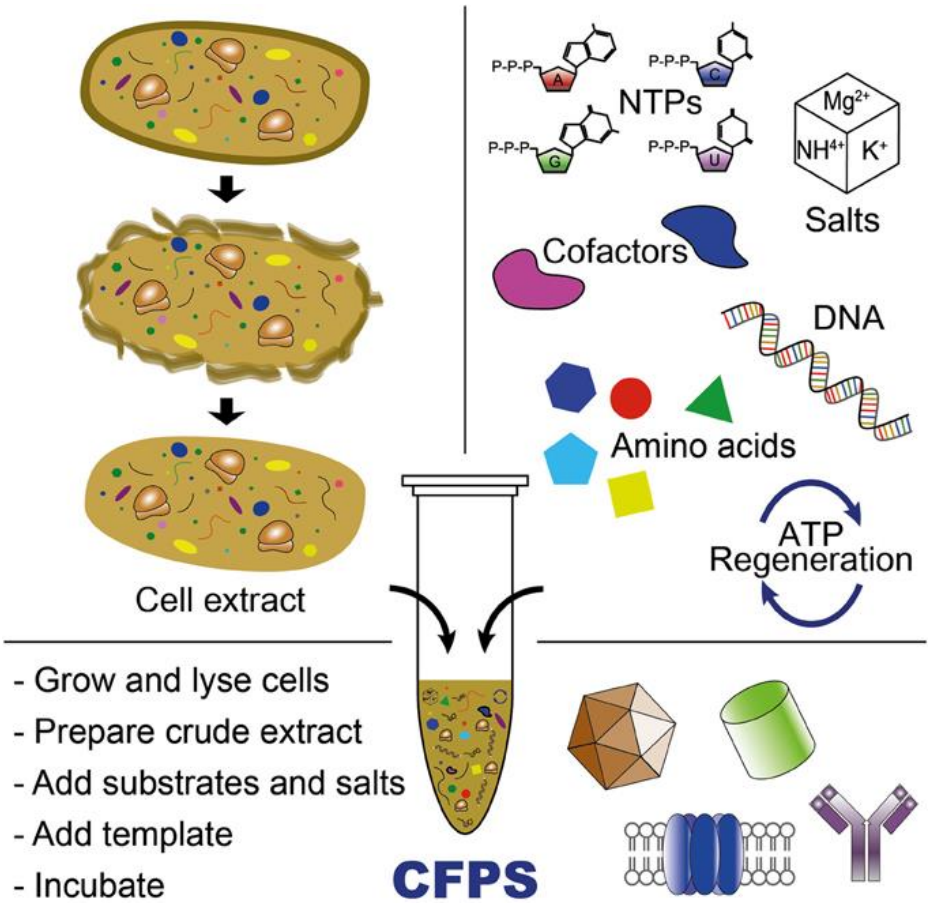

Figure 7.3 Schemes of cell-free protein (CFPS) synthesis systems for peptide/protein production. Reactions can be achieved in a test tube or can be scaled up by adding more cell extracts and essential components [7].

CFPS processes includes ATP, amino acids, salts, and template DNA (Figure 7.3 [7]). In recent decades, CFPS have been widely used to produce proteins from either plasmid DNA or DNA fragments (PCR products). Meanwhile, the extracted cell extracts can be lyophilized and stored, which enables more flexibility and possibility of scale-up.

CFPS can be used to enable both CPP and CPP-cargo fusion production in a test tube without host cells limitations. For peptide synthesis, the potential disadvantage is the stability and product yield. Due to the length of the peptides (< 3

kDa), the synthesis efficiency could be substantially lower than protein synthesis, as CFPS are often used to produce full-size proteins. To solve the problem, I can design a longer PCR fragments with multiple CPP units, separated by enzyme-cleavage recognition sites. The long fragments can be further purified using a fast liquid chromatography system (FPLC) and cleaved by an enzyme to recover CPP units (**Figure 7.4 A**).

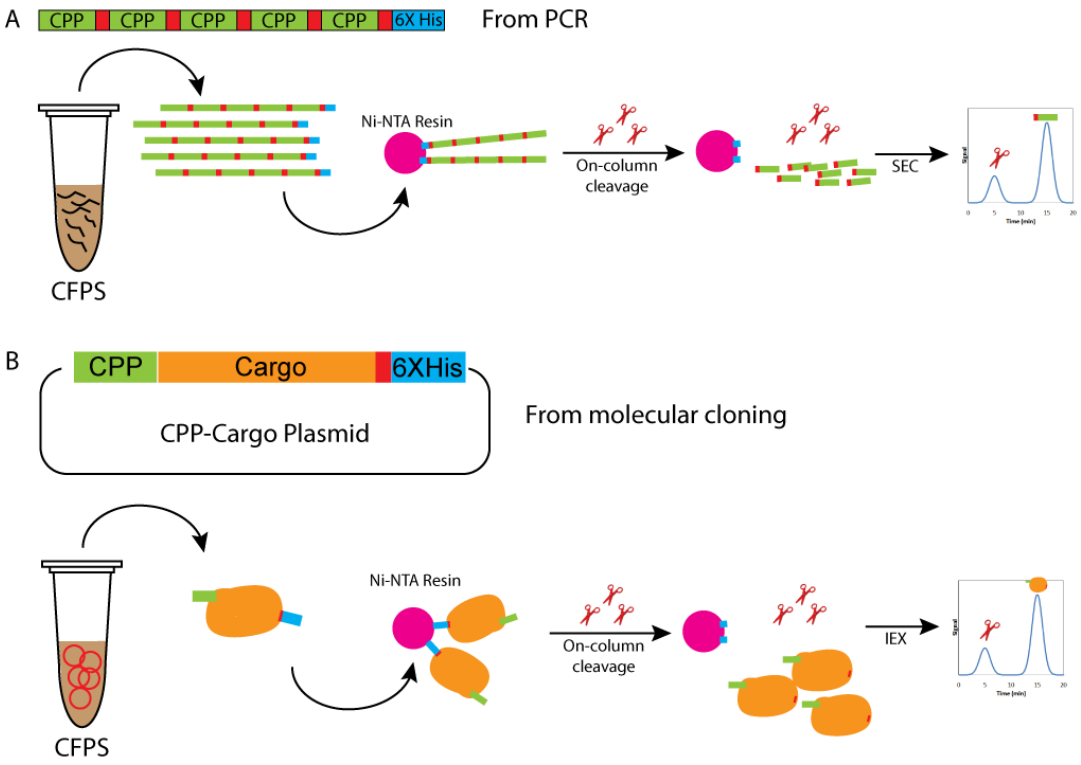

Figure 7.4 Schemes of producing CPPs or CPP-Cargo fusion proteins using CFPS. (A) Multiple CPP subunits will be produced by PCR on one bigger DNA fragment, which will be used for CFPS reactions. The big peptide will be recovered by affinity purification, followed by on-column cleavage by adding protease into the resin. Isolated CPP units will be separated from the enzyme in the flow-through by size-exclusion chromatography (SEC) and the latter elution represent the smaller CPP elution. (B) Plasmid DNA encoding CPP-Cargo fusions will constructed by cloning in bacteria. Purified plasmid DNA will be added into the tube for CFPS reactions. Protein will be recovered by affinity purification and released from the column by cleavage. Protein of interests and enzyme can be separated by ion-exchange chromatography by the difference in isoelectric point (pI).

To produce CPP-cargo fusion proteins, I can use molecular cloning techniques, similar to those in Chapter 6, to construct new plasmid DNA containing template DNA that combines the CPP and cargo protein on the same plasmid (**Figure 7.4 B**). Fusion proteins can be purified using FPLC, and the affinity tag can be removed by on-column purification methods. Additional work of CFPS system optimization and yield control will enable us to utilize this method to produce more peptides or fusion proteins.

7.2.2. Non-natural amino acid (NAA) incorporation

The toxicity of CPP-cargo fusions to the cells mainly comes from the peptides and no loss of cell viability is observed when I only express cargo proteins (GFP) in bacterial cells. An alternative to recombinantly producing fusions is to produce protein cargos alone recombinantly, have the CPP synthesized separately, and then perform peptide conjugation to the cargo *in vitro*.

Non-natural amino acid incorporation has been widely used to produce proteins with non-natural amino acids to study protein folding [8] and photoswitching [9] and to allow protein labeling using click chemistry [10, 11]. Ivana *et al.* successfully used several non-natural amino acids with alkyne groups to allow the conjugation of a fluorescent dye with azide modification through click chemistry [10]. Alkyne-containing proteins have been produced via codon-suppression methods in *E. coli*, yeast, and mammalian cells [12-14]. The amber codon (UAG) is one of the most commonly used codons to allow NNA incorporation. In addition to the template DNA encoding the cargo proteins with a UAG codon, specific plasmids encoding amber tRNA and aminoacyl-tRNA synthetase (aaRS) need to be used to co-transfrom

the host cells. aaRS will aminoacylate the tRNA to only allow NAA transportation at the UAG site (**Figure 7.5** [15]). In such a way, recombinant cargo proteins will allow bioconjugation to CPPs with an azide modification by click chemistry.

NAA incorporation can also be performed *in vitro* via CFPS methods. Hong *et al.* used CFPS to incorporate NAAs into proteins using *E. coli* extracts [7].

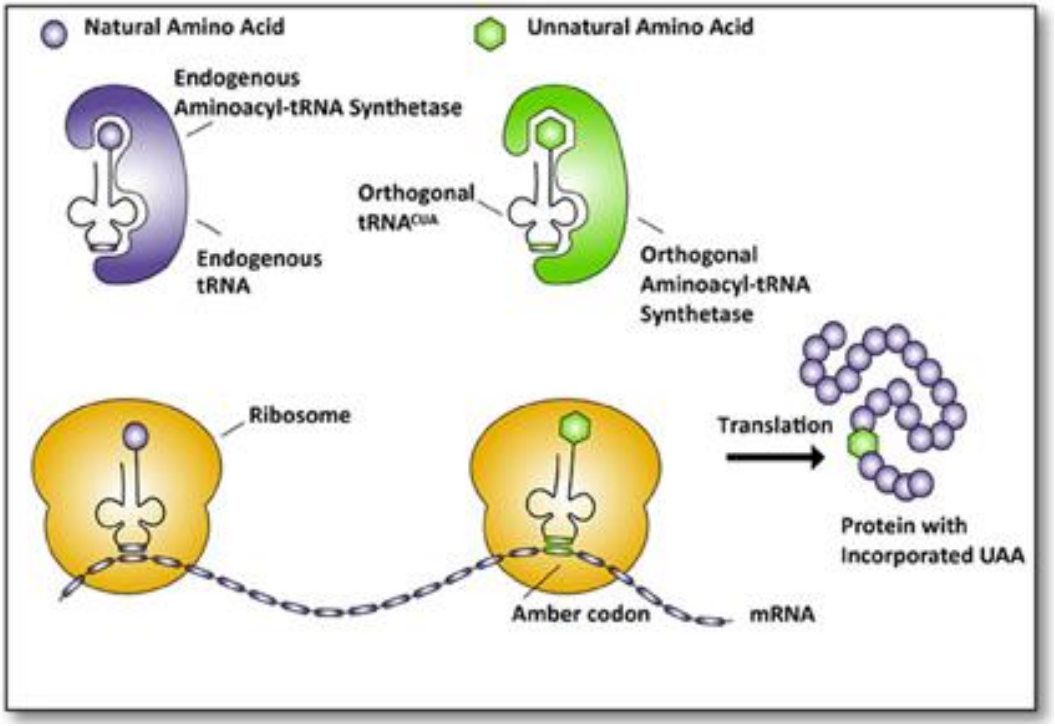

Figure 7.5 Schematic representation of NAAs incorporation via amber codon suppression. Plasmids encoding tRNA, aaRS, and the new protein synthesis DNA with amber codon need to be co-transformed. aaRS will target the tRNA with NAA to the amber site on mRNA sequence to substitute the stop codon with a new amino acid with modified side chain, allowing downstream bioconjugation [15].

Additional DNA encoding tRNA, aaRS will be added into the system on top of regular CPFS essential components. CFPS can resolve the potential toxicity due to overexpression of tRNA and aaRS. This work, along with cell-free synthesis of CPPs will enable complete biosynthesis and bioconjugation *in vitro* and allow a higher degree of freedom in choosing cargo proteins without limitations from the host cells.

7.3. CPP-cargo fusion protein secretion

As mentioned above, the potential toxicity from the CPPs is limiting the recombination expression and production of CPP-cargo fusion proteins in microbial cells. I have described the CPFS methods and NAA incorporation to allow the *in vitro* production of CPPs and CPP-cargo fusions to bypass the limitation from the host cells. Another method to reduce to cytotoxicity of the fusion proteins is to have the protein secreted after synthesis to prevent intracellular accumulation of toxic proteins.

7.3.1. Bacterial secretion pathway for protein expression

Most of *E. coli* secreted proteins are either translocated into the periplasmic space in soluble form or are anchored to the inner or outer membranes, with only a small portion of protein secreted into the extracellular space [16].

The twin arginine translocation (Tat) pathway is a widely studied protein secretion pathway in *E. coli*. The Tat pathway is capable of translocating correctly folded protein across the inner membrane. It requires a conserved, distinctive signal peptide to allow the secretion and periplasmic localization [17]. The enzymes on the inner membrane not only regulate the anchoring and translocation process, but also act as the "quality control" unit for proper protein folding and even disulfide bond formation. Although it has been suggested that the Tat pathway is less efficient than the secretory pathway [18], the quality control mechanism still makes the Tat pathway a promising way to secrete soluble recombinant proteins, which can be used to produce correctly folded CPP-cargo fusion proteins.

Instead of translocating proteins into the periplasm, secreting proteins into the growth medium can protect the proteins from being degraded by the intracellular

proteases and simplify downstream protein recovery and purification. Most of the outer membrane protein secretion is through non-specific pathways with compromised membrane permeability. Alternatively, *Salmonella entertica* has a Type III secretion mechanism to allow direct secretion via a membrane channel "needle", bypassing the periplasm. Metcalf *et al.* have shown stable protein expression and secretion via this Type III pathway, and they suggested that the needle can also act as a folding quality control mechanism to ensure the folding and the biological activity of the secreted proteins [19]. This method gives us an alternative way to produce CPP fusions and allow faster protein recovery.

7.3.2. Yeast secretion pathway for protein expression

Protein secretion in prokaryotic cells has several limitations including low secretion efficacy, missing folding quality control (in the secretory pathway), and lack of post translational modification (PTM). Secretory expression of heterologous proteins in eukaryotic cells such as yeast can allow correct folding and secretion of proteins with the help of the endoplasmic reticulum (ER) and Golgi, and, most importantly, the proteins can be glycosylated [20]. Several strains have been successfully engineered to allow high-efficiency recombinant protein secretion, including strains of *Pichia pastoris*, *Hansenula polymorpha*, *Saccharomyces cerevisiae*, and *Schizosaccharomyces pombe*. There are various expression systems with different promoters for protein expression, such as the inducible promoters ADH2 and SUC2 to allow controlled expression and constitutive promoters like GAPDH for continuous protein expression [21].

There are several challenges associated with yeast recombinant protein expression. The intracellular trafficking is difficult to control. Some of the secreted vesicles after the Golgi will be directed to vacuoles, significantly reducing extracellular protein concentration. The difficulty in controlling the degree of PTM also diversifies the protein properties. Compared with bacterial expression system, like T7, the overall protein expression level and yield in yeast is much lower than engineered bacterial strains. A high cell density fermentation is also important to increase the yield of production and extra experiments are needed for optimization. These limitations need to be further explored to enable better protein secretion in yeast cells.

7.3.3. Mammalian secretion pathway for protein expression

Although yeast cells can be engineered to enable robust protein over-expression and high-yield cell culture, the divergence from native human PTM and variability in expression levels limit the application of yeast expression systems for some routine therapeutic protein production [22].

Mammalian cell culture is promising for biopharmaceutical protein production. The protein folding, PTM, and secretion are more consistent compared with other expression system. There are well designed expression vectors such as CMV and SV40 to allow heterologous protein expression [23]. Various signal sequences allow stable protein production and secretion. Examples like interleukin-2, CD5, trypsinogen and prolactin are well described and show consistent protein secretion [24]. To ensure stable protein expression, a proper mammalian cell line is very important. One of the most commonly used engineering cell line is the Chinese

hamster ovary (CHO) cell line. CHO cells are widely used for monoclonal antibody and therapeutic protein production in the biopharmaceutical industry, and culturing of these cells can be scaled up to larger scale bioreactors. With these tools, I can explore the possibility to use mammalian cells to produce CPP-cargo protein fusions with less toxicity to host cells and more specificity toward fungal pathogens.

7.4. Conclusion

The work presented in this thesis allows more comprehensive understanding of the structure-function relationships of CPPs towards fungal pathogens. Antifungal agent conjugation to CPPs represents an application of using CPP to deliver drugs to combat fungal infections. Additional work on peptide/protein production will enable us to have a larger set of CPPs and CPP-cargo fusion proteins to enable future studies to understand the limitation on the types of cargos that can be delivered. CFPS methods will remove the limitation of cells in expression and allow high-yield *in vitro* CPP/CPP-cargo expression and conjugation. To help eliminate the potential cytotoxicity issue from the peptides inside production hosts, secretion expression systems with different types of cells should be widely studied. These studies will allow better understanding of CPP for cargo delivery and cargo conjugation.

7.5. Reference

1. Ghannoum, M.A. and L.B. Rice, *Antifungal agents: Mode of action, mechanisms of resistance, and correlation of these mechanisms with bacterial resistance.* Clinical Microbiology Reviews, 1999. **12**(4): p. 501-+.
2. White, T.C., K.A. Marr, and R.A. Bowden, *Clinical, cellular, and molecular factors that contribute to antifungal drug resistance.* Clinical Microbiology Reviews, 1998. **11**(2): p. 382-+.
3. Pore, V.S., et al., *Design and synthesis of fluconazole/bile acid conjugate using click reaction.* Tetrahedron, 2006. **62**(48): p. 11178-11186.
4. Huisgen, R., H. Seidl, and I. Bruning, *1,3-Dipolar Cycloadditions .49. Kinetics and Mechanism of Nitrone Additions to Unsaturated Compounds.* Chemische Berichte-Recueil, 1969. **102**(4): p. 1102-&.
5. Ten Brink, H.T., et al., *Solid-phase synthesis of C-terminally modified peptides.* Journal of Peptide Science, 2006. **12**(11): p. 686-692.
6. Hazen, K.C., et al., *Comparison of the Susceptibilities of Candida spp. to Fluconazole and Voriconazole in a 4-Year Global Evaluation Using Disk Diffusion.* Journal of Clinical Microbiology, 2003. **41**(12): p. 5623-5632.
7. Hong, S.H., Y.-C. Kwon, and M.C. Jewett, *Non-standard amino acid incorporation into proteins using Escherichia coli cell-free protein synthesis.* Frontiers in Chemistry, 2014. **2**(34).
8. Wang, L., et al., *Unnatural Amino Acid Mutagenesis of Green Fluorescent Protein.* The Journal of Organic Chemistry, 2003. **68**(1): p. 174-176.
9. Reddington, S.C., et al., *Directed evolution of GFP with non-natural amino acids identifies residues for augmenting and photoswitching fluorescence.* Chemical Science, 2015. **6**(2): p. 1159-1166.
10. Nikić, I., et al., *Labeling proteins on live mammalian cells using click chemistry.* Nat. Protocols, 2015. **10**(5): p. 780-791.
11. Tyagi, S. and E.A. Lemke, *Genetically encoded click chemistry for single-molecule FRET of proteins.* Methods Cell Biol, 2013. **113**: p. 169-87.
12. Deiters, A. and P.G. Schultz, *In vivo incorporation of an alkyne into proteins in Escherichia coli.* Bioorg Med Chem Lett, 2005. **15**(5): p. 1521-4.
13. Deiters, A., et al., *Adding amino acids with novel reactivity to the genetic code of Saccharomyces cerevisiae.* J Am Chem Soc, 2003. **125**(39): p. 11782-3.
14. Wang, Y.S., et al., *A rationally designed pyrrolysyl-tRNA synthetase mutant with a broad substrate spectrum.* J Am Chem Soc, 2012. **134**(6): p. 2950-3.
15. Ovaa, H. and k. wals, *Unnatural amino acid incorporation in E. coli: current and future applications in the design of therapeutic proteins.* Frontiers in Chemistry, 2014. **2**(15).
16. Georgiou, G. and L. Segatori, *Preparative expression of secreted proteins in bacteria: status report and future prospects.* Current Opinion in Biotechnology, 2005. **16**(5): p. 538-545.
17. Berks, B.C., F. Sargent, and T. Palmer, *The Tat protein export pathway.* Molecular Microbiology, 2000. **35**(2): p. 260-274.

18. DeLisa, M.P., et al., *Phage shock protein PspA of Escherichia coli relieves saturation of protein export via the Tat pathway.* J Bacteriol, 2004. **186**(2): p. 366-73.
19. Metcalf, K.J., et al., *Using transcriptional control to increase titers of secreted heterologous proteins by the type III secretion system.* Appl Environ Microbiol, 2014. **80**(19): p. 5927-34.
20. Klis, F.M., *Protein Secretion in Yeast*, in *Growth, Differentiation and Sexuality*, J.G.H. Wessels and F. Meinhardt, Editors. 1994, Springer Berlin Heidelberg: Berlin, Heidelberg. p. 25-41.
21. Mattanovich, D., et al., *Recombinant protein production in yeasts.* Methods Mol Biol, 2012. **824**: p. 329-58.
22. Dalton, A.C. and W.A. Barton, *Over-expression of secreted proteins from mammalian cell lines.* Protein Science : A Publication of the Protein Society, 2014. **23**(5): p. 517-525.
23. Backliwal, G., et al., *Rational vector design and multi-pathway modulation of HEK 293E cells yield recombinant antibody titers exceeding 1 g/l by transient transfection under serum-free conditions.* Nucleic Acids Res, 2008. **36**(15): p. e96.
24. Kober, L., C. Zehe, and J. Bode, *Optimized signal peptides for the development of high expressing CHO cell lines.* Biotechnol Bioeng, 2013. **110**(4): p. 1164-73.

List of publications

- **Gong Z.**, Walls M., Karley A., Karlsson AJ (2016). Effect of a flexible linker on recombinant expression of cell-penetrating peptide fusion proteins and their translocation into fungal cells. Molecular Biotechnology. 58 (12), 838-849
- **Gong Z.**, Karlsson AJ. Translocation of cell-penetrating peptides into *Candida* fungal pathogens. Protein Science (In press)
- Moghaddam-Taaheri, P., Ikonomova, SP., **Gong, Z.**, Wisniewski, JQ., Karlsson, AJ (2016). Bacterial inner-membrane display for screening a library of antibody fragments. J. Vis. Exp. (116), e54583, doi:10.3791/54583

- **Gong Z.**, Karlsson AJ. Secondary structure of cell-penetrating peptides and the interaction with fungal cells (To be submitted, 2017)
- **Gong Z**., Doolin M., Adhikari S., Karlsson AJ. Rational design of cell-penetrating peptides for understanding structure-function relationships in *Candida albicans*. (To be submitted, 2017)

List of presentations

- **Gong Z**., Karlsson AJ. Engineering cell-penetrating peptides for translocation into *Candida* fungal pathogens. ICBE, 2016
- **Gong Z**., Karlsson AJ. Investigation of the cellular uptake and cytotoxicity of cell-penetrating peptides in *Candida* fungal pathogen, AIChE, 2016
- **Gong Z**., Walls MT, and Karlsson AJ. Translocation of biomolecular cargo into *Candida albicans* using cell-penetrating peptides. American Society for Microbiology Conference on *Candid*a and *Candidiasis*, 2016

- **Gong Z**., Karlsson AJ. Effect of secondary structure of cell-penetrating peptides on their interaction with fungal cells, AIChE, 2017 (abstract submitted, 04/17/2017)